Cyprus University of Technology

Faculty of Engineering and Technology

Doctoral Dissertation

Shallow Geothermal Energy Systems: Investigating possible viable solutions in the building sector

Lazaros Aresti

Limassol, December 2020

in memory of my father, Georgios Aresti

CYPRUS UNIVERSITY OF TECHNOLOGY

FACULTY OF ENGINEERING AND TECHNOLOGY

DEPARTMENT OF ELECTRICAL ENGINEERING AND COMPUTER ENGINEERING AND INFORMATICS

Doctoral Dissertation

Shallow Geothermal Energy Systems: Investigating possible viable solutions in the building sector

Lazaros Aresti

Limassol, December 2020

Approval Form

Doctoral Dissertation

Shallow Geothermal Energy Systems: Investigating possible viable solutions in the building sector

Presented by

Lazaros Aresti

Supervisor: Paul Christodoulides, Assistant Professor, Faculty of Engineering and Technology

Signature 

Chair of the committee: Christakis Damianou, Professor, Faculty of Engineering and Technology

Signature 

Member of the committee: Georgios Florides, Adjunct Professor (co-supervisor), Faculty of Engineering and Technology

Signature 

Member of the committee: Konstantinos Tsagarakis, Professor, Faculty of Engineering, Democritus University of Thrace

Signature 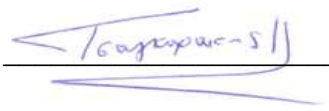

Cyprus University of Technology

Limassol, December 2020

Copyrights

Publications

Journal Articles

2020 Aresti L., Christodoulides P., Florides G., An investigation on the environmental impact of various Ground Heat Exchangers configurations, Renewable Energy, under second review

2020 Aresti, L, Christodoulides,P., Panayiotou, G.P., Florides, G. Residential buildings' foundations as a Ground Heat Exchanger and comparison among different types in a moderate climate country, Energies 13(23), 6287

2020 Christodoulides P., Vieira A., Lenart S., Maranha J., Vidmar G., Popov R., Georgiev A., Aresti L., Florides G., Reviewing the Modeling Aspects and Practices of Shallow Geothermal Energy Systems, Energies 13(16), 4273

2020 Aresti L., Christodoulides P., Panayiotou G.P., Florides G., The Potential of Utilizing Buildings ' Foundations as Thermal Energy Storage (TES) Units from Solar Plate Collectors, Energies 13(11), 2695

2019 Ramos R., Aresti L., Yiannoukos L., Tsiolakis E., Pekris J., Vieira A., Florides G., Christodoulides P., Thermal and physical characteristics of soils in Cyprus for use in Shallow Geothermal Energy applications, Energy, Ecology and Environment 4(6), 300-309

2019 Bianchi G., Panayiotou G.P., Aresti L., Kalogirou S.A., Florides G.A., Tsamos K., Tassou S.A., Christodoulides P., Estimating the waste heat recovery in the European Union Industry, Energy, Ecology and Environment 4(5), 211-221

2019 Christodoulides P., Aresti L., Florides G., Air-conditioning of a typical house in moderate climates with Ground Source Heat Pumps and cost comparison with Air Source Heat Pumps, Applied Thermal Engineering 158, 113772

2019 Stylianou I.I., Tassou S., Christodoulides P., Aresti L., Florides G., Modeling of Vertical Ground Heat Exchangers in the Presence of Groundwater Flow, Energy and Buildings 192, 15-30

2019 Agathokleous R , Bianch G., Panayiotou G., Aresti L., Argyrou M.C., Georgiou G.S., Tassou S., Kalogirou S.A., Florides G.A., Christodoulides P., Waste heat recovery in the EU Industry and proposed new technologies, Energy Procedia 161, 489-496

2018 Stylianou I.I., Christodoulides P., Aresti L., Tassou S., Florides G., Borehole ground heat exchangers and the flow of underground water, International Journal of Industrial Electronics and Electrical Engineering 6(9), 67-72

2018 Aresti L., Christodoulides P., Florides G.A., A review of the design aspects of Ground Heat exchangers, Renewable & Sustainable Energy Reviews 92, 757-773

2017 Panayiotou G.P., Bianchi G., Georgiou G.S., Aresti L., Argyrou M.C., Agathokleous R., Tsamos K., Tassou S.A., Florides G., Kalogirou S.,

Christodoulides P., Preliminary assessment of waste heat potential in major European industries, Energy Procedia 123C, 335-345

2016 Aresti L., Christodoulides P., Florides G.A., Computational Modeling of a Ground Heat Exchanger with groundwater flow, Bulgarian Chemical Communications 48, Special issue E, 55-63

2014 Kalogirou S.A., Aresti L., Christodoulides P., Florides G., The effect of air flow on a building integrated PV-panel, Procedia IUTAM 11, 89-97

2013 Aresti L, Tutar M, Chen Y, Calay RK, Computational study of a small scale vertical axis wind turbine (VAWT): comparative performance of various turbulence models, Wind and Structures 17 (6), 647-670

Conference Publications

2020 Aresti L., Christodoulides P., Makarounas C., Lazari L., Florides G., Computational Investigation of Dwellings Foundation as a GHE in Mediterranean Climate, 7th International Conference on Energy, Sustainability and Climate Change, ESCC 2020, 24-26 August 2020, Skiathos, Greece

2020 Christodoulides P., Aresti L., Messaritis V., Panayiotou G., Bianchi G., Florides G., Waste Heat Recovery Technologies: Recommendations on how to Overcome Barriers to their Adoption, 7th International Conference on Energy, Sustainability and Climate Change, ESCC 2020, 24-26 August 2020, Skiathos, Greece

2020 Aresti L., Christodoulides P., Florides G., An investigation on the environmental impact of GSHP systems, Alternative Energy Sources, Materials and Technologies (AESMT'20), 8-9 June, Varna, Bulgaria

2020 Aresti L., Christodoulides P., Florides G., Using buildings' foundation as a GHE in moderate climates, EGU General Assembly Conference Abstracts, 3684

2019 Aresti L., Christodoulides P., Messaritis V., Florides G. Ground Source Heat Pumps cost analysis in moderate climate, WAMS 2019 in 19th Asia Simulation Conference AsiaSim 2019, Singapore

2019 Aresti L., Christodoulides P., Lazari L., Florides G. Computational investigation on the effect of various parameters of a spiral Ground Heat Exchanger, WAMS 2019 in 19th Asia Simulation Conference AsiaSim 2019, Singapore

2019 Florides G., Aresti L., Messaritis V., Christodoulides P., Performance investigation of a Ground Source Heat Pump system for space heating and cooling of a typical house in moderate climates, 6th International Conference on Energy, Sustainability and Climate Change ESCC 2019, 3-5 June, Chania, Greece

2019 Aresti L., Ramos R., Vieira A., Messaritis V., Florides G., Christodoulides P., Ground thermal characteristics of typical soils in Cyprus for Ground Heat

Exchangers, 6th International Conference on Energy, Sustainability and Climate Change ESCC 2019, Chania, Greece

2019 Christodoulides P., Aresti L., Florides G., Experimental validation of a CFD model for spiral Ground Heat Exchangers, 6th International Conference on Energy, Sustainability and Climate Change ESCC 2019, 3-5 June, Chania, Greece

2019 Florides G., Aresti L., Messaritis V., Lazari L., Christodoulides P., Economics of a sustainable geothermal system for air-conditioning a typical house in moderate climates, SIAM Conference on Mathematical & Computational Issues in the Geosciences, Houston TX, U.S.A.

2019 Christodoulides P., Zerun M., Aresti L., Kalogirou S., Florides G., Performance and cost analysis of single and double U-tube ground heat exchangers, SIAM Conference on Mathematical & Computational Issues in the Geosciences, Houston TX, U.S.A.

2018 Florides G.A., Aresti L., Panayiotou G., Messaritis V., Christodoulides P., Optimization of floor elements to cover the heating needs of buildings using solar collectors, 8th International Conference on Energy and Environment of Residential Buildings ICEERB 2018, Wellington, New Zealand

2018 Agathokleous R , Bianchi G., Panayiotou G., Aresti L., Argyrou M.C., Georgiou G.S., Tassou S., Kalogirou S.A., Florides G.A., Christodoulides P., Waste heat recovery in the EU Industry and proposed new technologies, 2nd ICSEF International Conference on Sustainable Energy and Resource Use in Food Chains, Paphos, Cyprus

2018 Ramos R., Aresti L., Christodoulides P., Vieira A., Florides G., Assessment and Comparison of Soil Thermal Characteristics by Laboratory measurement, International Symposium on Energy Geotechnics SEG 2018, Lausanne, Switzerland

2018 Stylianou I.I., Christodoulides P., Aresti L., Tassou S., Florides G., Borehole ground heat exchangers and the flow of underground water, 143th ISER International conference (359th International Conference on Heat Transfer and Fluid Flow ICHTFF), Melbourne, Australia

2018 Aresti L., Florides G., Messaritis V., Lazaris L., Christodoulides P., Ground Heat Exchanger model validation through software comparison, 5th International Conference on Energy, Sustainability and Climate Change ESCC 2018, Mykonos, Greece

2017 Christodoulides P., Yiangou E., Aresti L., Kaouri K., Florides G., Kalli K., Heat transfer and pressure-driven flow in circular and elliptical microstructure fibres, 5th Workshop on Specialty Optical Fiber and Their Applications WSOF'2017, Limassol, Cyprus

2017 Aresti L., Christodoulides P., Panayiotou G., Theophanous E., Kalogirou S., Florides G., Integrated solar flat plate collectors and passive solar floor heating in buildings, 4th International Conference on Energy, Sustainability and Climate Change, Santorini, Greece

2017 Aresti L., Florides G., Christodoulides P., Lazari L., Groundwater flow and Ground Heat Exchangers, 10th IMACS International Conference on Nonlinear Evolution Equations and Wave Phenomena, Athens GA, U.S.A.

2017 Aresti L., Christodoulides P., Panayiotou G., Theophanous E., Kalogirou S.A., Florides G., Passive Solar Floor Heating in Buildings utilizing the Heat from an Integrated Solar Flat Plate Collector, First International Conference on Building Integrated Renewable Energy Systems (BIRES), Dublin, Ireland

2016 Aresti L., Florides G., Christodoulides P., Messaritis V., Effect of groundwater flow on a ground heat exchanger, XXIV International Congress of Theoretical and Applied Mechanics, Montreal, Canada

2016 Aresti L., Christodoulides P., Florides, Computational Modeling of a Ground Heat Exchanger with groundwater flow, RE&IT Conference, Plovdiv, Bulgaria

2015 Christodoulides P., Aresti L., Florides G., Messaritis V., Analytical and numerical modeling of Ground Heat Exchangers, SIAM Conference on Analysis of partial Differential equations, Phoenix AZ, U.S.A.

2014 Kalogirou S., Agathokleous R., Aresti L., Christodoulides P., Florides G., The effect of the air flow on the temperature of the PV panel examined for two BIPV panels of different shape, 17th Conference on Process Integration, Modelling and Optimisation for Energy Saving and Pollution Reduction, Prague, Czech Republic

2013 Kalogirou S.A., Aresti L., Agathokleous R., Christodoulides P., Florides G., Air flow effect on the temperature of a building integrated BIPV-panel, COMSOL Conference, Rotterdam, Netherlands

2013 Kalogirou S.A., Aresti L., Christodoulides P., Florides G., The effect of air flow on a building integrated photovoltaic (BIPV), IUTAM Symposium on nonlinear interfacial wave phenomena from the micro- to the macro-scale, Limassol, Cyprus

I would like to express my deepest gratitude to my supervisors, Prof. Paul Christodoulides and Prof. Georgios Florides, for believing in me from the very first moment, along with their invaluable guidance and their enthusiastic support. Their advice and encouragement have strongly inspired me to complete this research successfully.

Finally, I own my deepest gratitude to my family; my parents in law Thedoros and Paraskevi, my sister Maria with my two little nieces Despoina and Eleftheria, my godson Giorgos, and, my wife and partner in life Elpida Skeparnidou, for their patience, support, understanding, and standing next to me during difficult times. But most importantly, I am truly indebted to my parents, Dora and Giorgos Aresti, for their guidance, support and all the sacrifices they have made for me.

Abstract

Shallow Geothermal Energy (SGE), a renewable resource, finds application through the use of Ground Source Heat Pumps (GSHPs) coupled with Ground Heat Exchangers (GHEs) for space heating and cooling of buildings. GSHPs are an emerging technology and have received more attention in the recent years due to their high efficiency in comparison to the conventional Air Source Heat Pumps (ASHPs). Despite their evident advantage, the technology of GSHPs has not reached a steady and popular state, owing to high initial costs of installation and manufacturing. Depending on the building's loads, and therefore on the climate of the area, the GSHP system could be a smart investment for the building's owner. To address this, the main objective of this research is to study and suggest ways of improving GSHP systems so that a system could stand out as an attractive Renewable Energy System (RES).

Initially, an economic evaluation of two types of systems, ASHP systems and GSHP systems, was conducted for a residential building in moderate climate conditions. An example of possibly enhancing the performance of GHEs is studied for a certain characteristic of the surrounding ground, namely through the possible groundwater effect on the outlet temperature, and hence, the length of the GHEs. The length of a GHE could also depend on the configuration/geometry type of the GHE. To that extent, the implementation of the building's foundation was subsequently considered to act as GHE. The use of a residential building's foundations, namely the foundation piles or the foundation bed, were considered for investigation within the framework of the newly developed nearly Zero Energy Buildings (nZEB) concept. Such hybrid elements (energy piles and foundation bed) demonstrate promising results with low payback periods and a low environmental impact. Such systems could potentially attract more homeowners to invest in geothermal energy and to see this technology flourish in the near future.

Keywords: Ground Heat Exchanger; Energy Geo-Structures; Shallow Geothermal Energy; GSHP system cost analysis; building foundation GHE; GSHP cost analysis; GHEs LCA analysis

Table of Contents

List of Tables

List of Figures

Nomenclature

Abbreviations

AP	Acidification potential
ASHP	Air Source Heat Pump
CUT	Cyprus University of Technology
DPP	Discounted Payback Period
EGS	Energy Geo-Structures
EP	Energy Piles
EP	Eutrophication potential
FAETP	Freshwater Aquatic Eco-toxicity potential
GSHP	Ground Source Heat Pump
GWP	Global Warming potential
HGSHP	Hybrid Ground Source Heat Pump
HP	Heat Pump
HTP	Human toxicity potential
nZEB	nearly Zero Energy Buildings
ODP	Ozon layer depletion potential
RES	Renewable Energy Systems
SGE	Shallow Geothermal Energy
SPP	Simple Payback Period
TAS	Thermo-Active Structures
TES	Thermal Energy Storage
TETP	Terrestrial Eco-toxicity potential
TRT	Thermal Response Test

Math

COP	Coefficient of performance

Ei Exponential Integral

$erfc$ Complementary Error Function

f_D Darcy's friction factor

F_O Fourier Number

G Dimensionless temperature introduced as the G-Function

h Convection heat transfer coefficient [W m^{-2} K^{-1}]

H, L Borehole depth [m]

J, Y Bessel functions

m Borehole mass [kg]

$\dot{m}$ Mass flow rate [m s^{-1}]

Q Heat transfer rate per volume [W m^{-3}]

$\dot{q}$ Heat transfer rate per unit length [W m^{-1}]

r Radial coordinate [m]

R_b Borehole Thermal resistance [K W^{-1}]

r_b Borehole radius [m]

T Temperature [K]

t Time [s]

u Velocity [m s^{-1}]

Greek Letters

α Thermal diffusivity [m^2 s^{-1}]

Γ Gamma function

γ Euler's constant

λ Thermal conductivity [W m^{-1} K^{-1}]

ρ Density [kg m^{-3}]

Chapter 1*

1. Introduction

Global climate change is globally noted as a critical issue needing a swift resolution. Many companies invest into renewable energy in order to overcome the issue of the inevitable elimination of fossil fuels. Renewable energy systems, including wind turbines, hydroelectric, photovoltaic systems and geothermal energy, have already started to power not only individual buildings but many cities around the world.

The meaning geothermal originates from the Greek word "γεωθερμική" (geo̱thermiki̱), which is in fact a combination of two words. The first word is "γή" (gi̱), meaning earth, and the second one is "θερμός" (thermós), meaning hot. This states that geothermal energy is the thermal energy contained in the forms (ground, soil) of the earth. Geothermal energy was first introduced as an energy source in Larderello, Italy 1904 (DiPippo, 1980). On a later stage it was introduced as a heat source for heat pump systems and the first known record was found in a Swiss patent in 1912 (Ball et al., 1983). Geothermal energy can be categorized by depth as shallow or deep geothermal, and by resource type as high or low enthalpy. Main applications of geothermal energy are power generation and direct use for space heating and cooling of buildings, with the latter having a higher capacity in Europe (Antics et al., 2013). In both cases, heat is extracted or rejected from/into the ground at a specific depth according to case (Jensen and Kaminski, 2005). Geothermal energy, despite being used for many years, has not yet reached a stable and popular state to allow a wide use.

A commonly used type of shallow Geothermal Energy Systems is the Ground Source Heat Pump (GSHP) system. These have higher energy efficiency and lower environmental impact compared to Air Source Heat Pumps (ASHP) (Yu et al., 2013). However, they have not been so extensively used due to their high manufacturing and installation cost compared to conventional not so effective systems. For example, the capital cost of an ASHP is lower than that of a GSHP

* Material from published paper (Aresti et al., 2019a, 2018)

system, although the operation cost is lower for the GSHP system. Only recently the GSHP systems have gained more recognition due to the energy shortage. It is noted that GSHP installations have increased dramatically in the recent years (after 2010) with an annual rate of 10–30% (Yang et al., 2010).

Ground Heat Exchangers (GHEs) act essentially as conventional heat exchangers, with a network of tubes concealed underground, gaining or rejecting heat from/to the ground. GHEs can be coupled with GSHP systems for heating and cooling a building. There are two main categories of GHEs: the horizontal and the vertical types. Vertical type GHEs, being the conventional type, require less space and have higher performance per meter compared to the horizontal types (Aresti et al., 2018). The main configurations of vertical types are the U-tube, double U-tube, and coaxial GHEs. In recent years, a different configuration has become popular, namely the spiral or helical type GHE. Spiral GHEs was introduced to reduce the GHE depth and has been used in foundation piles, identified as "energy piles" (Carotenuto et al., 2017). The overall aim of this configuration is to reduce the initial capital and the cost of the GSHP system in order to make it more attractive for investment. To that extent the incorporation of GHEs in the building structural elements potentially reduces the initial cost of a GSHP system. Such systems are referred to as Thermo-Active Structures (TAS) or Energy Geo-Structures (EGS), where structural building elements act as GHEs as well (hybrid elements). In particular, so-called energy piles, are nothing else than the foundation piles utilized with a network of tubes during the building foundation construction to provide space heating and cooling. The typical sizing of the energy piles is between 20–40m in depth and 0.4–1.5m in diameter, as reported by Brandl (2013). Apart from energy piles, another EGS system can be realized (as proposed in this Thesis), by the incorporation of the whole building's foundation bed as a GHE. Foundation piles are not required in all constructions, but a building's foundation bed is a mandatory element. This configuration is also based on the principles of the energy pile.

1.1 Problem-Statement and Hypothesis

GSHP systems constitute an evolving technology that has been given significant attention in recent years. Such systems owe the attention given to them to their high

performance compared to ASHP systems. For optimized performance, GSHPs require yearly both heating and cooling loads, something provided by the mild Mediterranean climate in Cyprus. The main concern with this technology however is the high initial costs, making it a difficult decision for the homeowners to incorporate the systems into their buildings.

The use of the building's foundations as a GHE could be examined in the framework of EGS, whereby the proposed GSHP system, compared to other existing GSHP/GHE systems or ASHP systems, could potentially prove to be an advantageous investment with regard to initial costs and payback period, but as well as an environmentally friendly application with regard to Life Cycle Analysis (LCA). Energy piles have yet to be applied in Cyprus and, thus, a preliminary assessment considered and investigated before application would be useful. The potential of the GSHP systems by utilizing the building's foundation is also considered here, for a moderate climate such as Cyprus; these can be studied in the framework of the European Union's demand of the penetration of nearly Zero Energy Buildings (nZEBs).

1.2 Objectives

The overall aim of this Thesis is to undergo a study of the existing performance of GSHPs, study and improve their efficiencies and reduce the total manufacturing or installation costs (Capital cost), in order to make the system more attractive to the public. To this end, the following objectives were considered:

i. Investigation on the design aspects affecting the efficiency of the GSHP systems;
ii. Economic evaluation and comparison of various GSHP systems and conventional ASHP systems, using simple payback methods such as SPP and DPP;
iii. Study of the groundwater flow effect on GHEs with the use of the COMSOL Multiphysics Computational Fluid Dynamics software package;
iv. Introduction to Energy Geo-Structure elements in the residential housing sector, and computational evaluation on their performance for a nZEB case study, using TRNSYS and COMSOL Multiphysics software;

v. Finally, a Life Cycle Analysis of the different processes of the proposed systems with the aid of the open-source software openLCA.

1.3 Approach

Following the brief introduction from Chapter 1, an initial investigation on the design aspects of GHEs and their effect of their performance on the system is given in Chapter 2. Then, an economic evaluation comparison between the conventional ASHP system and a GSHP system for a residential building at moderate climate is considered in Chapter 3. The results point to long payback periods and, as a consequence, the need for the reduction in costs arises so as to achieve an attractive investment for the systems. In Chapter 4, an example of possibly enhancing the performance of GHEs is studied for a certain characteristic of the surrounding ground. Namely, the presence of groundwater was examined with regard to its possible effect on the outlet temperature of vertical GHEs, which could lead to the reduction of GHE length. With the aid of COMSOL Multiphysics, a CFD software, the effect of the outlet temperature was observed, using data for an existing location in Cyprus. Indeed, a reduction of the outlet temperature was observed, leading to a reduction in the GHE length and, consequently, to a reduction in the initial costs required. Unfortunately, not many buildings come with the privilege of an underground aquifer at the construction site.

The implementation of the buildings' foundation, a mandatory requirement for all buildings, was subsequently considered as a GHE, in Chapter 5. As above-mentioned, such GHEs are categorized as EGS or TAS. Foundation piles coupled with a network of pipes, also referred to as energy piles were studied for a residential building. In the Mediterranean island of Cyprus however there is a limited use of foundation piles in buildings, and hence a new configuration was proposed, the use of the whole foundation bed as a GHE. Energy piles and the foundation bed as a GHE were investigated for a typical house in Cyprus with the heating and cooling loads of a nZEB.

Finally, a Life Cycle Analysis (LCA) of different GHEs types is considered, in Chapter 6, to investigate whether the RES technology under investigation, namely

the GSHP system, could not only address a reduction in CO_2 emissions but produce a lower impact in all environmental aspects.

Chapter 2*

2 Literature review of the design aspects of Ground Heat Exchangers

Summary: The advancement of technology and renewable energy systems (RES) have evolved considerably through the years. Geothermal energy was first introduced in Italy in 1904 and has ever since dramatically increased in efficiency. One of the main types of RES, Ground Source Heat Pumps (GSHPs), are used for heating and cooling a space when coupled with Ground Heat Exchangers (GHEs). GSHPs extract or reject heat to the Earth via a network of tubes. The closed loop system, either vertical or horizontal, is the most common of the configurations. Alternatively, pipes can run all the way down to utilize natural underground water sources, when present, in an open loop configuration. GHEs have significantly higher performance over conventional air-to-air heat exchanger systems and the reduction of their cost and the improvement of their overall efficiency through their design are crucial in research.

In this chapter the design aspects of GHE systems are presented and reviewed. In particular the types of GHEs such as open or closed loop systems, vertical or horizontal, U-tube or spiral, energy piles and hybrid systems are discussed. A comparative analysis through the literature of the various geometrical aspects of GHEs and the geothermal investigation of the ground environment and the materials used in the construction of GHEs are also presented. Then the modelling – experimental and mathematical – of GHEs is analysed, with terms that have been extensively studied, like borehole thermal resistance, thermal characteristics, thermal response test, line-source and cylindrical-source models, discussed in detail. Next a demonstration of designing a numerical model of a GHE system through a software, taking into consideration the thermal characteristics, is given. Finally, a comparative detailed list in the form of a table of more than 30 mathematical and/or experimental GHE studies is provided, focusing on the important factors analysed and findings of each. The overall aim of the current

* Material from published paper (Aresti et al., 2018)

review study is to help improve the efficiency and the total manufacturing cost of GHEs.

2.1 Overview

A GHE can be classified as the system that connects the heat pump system with the ground and allows heat rejection or injection into the ground. There are several types of GHEs, which can be broken down into three general type categories: open loop systems, closed loop systems and other type systems. In an open type system, there are two sub-sections where a medium can be used, where the groundwater can be used as a medium, whereas in a closed system a heat exchanger is located in the ground and the medium (refrigerant) is circulated through the pipes transferring heat from/to the ground. In a closed system, there is no contact between the heat carrier (refrigerant) and the ground (soil/rock) in contrast with the open system where there is no separation (Omer, 2008). There is also a third category for some cases where they do not fall exactly in the open or closed loop systems. Some examples of these systems are the standing column wells as well as mine water wells, which usually consist of a borehole filled with water transferred from the bottom of the well to the heat pumps and then rejected either in the well itself or in another rejection well (Nguyen et al., 2015; Pasquier et al., 2016).

The closed loop system, either vertical or horizontal, is the most common of the configurations. Pipes can be buried by drilling either vertical boreholes or horizontal trenches. Alternatively, if the building has access to an aquifer, pipes can run all the way down to utilize this natural underground water source as an open loop configuration.

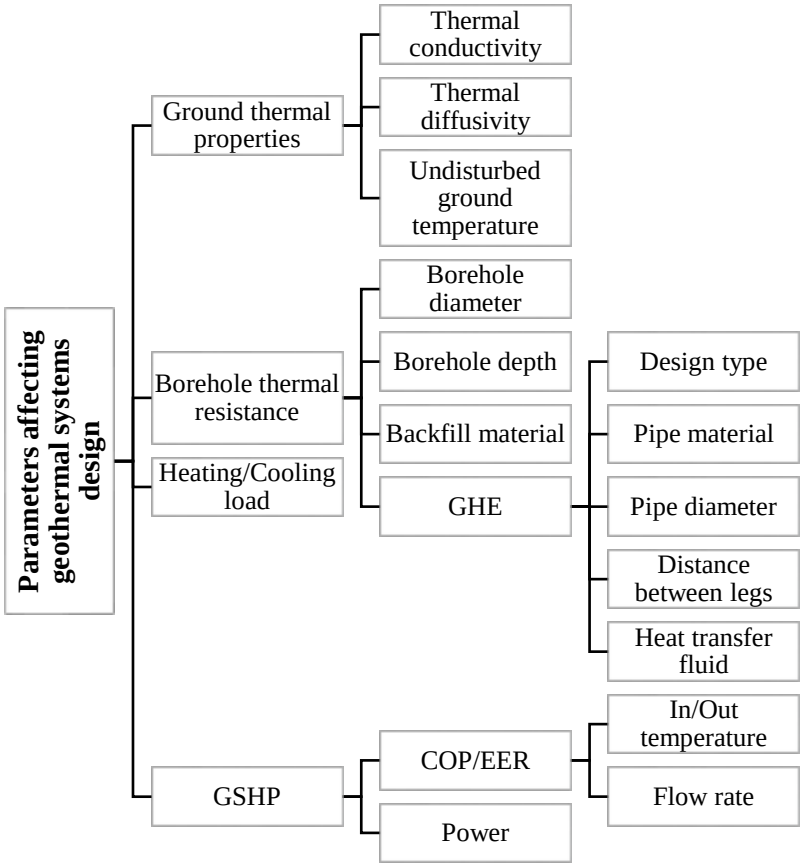

Figure 2.1 Factors affecting the design of GHEs (modified from (Pouloupatis et al., 2017))

Figure 2.1 is a schematic of the factors affecting the design of GHEs. The overall aim of the present paper is to undergo a review study of the design aspects of GHEs. The most important factors that one should consider before building a GHE system include (not necessarily in order of importance): (i) the choice of an open or closed loop; (ii) the choice between a horizontal GHE, a vertical GHE, or an energy pile; (iii) a U-tube, a spiral, a co-axial, a helical, a slinky tube configuration, (iv) the choice of a single or multiple tubes (in parallel or series connection), (v) the length and the diameter of the borehole and the pipes and the flow direction; (vi) the centre-to-centre distance between pipes; (vii) the characteristics of the backfill grout material; (viii) the thermal characteristics of the ground; (ix) the experimental methodology and the mathematical model chosen for the computation and the behaviour of parameters affecting the GHE system. Note that the current review is not concerned with the efficiency of GHEs (see for instance (Pouloupatis et al., 2017)).

In the following sections, an overview of such factors is given. In Section 2.2, GHE systems are introduced and separated into groups according to their sources. Section 2.3 presents a comparative study on the Geometry of GHEs, while materials of the GHE are introduced in Section 2.4. In Section 2.5, the widely used analytical and computational models are presented and discussed, while the borehole thermal resistance and Thermal Response Test are being introduced. A numerical model demonstration is presented in section 2.6, along with a detailed list of mathematical and/or experimental GHE studies for comparison reasons. Section 2.7 concludes with a discussion and future recommendations.

2.2 Types of GHE systems

2.2.1 Open loop systems

The open loop GHE systems can be separated into two sub-categories: ground pre-heating/pre-cooling of air or ground water heat pump (see Figure 2.2). The basic principle of the pre-heating or pre-cooling the air is to increase the efficiency of the air-to-air heat exchanges and this is achieved with the ambient air passing through the tubes that follow down in the ground before it enters a conventional air conditioning unit (Florides and Kalogirou, 2007).

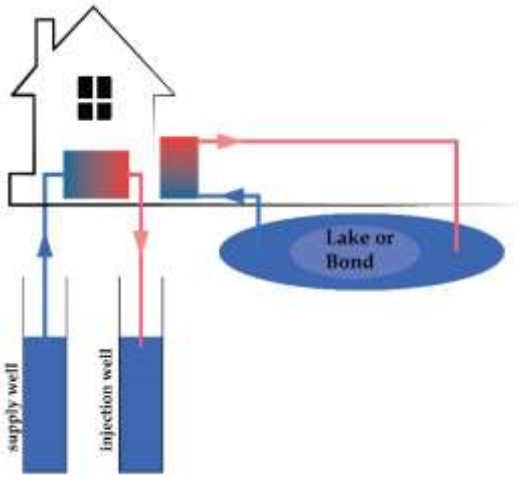

Figure 2.2 Ground water heat pump with open loop (doublette) (Lok Do and Haberl, 2010)

Overall the open loop systems are considered to have better thermodynamic performance and lower cost compared with the closed loop systems (Omer, 2008).

This is due to the fact that they have low drilling requirements (in the case of one well) and the groundwater delivered is at ground temperature. In contrast the water availability may not always exist and also the heat exchanger is subject to corrosive agents, scaling and bacterial contents (Omer, 2008). In addition, for the case where a re-injection well is required, the cost is relatively high. The larger water flow requirements point to a higher pumping power desired compared with the closed loop systems.

2.2.2 Closed loop systems

In a closed loop system, the heat carrier fluid is circulated within the heat exchanger as opposed to the open loop system where the fluid is the ground water and is not circulated in the system. The closed loop system is separated into the categories of the horizontal and the vertical systems. In both systems pipes are buried in the ground.

2.2.2.1 Horizontal and Vertical GHE types

In the horizontal type, pipes are buried into a depth of 1–2m and the loop is 35–60m long per kW of heating or cooling (Florides and Kalogirou, 2007). It is a more cost-effective system and appropriate when there is space available and when trenches are easy to dig. It is noted by Florides and Kalogirou (2007) that the horizontal ground loops are easier to install when the building is under construction, but with new digging equipment it is also feasible to install it post construction, for example in the driveway. The horizontal systems can be arranged into different configurations such as trench connection or slinky-type connection (Figure 2.3), as well as series- or parallel-tubes connection. The parallel connections are more common due to the advantage of lower pumping power consumption as compared with the series connection. In addition, the parallel loops use smaller diameter pipes, therefore the heat transfer fluid volume is reduced. The series connection on the other side requires a smaller number of pipes.

An improvement of the horizontal type can be seen in the slinky-type ground heat exchanger (Figure 2.3), where more pipe length (pipe density) occupies less area. The use of this configuration is suitable when not enough land area is available and

natural temperature recharge of the ground is not vital (Florides and Kalogirou, 2007). The trench/slinky type can be set into two different configurations. Either in overlapping loops or in vertical spiral loops. In the overlapping connection attention to the filling process must be given in order to avoid any gaps between the overlapping pipes. In the case where air gaps are left, air thermal resistance may be produced and a reduction in heat transfer performance will occur (Ping et al., 2015). The thermal interference between the vertical coils, in the vertical spiral connection, is more significant when compared to the overlapping slinky coils, but requires higher installation costs and time compared to overlapping pipe connection (Congedo et al., 2012).

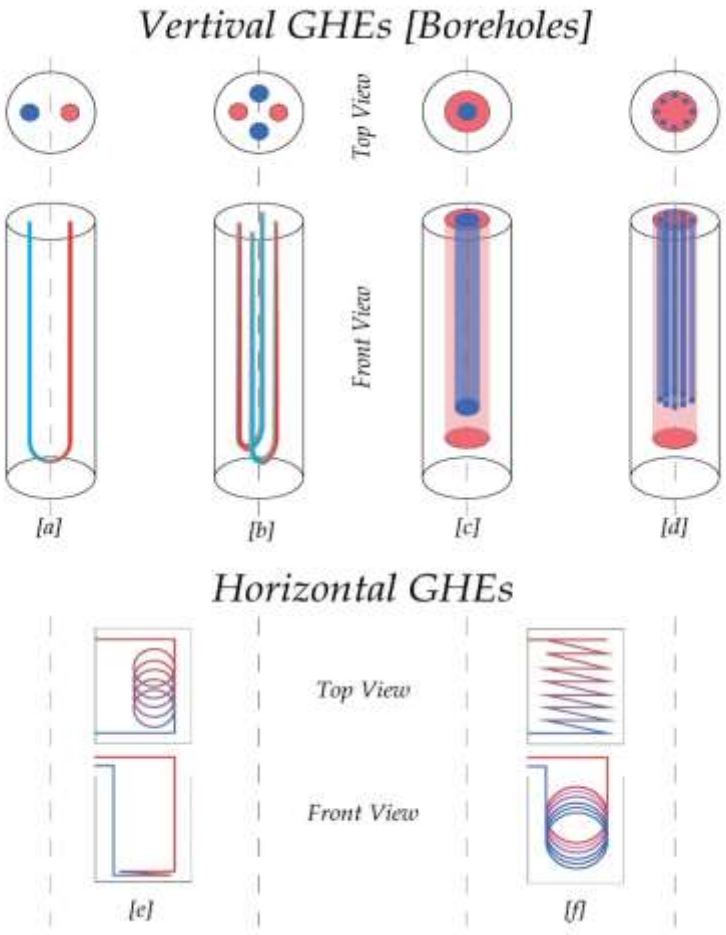

Figure 2.3 (a) Common vertical GHE designs – single U-tube, (b) double U-tube, (c) simple coaxial, (d) complex coaxial, (e) overlapping slinky loops, (f) vertical spiral loops

The vertical GHEs are used in contrast to the horizontal types when, not enough land area is available, the ground surface is rocky, or even when interfering with the

landscape is not desirable. Vertical GHEs consist of plastic pipes (commonly used material is polyethylene or polypropylene), refrigerant fluid and backfill material, which enables a reduction in thermal resistance between the pipes and the ground as well as a good contact between the two materials. With studies showing that the temperature over a certain depth in the ground remains constant, vertical GHEs require less pipe length to produce the same efficiency as the horizontal but have higher installation cost due to the high depth required (Pouloupatis et al., 2011). The vertical GHE or borehole heat exchanger (BHE) is separated in two subcategories according to the installed pipe design, the U-pipes and the coaxial pipes (see Figure 2.3).

The U-pipe design consists of a one or more pairs of pipes connected with a U-turn on the deepest point of the borehole. The most commonly used are the single U-pipe or the double U-pipe configuration. The coaxial pipes design consists of a pipe in pipe configuration where a smaller pipe is inserted in a larger diameter pipe or with complex configuration where more than one pipe are put together on the outer surface of the centre pipe (shown in Figure 2.3).

In general, a global performance comparison (efficiency, etc.) of the different types of GHEs is hard to achieve (and hence does not exist), as the performance of each GSHP is case specific. Although, as already stated in Section 2.1, the current review has not set a goal to deal with the efficiency of GHEs, some indicative (and surely not exhaustive) cases are presented in Section 2.3, where a comparison analysis of various geometrical aspects of GHEs is attempted.

2.2.2.2 Energy pile systems

The GHE can also be utilized in the building foundation. This method is known as "energy piles" and can dramatically decrease the drilling and backfill material cost of the system. Furthermore, it is ideal where the land is limited, and the building consumes a high percentage of the area. Foundation piles are thicker in diameter and shorter in depth compared with the boreholes. The first experiments for energy piles came from Morino and Oka (1994) while later many researchers tried to adopt this concept into experimental and numerical investigations (see for instance (Pahud et al., 1996)).

Morino and Oka's approach was to reduce the installation cost of the heat exchangers by utilizing the steel piles used for foundations as heat exchangers (Morino and Oka, 1994). They contacted an experiment using a steel pile for building foundations with 400mm diameter and a depth of 20m.

Pahud et al. (1999) presented a study, with TRNSYS as a simulation tool, based on the Dock Midfield terminal building at Zurich airport. The foundation piles were 30m in depth and 1–1.5m in diameter, filled with concrete, and were equipped with pipes coupled to a heat pump. The authors demonstrate that a reduction of fossil fuel consumption will be achieved without increasing the overall energy demand, when the GHE piles are in optimal use.

Laloui et al. (2005) performed a thermo-hydro-mechanical investigation of an energy pile using experimental and numerical solutions. A four-storey building with 97 piles at a depth of 25m was chosen as an in-situ test for GHEs, and the test borehole drilled had a 25.8m depth and a 0.88m diameter.

Hamada et al. (2007) performed an experimental investigation at a building with office and residential use. Twenty-six concrete piles were used with a 0.302m outer diameter and a 9m depth. Four design types of GHE were considered (U-shaped, double U-shaped; indirect double-pipe and direct double-pipe), with the most preferable (heat transfer characteristics), being the direct double-pipe type, given the assumption of no possible leakage to occur when using an antifreeze solution. The specific U-shaped type, having the economic and workability advantage, gave a relatively high coefficient of performance (COP) of 3.9.

Sekine et al. (2007) performed a cast-in-place concrete piles experiment (piles with a 1.5m diameter, a 20m length and having 8 U-tubes installed on the outer surface) to investigate the GHE capabilities, subterranean temperature changes and heat pump performance. The COP obtained was a high 4.89 in cooling mode, indicating that the system was 1.7 times more efficient than common an Air Source HP system.

The energy piles can accommodate the spiral/helix coil geometry configuration. This configuration differs from the U-tube configuration in the sense that a spiral coil being used instead of a straight tube. The spiral coil configuration has the

advantage of larger heat transfer area and better flow patterns, without air chocking in the pipes at the turning tips when connected in series (Man et al., 2010; Ping et al., 2015). In addition, the borehole diameter is relatively larger than the U-tube pipe and the depth is reduced as an outcome of the stated advantages. The spiral coil configuration would be more ideal to be used in an energy pile method as it requires wider diameter.

2.2.2.3 Hybrid Ground-Source Heat Pumps

The Ground-Source Heat Pumps (GSHP) perform better when heating and cooling loads are balanced all year round due to the long term transient heat transfer (Ping et al., 2015). It is also observed that in warmer or colder climate areas, unbalanced cooling and heating loads are distinguished. In such cases when heat is rejected or extracted in the ground, in the long term these unbalanced loads will cause an increase or decrease in the ground temperature.

Ping et al. (2015) state that the issue above causes a performance reduction since the entering and exiting fluid temperatures will change. This issue can be overcome by increasing the borehole depth or the boreholes spacing, if more than one borehole is used. These solutions result in increasing the capital cost and the area required. A different solution to overcome the unbalancing loads is to use a Hybrid Ground Source Heat Pump (HGSHP) system. The HGSHP suggest the use a supplemental heat rejecter or supplemental heater, to reject the unbalanced heat from the cooling load or gain heat from the supplemental heater for the heating loads.

In the case of hot environments, a GSHP is incorporated with a supplemental heat rejecter. The GHE will be of reduced depth resulting in reduced capital cost. The conventional system of the supplemental heat rejecter consists of a cooling tower in an open system that is connected with the GHE using a plate heat exchanger. The conventional HGSHP system mainly consists of a heat pump, a GHE, a cooling tower, a plate heat exchanger, and an optional domestic hot water (DHW) production device (the super-heater) (Ping et al., 2015).

The procedures from ASHRAE manual (ASHRAE, 1996) inform the public about the advantages of using a HGSHP system in a warm environmental area

considering the capital costs and the area limitations. Many studies have been performed for rating the optimal operation control, for simulation of system operating performance and the experimental investigation on the HGSHP systems. For instance, Gilbreath (1996) presented a study on HGSHP systems giving design guidelines for hybrid systems. Furthermore, Kavanaugh and Rafferty (1997) suggested the use of a cooling tower heat rejecter sized according to the peak block loads.

The impact of a cooling tower and the design methods were studied and presented by Kavanaugh (1998). The author suggested that the GSHP system be designed for the heating mode (lengthwise). In addition, he suggested that a cooling tower be incorporated in order to reduce the borehole length needed for the cooling mode. The revised method proposed for the design procedure of a HGSHP system included a method to calculate the required cooler operating hours to balance ground-loop energy flow; subsequently the heat loads were balanced throughout the year.

Yavuzturk and Spitler (2000) presented control strategies and a comparative study with various GSHP (among which HGSHP) systems operating. The best control strategy (lowest initial and operational cost), as suggested by the authors, was decided through the determination of the difference between the fluid temperature exiting the heat pump and the outside wet-bulb temperature. A life circle cost analysis conducted gave an advantage to the hybrid systems.

Xu (2007) focused on optimal control strategies comparison for hybrid models using computational models through the HVACSIM+ software and experimental analysis. Three HGSHP system procedures were compared with emphasis given to reducing the cooling tower size and the systems cycle costs.

2.3 Comparative analysis of various geometrical aspects of GHEs

Several studies (with several indicative ones presented below) have been conducted in order to find the best configuration and the most efficient design with given grouting material of a GHE. The coaxial design can be performed with two flow directions; downward flow through the outside tube and upward through the inside

and opposite. In the U-pipe system the diameter and the complexity of the pipes can be utilized for the system to perform best.

A comparative performance between the U-tube and coaxial loop designs was performed by Wood et al. (2012) and the tests were conducted experimentally. The hydraulic performance tests indicated the coaxial design has a lower pressure drop compared to the U-tube design and this can be easily explained with the smaller cross-sectional area of the U-tube loop. The higher velocity of the U-tube can reach transitional to turbulent flow at a lower flow rate. The thermal performance tests have indicated that the heat output of the U-tube system is higher than that of a coaxial design and this is related to the turbulent flow as suggested by the authors. In addition, this significance can be seen in the COP of the two systems, where the U-tube outperforms the coaxial design. It is stated by the authors that the coaxial loop did not provide any increase in the heat output, with the same flow rate as the U-tube design, due to the fact that the flow in the annulus remains laminar.

Desmedt et al. (2012) took in consideration the geometry of the borehole by changing some parameters that affect the performance; change of the flow direction, installing larger diameter tube, single or double U-tube pipe. By changing the flow direction of the coaxial pipe-in-pipe design BHE (downward flow through the inside tube and upward flow through the outside tube) resulted in an 11% reduction (for the specific case under their consideration, of course) in the thermal resistance of the borehole giving a better efficiency to the system. Following on, the coaxial tube diameter was increased and a reduction of 28% on the thermal resistance was achieved. The authors did not discuss nor compared the effect of tube diameter size in relation to the performance or thermal resistance. A comparison between the reference coaxial borehole with a single U-tube and double U-tube borehole configurations was presented. The best geometry design was achieved with the use of the double U-pipe with a reduction of thermal resistance to 52% in comparison to the reference borehole (initial test using single pipe borehole). The second best was the single U-tube, with the coaxial being the last. The single U-tube configuration gave very similar results with the larger diameter tube on the coaxial design.

Zanchini et al. (2010a) computationally tested the effects of flow direction in a small coaxial GHE (20m). The results were obtained using the COMSOL Multiphysics software on a 2D geometry and tetrahedral meshing. The results differ from those obtained by (Desmedt et al., 2012) and the authors showed that the annulus-in flow direction (downward flow through the outside tube and upward flow through the inside tube) is more effective than the centre-in-flow. They observed that the effect of the flow direction is of high importance in winter operation and during the first 6 hours, where an increase of 40% in noticed in the first 5 minutes and 2% after the 6 hours operation (for the case under their consideration).

Lee et al. (2012) suggested a new 3-pipe configuration to eliminate the interference between the inlet and the outlet pipes (see Figure 2.4). The results of the thermal response test (TRT) have shown that the 3-pipe type has an increase in thermal conductivity by 14.1–14.5%, in contrast with the single U-pipe conventional configuration (for the case under their consideration). The authors are outlining the need that not only the enhancement of the grouting materials should be considered but also the thermal interference between the pipes in order to improve the overall performance of the GHE.

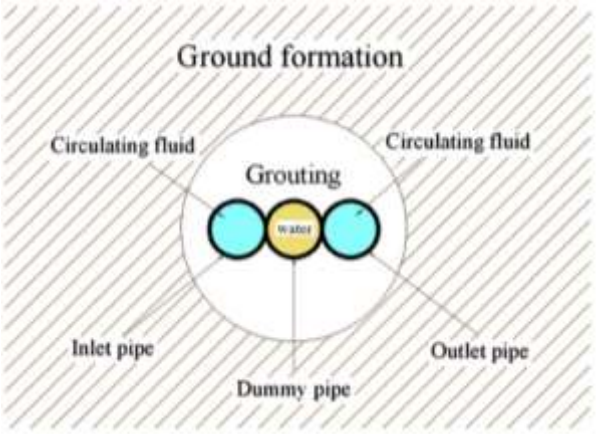

Figure 2.4 Schematic diagram of 3-pipe type (Lee et al., 2012)

Different drill-hole diameters were experimentally tested using the TRT by Luo et al. for three sizes: 121mm, 165mm and 180mm (Luo et al., 2013). The thermal efficiency data comparison was taken during the heating mode system operation and the base model was set to be the drill-hole diameter of 121mm. The results

indicated that with this specific borehole set up a drill-hole diameter of 180mm provides a 6.7% (with a maximum of 10%) increase on an average daily thermal exchange ratio compared to the base model, and the 165mm a 2.16% increase. The authors come to the conclusion that despite the fact that the thermal conductivity of the grout material is smaller than that of the ground, the drill-hole diameter increase will improve the thermal performance of the BHE.

Florides et al. (2013) tested computationally the centre-to-centre distances for both the vertical and horizontal GHE and compared their efficiency. It was observed that the centre-to-centre distance affect the mean fluid temperature. The horizontal GHE is subject to an increased performance compared to the vertical BHE where the centre-to-centre distance is higher than that of the vertical BHE. If the centre-to-centre distance is kept the same for both GHE configurations, then the vertical exceeds in performance the horizontal configuration. The authors also indicate that, in practice, increasing the width of the trench on a horizontal BHE can be achieved easily and with a low cost compared to the vertical BHE.

The double U-pipe GHE can be placed in a single borehole (seen in Figure 2.5 below) and can be divided into two arrangements; parallel connection and series connection. Florides et al. (2013) studied these configurations computationally using the FlexPDE software. In the connection, the fluid exiting one pipe reenters another pipe before entering the heat exchanger, where in the parallel connection the fluid is simultaneously entering two pipes and exits from the remaining two before entering the heat exchanger. The results for the parameters used indicated that both configurations of the double U-pipe GHE have an increased efficiency compared to the single U-tube GHE, with 26% more heat absorbed in the parallel connection and 59% in the series connection (for the case study under their consideration). In addition, the authors performed a cost analysis in order to demonstrate if the additional cost for the improved efficiency is a feasible solution. The conclusions from the costs analysis indicate that an additional cost of 22–29% for the double U-pipe connection is worth spending and balanced out with an increased efficiency of 26–29% in parallel connection and 42–59% in series connection.

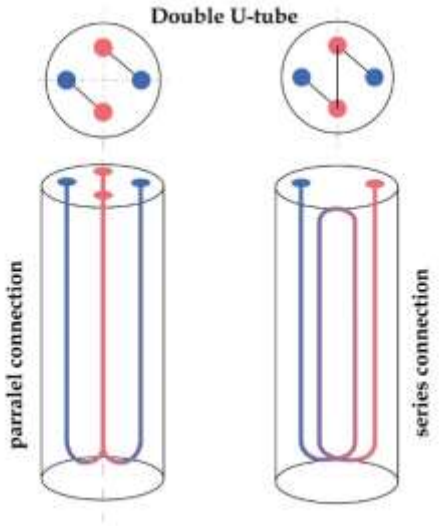

Figure 2.5 Top view of a double U-tube GHE in a single borehole

The diameter of the coaxial pipes was also computationally tested by Zanchini et al. (2010b) using COMSOL Multiphysics software package. They showed that the water flow rate and the inner tube diameter have a significant impact on the effect on the long coaxial borehole heat exchanger. As the water flow rate increases, the obtained energy gain increases and is larger during the summer period than in winter. According to the authors this is due to the fact that the water flow rate turns turbulent during the specific conditions. A combined optimization is suggested, with regard to the water flow rate for the thermal energy gain and the electric energy consumption. An increase in thermal efficiency is proposed with an increase in the inner circular tube diameter while the outer annular tube remains constant. An increase of 5% (for the case under consideration in (Zanchini et al., 2010b)) is observed by following the suggested design during winter operation but it is lower during summer operations. This can be explained that by reducing the mean tube diameter, a reduction in the Reynolds number is also achieved.

In another study, Congedo et al. (2012) compared computationally three different geometry configurations in a horizontal axis type GHE. The three configurations included the linear single tube, the helical type and the slinky type configurations. The working conditions of both summer and winter were taken into account, while the variables were the heat exchanger depth, the fluid velocity and the thermal conductivity of the ground. The variable with the highest impact on performance

was the ground thermal conductivity; higher ground thermal conductivity gave the optimal performance. The helical geometry configuration was also the one to perform best but with higher installation cost. The authors also concluded that the depth (varied between 1.5m and 2.5m) did not significantly improve the performance of the horizontal GHE.

More recently, in an experimental study, Sicasakthivel et al. (2017) compared the thermal performance of a single and a double U-tube GHE. Results indicated that the double U-tube GHE provides higher average performance in the range of 26% during the heating mode and 30% during the cooling mode. Furthermore, observations by the authors stated that in the short-term operation of the systems, the thermal potential for heat transfer of the double U-tube is higher. This is due to the fact that the double U-tube GHE has a larger heat transfer surface area for heat exchanging.

Three different GHE types (U-shaped, W-shaped and spiral-shaped) in foundations piles were compared using transient solutions by Zhao et al. (2016). The average external thermal resistance and the pile average temperature were almost the same in all cases (different design types). The best thermal performance, as described by the authors, was provided by the spiral shape due to the longer pipe and the geometrical arrangement form.

Another evaluation was performed by Kim al. (2016) to determine the thermal performance of horizontal GHEs. Horizontal slinky type and spiral coil type were tested using TRT and the results showed that the best performance was provided by the slinky type. Furthermore, the authors conducted a numerical analysis and a parametric study to determine the parameters affecting the performance of a horizontal GHE, and noted that the pipe diameter did not affect the GHE performance, while the design type and the ground thermal conductivity were the main factors.

Different horizontal GHE layouts and materials were investigated using numerical modelling by Selamat et al. (2016). Six different configurations, orientation and pipe material were explored, namely straight, slinky, horizontal, vertical and inverted vertical orientation, HPDE, copper and composite pipe material. Based on the results, the authors commented that the additional length of pipe in the slinky

configurations were compensated since the effective period was extended. Additionally, the vertical orientation provided 14% longer effective heat exchange rate compared to the horizontal orientation.

2.4 Geothermal Investigation and Materials

Boreholes consist of the buried pipes, the refrigerant fluid and the backfilled material. The ground thermal conductivity has a fixed value and can only be changed by changing the location of the borehole, but the borehole resistance is a function of the grouting material and the installation set-up. In order to increase the efficiency of a BHE the heat exchange between the refrigerant and the ground needs to be enhanced. The characteristics of the backfill grout material are an important factor for the performance of the BHE. High Density Polyethylene (HDPE) is the most commonly used material for the pipes.

The most common model for experimental investigation and testing is the TRT (see Section 2.5), for determining the thermal ground properties. It is a usual procedure for the experimental setup to conduct several TRTs and determine the average thermal conductivity of the ground (Georgios Florides et al., 2013). The line-source model (see Section 2.5) on the other hand is a common analytical model (see for instance Signorelli et al. (2007)) that constitutes a reliable fast tool (analysis under ideal condition) for evaluating the thermal response data.

It is also accepted that the soil particle size is an important factor for evaluating the thermal performance since the smaller the particles the better performance they have to retaining heat. The soil is categorized by its size to the following types: clay, gravel, peat, sand and silt (Birsen, 2010).

Kara et al. (2007) followed a Spilker el al. (1998) suggestion, that by using low thermally conductive material as a backfill, a longer borehole will be needed. They came to the conclusion that (for the parameters used) by using a standard bentonite grout, instead of sand, the overall length is increased by 49% for the same heat extraction rate. In addition, the use of standard bentonite grout, instead of thermally improved bentonite grout, increases the loop length by 24%, and the thermally improved bentonite grout increases the loop length by 10% compared to using sand.

A double U-pipe GHE was introduced and a TRT was carried out by Pahud et al. (2001) for six different boreholes. The different materials used for the borehole backfilling were standard mixture of bentonite and cement, addition of quartz sand and only quartz sand. The results showed that the lowest borehole thermal resistance was provided by the mixture of quartz sand with spacers. The spacers are used to prevent the interference between the polyethylene pipes and ensure a distance from the borehole wall.

Using the analytical line source model, Jun et al. (2009) proposed that the thermal conductivity of the grout mix should be kept higher than the ground thermal conductivity in the absence of groundwater flow. These were the conclusions that came upon analysing the effect of the thermal conductivity of grout mix on both the thermal resistance and the heat exchange rate. The authors determined that by increasing the thermal conductivity of the grout, the thermal resistance decreases while the heat exchange rate increases.

Different grouting materials and soil properties (thermal conductivity) affect the performance of the BHE. Effects of different grouting materials were investigated by Desmedt et al. (2012), using a coaxial BHE filled with low thermal conductivity grouting material (cement and bentonite mixture). In this specific experiment the tests conducted for different borehole materials were as follows: use a mixture of drilling rests as grouting material, adding sand to the cement-bentonite mixture, replacing the outside tube of the coaxial type from polyethylene (PE) to galvanized steel and using of thermally enhanced grouts (TEGs). The best configuration with the lowest borehole resistance was noticed in the replacement of the outside coaxial tube from polyethylene with galvanized steel, which is not as durable, has a higher cost and is subject to corrosion and shorter life span. The resulting borehole resistance dropped by 35%, from the reference borehole (for the case study under their consideration). This is so due to the low thermal resistance of the material. The next to best configuration was noticed with the use of a mixture of drilling rests as grouting material, with a reduction of borehole resistance of 34%. The high thermal conductivity of the sand in the drilling rests led to higher thermal conductivity of the mixture. Similar results were obtained when sand was added to the standard cement-bentonite mixture, with a 28% reduction of borehole resistance. Lastly the

use of TEGs did not significantly improve the performance, compared to the sand addition (which is a low-cost grouting material) to the standard mixture.

Another research by Bernier and Eslami-nejad (2013) attempted to reduce the length of the borehole ground heat exchanger in cooling-dominated climates. The proposal of the project was to use single U-tube borehole surrounded by a ring made of thermally enhanced phase material (PCM) mixed with sand. During the cooling mode, the PCM-sand ring is allowed to melt to take advantage of the relatively high energy content. The numerical results showed that the use of the PCM-sand ring reduced the length of the borehole by 7.3% (in this particular case) and with the use of 3.4cm thickness of ring. The reduction in the borehole length resulted in an increase of the heat pump energy consumption by 2%. By increasing the ring thickness to 4.1cm, so that melting does not go beyond the ring radius at peak conditions, the reduction of the borehole length can be reduced by 9.3%, with an increase in heat pump energy consumption by 2.7%.

A different approach was followed by Borinaga-Trevino et al. (2013b) where the authors analysed the use of natural and recycled materials as an alternative to the borehole backfilling materials. The experiments were performed in a lab and a sample was tested. Only cement based grouting materials were tested as bentonite-based grouts do not fulfil the minimum strength requirements. The mortars were made of water, cement, super plasticizer and different types of aggregates. The aggregates were silica, limestone, electric arc furnace slag and construction and demolition waste. The results showed that the four aggregates gave an improvement of the thermal conductivity over the pure cement material with the silica providing the highest thermal conductivity and the construction and demolition waste the lowest. In addition, a computational modelling was employed in order to examine the thermal resistance and the total borehole length. The silica sand aggregate provided an 18% reduction of the total borehole length, with limestone following at 16%, electric arc furnace slag at 12% and construction and demolition waste at 9% (for the case study under their consideration).

The results from (Borinaga-Treviño et al., 2013b) were applied to a realistic situation and with the use of the thermal response and the thermal resistance of the borehole, four different grouting materials were studied by Borinaga-Treviño et al.

(2013a). The four grouting materials consisted of cement-bentonite-graphite mix, and 3 different cement-based mortars, containing blast oxygen furnace slag, silica sand, and construction and demolition waste. The best grouting material was found to be the 40% solid cement-bentonite-graphite mix. In addition, the higher thermal conductivity of the cement-based grouting materials did not contribute in an improved contact resistance between the pipes and the grout. In addition, the authors were sceptical about the cement-based grouting materials injection process as it could result in a segregation issue.

Different grouting materials were also tested experimentally (through TRT) by Chulho et al. (2011) for the effective thermal conductivity in a closed-loop vertical GHE. Six boreholes with different construction conditions (grouting materials and additives; silica sand and graphite) were constructed and analysed. The results obtained were that the boreholes with the cement grouting material provide better thermal conductivities in comparison with the bentonite grouting material (7.4–10.1%). Also the boreholes grouted with silica sand and graphite provide higher thermal conductivity than the ones with grout silica sand only. The results were further analysed by Lee et al. (2012) yielding the same conclusions. Cost analyses have shown that the use of cement grouting material as opposed to bentonite reduce the construction cost by 40% (for the case study under their consideration). The configuration of the new proposed 3-pipe type (see Section 2.3) with the addition of graphite and silica sand to the cement grout has the lowest construction cost and thermally outperforms the other types.

The experimental test of different grouting materials in (Chulho et al., 2011) verifies the laboratory experimental results by Lee et al. (2010) who investigated the thermal conductivity and viscosity of seven bentonite grouts from different product sources for BHEs backfilling materials. The results indicated that the addition of silica sand in the bentonite ground does not significantly increase the thermal conductivity, even in the case of 60% silica sand. In contrast, the addition of graphite power can enhance the thermal conductivity with the addition of 20% of graphite resulting the thermal conductivity of the bentonite grout close to the geological formation. In addition, it was noticed that the bentonite grout's viscosity increases with time, especially in the case of bentonite produced for civil

engineering constructions with graphite additives. The authors recommended that there should not be any significant delay in the ground pumping operation after preparing the grout paste in the field.

Delaleux et al. (2012) tested different kinds of graphite particles as an enhancement to the conventional bentonite mixture; graphite flakes, expanded natural graphite (ENG) and composites made of raw expanded natural graphite (CENG). The highest thermal conductivity was observed using the larger particles (KS300 from Timcal) and this can be explained through the fact that the larger particles tend to form an interconnected thermal network more easily. The use of CENG with density of 100 kg m^{-3} gave the best results with the minimum percentage of graphite content (5%) compared to the results obtained from KS300 and the literature.

Delaleux et al. (2012) followed and extended the results from Jobmann et al. (Jobmann and Buntebarth, 2009) that at 15% graphite content, the thermal conductivity increases linearly with the water content, and with similar trends in both materials (bentonite + graphite, bentonite + CENG). The authors advice that this effect be taken into account in dry seasons to avoid a decrease in borehole performance.

Three-pipe materials in a long coaxial BHE were computationally investigated using COMSOL Multiphysics by Zanchini et al. (2010b) during both winter and summer operation. The different materials for the inner tube are the high-density polyethylene PE100, polypropylene random copolymer PPR80, an ideal material with a varnishing conductivity, and AISI304 steel for the outer tube. With an internal tube of PPR80 the effect of thermal short-circuiting is reduced considerably. With reference to a time interval of 5 days, the reduction obtained is: 24–25% for winter operation, about 30% for summer operation in a grout with thermal conductivity of $\lambda = 1$ W m^{-1} K^{-1}, and 40% for summer operation in a grout with thermal conductivity of $\lambda = 2$ W m^{-1} K^{-1}. An inner tube of PPR80 is recommended by the authors.

More recently, laboratory experiments and numerical investigation was performed by Daehoon et al. (2017) in order to determine the thermal properties of cement-based grouts. The authors experimented with nine different mix portions, involving

different water to cement ratio, silica sand to cement ratio, as well as dried and saturated conditions. The results showed that under saturated conditions, the thermal conductivity of the cement-base ground increases, as the silica sand to cement ration increased and the water to cement ratio decreased. In terms of the specific heat capacity of the cement-based grouts, the results revealed an increase, where the water to cement ratio was increased and the silica sand to cement ratio was decreased. Lastly, as noted by the authors, the overall performance of the GHE did not depend only on the thermal conductivity of the grout but also on the high specific heat capacity.

Another important factor concerning the ground thermal properties is the ground temperature recovery time, as outlined by Baek et al. (2017). A new transient approach based on the implicit finite difference method (FDM) was developed by the authors. The results showed that ground with low thermal conductivity required more time to recover with high thermal conductivity ground. A suggestion, following their findings, indicate that a height reduction of the GHE could be achieved by considering the ground temperature recovery time.

Finally, Christodoulides et al. (2016) presented a practical way of estimating the thermal ground properties, namely the ground thermal conductivity, the thermal diffusivity and the volumetric heat capacity in a reliable manner, for sizing GHEs.

2.5 Modelling GHE systems

2.5.1 Borehole Thermal Resistance and Thermal Response Test

The length of the GHE is major in the initial cost of the system and its performance. Overestimating a GHE system and Thermal Response Test will result in a higher cost for the system, whereas underestimating will result in limited performance. Many procedures have been introduced through the years for designing a GHE. In all of these, the length of the borehole is calculated by specifying maximum and minimum fluid temperatures (Lamarche et al., 2010). These temperatures depend upon the Borehole Thermal resistance (R_b), with their relation being given by the following equation (Lamarche et al., 2010):

$$T_f - T_b = R_b \dot{q} \qquad 2.1$$

where T_f is the mean fluid temperature (averaging the two borehole legs temperatures) [K], T_b is the temperature at the borehole wall and $\dot{q}$ is the heat transfer rate per unit length [W m^{-1}].

Marcotte and Pasquier (2008) state that the use of the mean fluid temperature (T_f) does not represent all the cases but only the cases where a constant heat flux is assumed. When the approximate mean fluid temperature is fitted into the line-source model (introduced in Section 2.5.2) the borehole resistance is overestimated resulting in a higher manufacturing cost. Instead the authors are suggesting the use of the p-linear average, with $p \rightarrow -1$, for estimating the mean fluid temperature. The *p*-linear average is based on Incropera and Dewitt's (1985) logarithmic mean temperature between the entering and leaving water as the mean temperature. This method assumes a constant temperature at the borehole wall, which is still not a realistic case as the temperature varies.

Following Marcotte and Pasquier's p-linear method, Zhang et al. (2014) developed the $p(t)$–linear average method, for estimating the ground thermal properties of the GHE. The authors that the previous p-linear method did not take into account that when the undisturbed soil temperature is used as the reference temperature, the water temperature profile derived by the p-linear average model will vary with time. The newly developed $p(t)$ – linear average proves to be an effective approach with less than 5% relative error, when $p = 1$. This method can be used to accurately estimate the borehole thermal resistance.

For designing a GHE the two most important parameters are (as already mentioned) the soil thermal conductivity as well as the borehole thermal resistance. The borehole thermal resistance depends upon borehole diameter, pipe size and configuration (see Section 2.3), pipe material and the backfill material (see Section 2.4) (Zhang et al., 2014). It is specified that for high soil thermal conductivity and a low borehole thermal resistance, the heat exchange rate will be higher for a given borehole (Zhang et al., 2014). Therefore, it is of high importance to determine the thermal characteristics of the ground prior to the system design. For larger installations borehole tests are carried out in a test borehole.

There are several methods developed to determine ground thermal characteristics (Zhang et al., 2014); soil and rock identification (Bose, 1989), experimental testing of drill cuttings (Sass et al., 1971), in situ probes (Choudhary, 1976), and inverse heat conduction models. However, the most commonly used is the thermal response test. The Thermal Response Test (TRT) is a method to determine the ground thermal characteristics and it was first introduced by Mogensen in (1983). The initial system used a chilled carrier fluid, and in later stages the chiller was replaced by a heater. TRT suggests heat injection in the borehole at constant power whereas the mean borehole temperature is defined on output. The recorded fluid temperature response is the temperature developed over time, which is evaluated to obtain the thermal characteristics of the borehole such as the thermal resistance, the volumetric specific heat capacity, and the soil conductivity by using inverse heat transfer analysis (Gehlin, 2002).

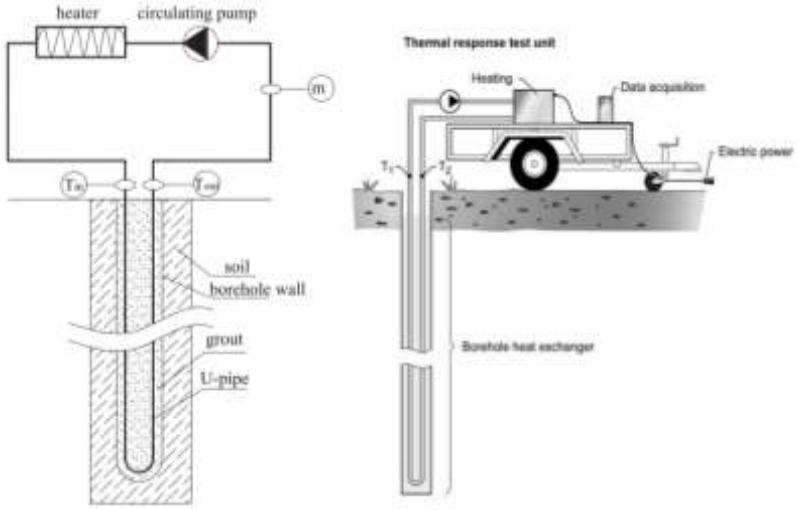

Figure 2.6 Thermal Response Test set-up, left: U-pipe borehole set-up (Zhang et al., 2014), right: mobile test-rig (Gehlin, 2002)

The TRT duration has undergone different recommendations in the literature. The recommendations start with a minimum of 12–40 hours (Smith and Perry, 1999), go to 36–48 hours in the ASHRAE handbook (2007), then to 48 hours with data to be collected for a minimum of 10 minutes' steps (Yu et al., 2004), to 50 hours (Austin and Yavuzturk, 2000) and finally to 60 hours (Gehlin and Hellstrom, 2000). The longer the TRT duration is the more expensive it will be, but the shorter durations could underestimate the thermal conductivity, leading to incorrect design

estimations of GHEs, and/or overestimate the borehole length with increased initial and running cost.

Through the advancement of the technology, TRT equipment has reduced its size in order to develop mobile test rigs units (see Figure 2.6) (Gehlin, 2002). Guidelines are provided for the site and test equipment by the International Ground Source Heat Pump Association with the latest standards in designing and installing a GSHP systems (IGSHPA, 2013).

In addition to a great many TRT applications (Bose, 1989; Choudhary, 1976; Mogensen, 1983; Sass et al., 1971; C. Zhang et al., 2014), an indicative study is Javed and Fahlen's (Javed et al., 2011) who performed TRTs for nine different boreholes. The authors have compared two methods for determining the undistributed ground temperature, with the start-up exit fluid temperature approach providing more accurate results in comparison with the fluid circulation approach. Gehlin and Nordell (2003) estimated temperatures in a groundwater-filled borehole in three different ways: (i) temperature logging with sensors placed along the borehole, (ii) temperature of a circulating fluid measurements (TRT) per 10 seconds, (iii) flow temperature calculation after a period of circulations. The authors assumed that the temperature logging method provided the correct undistributed ground temperature profile. For the specific case they concluded that 20 minutes of circulation is the limit for determining the ground temperature accurately.

TRT can also be characterized as 'enhanced', as suggested by Sanner et al. (2008), when supplementary information is provided in the results, as for instance the thermal conductivity distribution along the GHE and the accuracy of the sensors (thermocouples). Such studies can be seen, for instance, in (Luo et al., 2015b) and (Bozzoli et al., 2011).

Another TRT technique was proposed by Acuna (2010) and is referred to as the Distributed TRT (DTRT). In this method the thermal conductivity is measured along the borehole at multiple depths, achieved by placing a fiber optic cable in the borehole to measure temperature and hence thermal conductivity at every length step. Another variation of the DTRT was firstly introduced by Raymond et al. (2010) and subsequently furthered varied by Mazyar and Mogaddam (2015), where instead of the use of a pump, heating cables attached with the fiber cable are

submerged into the borehole to monitor temperature. The DTRT method with the use of heat cables allows for the calculation of heating power by controlling the current and the voltage supplied to the cable. Other DTRT studies include (Beier, 2014), (Lanini et al., 2014) and (Ruiz-Calvo et al., 2015).

2.5.2 Analytical and numerical models

There are several models that have been developed throughout the years to implement fast and reliable predictions of GHE. There are analytical and numerical models. All the models are based on the Fourier's law of heat conduction (Florides and Kalogirou, 2007).

The GHE modelling approaches can be divided in two categories as reviewed by Javed et al. (2009); calculating borehole length by predicting the long-term performance of the GHE (conventional models), and the short-term models. The main difference is that the long-term models use steady-state solutions or long-time steps in a transient solution for the calculating heat transfer in the GHE, whereas the short-term models use hourly time-step variants or less in a transient solution. The models can also be categorized with regard to the type of the 'source' heat (infinite or finite, linear or not) and are the each appropriate to use depending on the nature of the problem under investigation.

2.5.2.1 Infinite-length line-source method

The classical line-source theory (infinite line-source method) was developed by Kelvin (Kelvin, 1882), while later Ingersoll L. et al. (1950, 1955) applied it to model radial heat transfer. Based on this model one assumes that the GHE is a line and a constant heat output is achieved, where the GHE has an infinite length and is surrounded by an infinite homogeneous medium. Then the solution of heat conduction is as follows:

$$T_b - T_0 = -\frac{\dot{q}}{4\pi\lambda}\,\mathrm{Ei}\left(-\frac{r_b^2}{4\alpha t}\right) \equiv \frac{\dot{q}}{4\pi\lambda}\int_{r_b^2/(4\alpha t)}^{\infty}\frac{e^{-u}}{u}\,du \qquad 2.2$$

where Ei(.) is the exponential integral, $\dot{q}$ is the constant heat injection rate [W m^{-1}], T_b is the temperature at $r = r_b$, T_0 is the undistributed ground temperature or the initial borehole temperature, r_b is the borehole radius [m], t is time [s], λ is the

borehole thermal conductivity [W m^{-1} K^{-1}], and $\alpha = \lambda/(\rho c_p)$ is the ground thermal diffusivity [m^2 s^{-1}], ρ being the density [kg m^{-3}] and c_p the specific heat capacity [J kg^{-1} K^{-1}]. When the effect of the borehole thermal resistance (see Equation 2.1) is taken into account, Equation 2.2 can be approximated into (Christodoulides et al., 2016; Monzo, 2011):

$$T_b - T_0 \approx \frac{\dot{q}}{4\pi\lambda}\left[ln\left(\frac{4\alpha t}{r_b^2}\right) - \gamma + 4\pi\lambda R_b + \frac{r_b^2}{2\alpha t}\left(ln\left(\frac{4\alpha t}{r_b^2}\right) - \gamma + 1 - \frac{\alpha m c_p}{\pi r^2 \lambda L}\left(ln\left(\frac{4\alpha t}{r_b^2}\right) - \gamma + 4\pi\lambda R_b\right)\right)\right] + O\left(\frac{r_b^2}{\alpha t}\right)^2 \quad 2.3$$

where m is mass of the borehole [kg], L its length [m] and γ = 0.57722 is the so-called Euler's constant.

Ingersoll and Plass (1948) have recommended using the infinite line-source model for applications with Fourier number larger than 20. With this suggestion a distorted solution at smaller time steps is avoided (Javed et al., 2009). In addition, the classical line-source theory does not take into account the end effects of the heat source as infinite length is assumed. Hart and Couvillion (1986) have developed a method based on the infinite line-source model with improved accuracy compared to the first approach.

2.5.2.2 Cylindrical heat source method

The cylindrical source method is another approach for the analytical modelling of heat transfer in GHE. It has similar assumptions as the infinite line-source method where the cylinder is surrounded by an infinite homogeneous medium (as firstly suggested by Carslaw and Jaeger (1959)). The cylinder represents the outer surface of the borehole and constant heat flux is assumed. A modification of the cylindrical model came from Ingersoll et al. (1954) to size buried heat exchangers, and it was later on re-modified by Kavanaugh (1985) for the determination of the temperature distribution or the heat transfer rate around a buried pipe. Later contributions came from Hellstrom (1991) and Bernier (2001). The modified model by Kavanaugh has been included in the ASHRAE (American Society of Heating, Refrigerating and Air-Conditioning Engineers) guidelines (ASHRAE, 2007).

The general solution (Hellstrom, 1991; Man et al., 2010) is given (as a function of radial coordinate r[m]) by

$$T_b - T_0 = \frac{\dot{q}}{\pi^2 \lambda r_b} \int_0^\infty \left(e^{-\alpha u^2 t} - 1\right) \frac{[J_0(ru)Y_1(r_b u) - J_1(r_b u)Y_0(ru)]}{u^2[J_1^2(r_b u) + Y_1^2(r_b u)]} du \qquad 2.4$$

where J_0, Y_0, J_1, Y_1 are Bessel functions of the first and second kind, namely (for $i = 1, 2$)

$$J_i(u) = \sum_{k=0}^{\infty} \frac{(-1)^k}{k!\Gamma(k+i+1)} \left(\frac{u}{2}\right)^{2k+i}, \; Y_i(u) = \frac{J_i(u)\cos(i\pi) - J_{-i}(u)}{\sin(i\pi)}, \; \Gamma(n) = (n-1)!$$

Under certain circumstances Equation 2.4 can be approximated to a form analogous to Equation 2.3 containing R_b (see for instance (Monzo, 2011)).

2.5.2.3 Finite-length line-source method

Apart from the infinite line-source model there is also, as mentioned earlier, a finite-length line-source model. Eskilson (1987) and Claesson and Eskilson (1988) were the first to develop an analytical g-function expression, where the solution is determined using a line source with finite length (Javed et al., 2009). The authors assumed a constant temperature of T_f and evaluated the given temperature at the middle of the borehole (Lamarche and Beauchamp, 2007a). The general solution is given (as a function of radial coordinate r[m] and axial coordinate z[m]) by

$$\mathrm{T_b} - \mathrm{T_0} \approx \frac{\dot{\mathrm{q}}}{4\pi\lambda} \int_0^{\mathrm{L}} \left(\frac{\mathrm{erfc}\left(\sqrt{\mathrm{r}^2 + (\mathrm{L}/2 - \mathrm{u})^2}/\sqrt{4\alpha \mathrm{t}}\right)}{\sqrt{\mathrm{r}^2 + (\mathrm{L}/2 - \mathrm{u})^2}} - \frac{\mathrm{erfc}\left(\sqrt{\mathrm{r}^2 + (\mathrm{L}/2 + \mathrm{u})^2}/\sqrt{4\alpha \mathrm{t}}\right)}{\sqrt{\mathrm{r}^2 + (\mathrm{L}/2 + \mathrm{u})^2}} \right) \mathrm{du} \qquad 2.5$$

where erfc(.) is the complementary error function, defined as

$$\mathrm{erfc}(u) = \frac{2}{\sqrt{\pi}} \int_u^\infty e^{-\tau^2} d\tau$$

Later on Zeng et al. (2002) proposed a modification of the model above as they observed that the temperature at the middle of the borehole overestimates the reference temperature. The specific modification, as stated by Lamarche and Beauchamp (2007a), is difficult to use for practical applications and the difference from Claesson and Eskilson (1988) solution is not so important. Hence, Lamarche

and Beauchamp (2007a) introduced an approach that adapts Zeng et al.'s (2002) solution using the mean temperature in the evaluation of the analytical g-function in a way that is faster than Claesson and Eskilson solution, with results comparing well with the numerical values available in the literature (Eskilson, 1987).

2.5.2.4 Models Comparison

A comparison between the infinite line-source and the cylindrical-source models was performed by Yu et al. (2013). The two models were validated with experimental results through Bland-Altman analysis for comparison between the experimental and the simulated data. The results showed that the time required to achieve a quasi-steady state in the ground is a function of the heat load. The authors suggested that the test duration of the TRT should be extended as the heat load increases. The authors also observed that the values of thermal conductivity estimated with the line-source model are slightly lower than that of the cylinder-source model and was noted that the greater the heat load is, the higher the values of thermal conductivity estimated by the line source model and cylinder source model are.

Jun et al. (2009) performed a comparison of the ILST (infinite line source theory) and CST (cylindrical source theory) against experimental data. The authors observed a relative error of 10.2–15.5% (for a certain case study) between the theoretical and experimental results, speculating that the difference was due to the vapor migration and groundwater advection in the soil. It was thus suggested that both theoretical models can be used where the groundwater flow and the moisture transfer in the soil are weak.

Yang et al. (2010) noted that both the one-dimensional model using Kelvin's theory (infinite line-source model) and the cylindrical-source model developed by Kavanaugh neglect the axial heat flow along the borehole depth. Therefore, they can be inadequate for analysing the long-term operation of the GHE/GSHP systems. Lamarche and Beauchamp (2007a) also compared the G-function of the cylindrical-source model and the line-source model. Their results showed that both solutions are similar and that neither solution reaches a steady state value. This is due to the

logarithmic behaviour of the solution at infinity and therefore is not the appropriate physical model for a large time value.

Spitler el al. (2009) performed a comparison of GHE design programs using the ILST and CST models. The authors observed that there are differences between the model assumptions and the experiments with regard to the uniform undisturbed ground temperature, the lack of groundwater flow, the lack of moisture transport in the upper unsaturated regions of the ground, and the uniform heat transfer along the length of the borehole.

Beier et al. (2014) proposed an analytical model for coaxial BHEs. The authors compared the proposed model with the ILST model, the composite model proposed by Beier and Smith (2003) and experimental data. In both models, it was observed that the use of the mean temperature (between the inlet and the outlet pipes of the system) approximation overestimates the borehole resistance.

Following an extended literature review, one can inspect a lack of sufficient direct comparisons among theoretical models and experimental data, constituting a task for researchers for future investigation.

2.5.2.5 Spiral coil models and Energy piles

Through the years not many analytical models have been developed for the spiral pipe configuration. The widely used model in recent years was the cylindrical-source model. This model as described in a previous section, when applied with a spiral configuration it does not take into consideration the heat capacity of the spiral coil, as it considers heat flux directly on the cylinder surface (borehole wall). Man et al. (2010) referred to this model as a “hollow” cylindrical-source model and the authors introduced a new “solid” cylindrical-source model (seen in Figure 2.7).

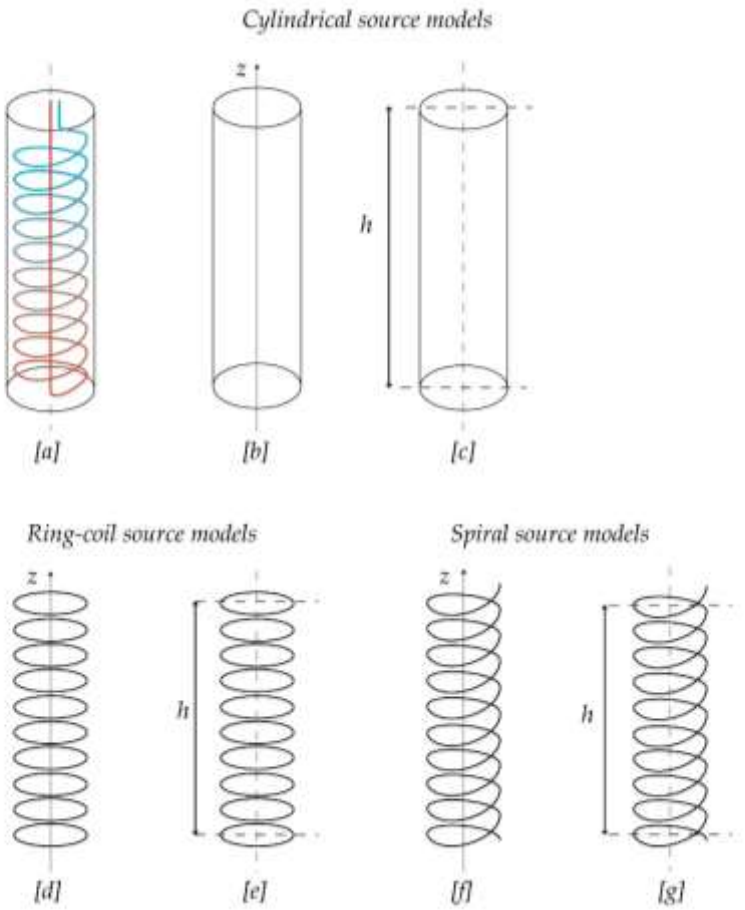

Figure 2.7 Established models of the GHE pile. (a) GHE pile with spiral coil, (b) infinite cylindrical source model (solid), (c) finite cylindrical source model of length h (solid), (d) infinite ring-coil source model, (e) finite ring-coil source model of length

In the proposed method, the radial dimension and the heat capacity of the borehole or pile are taken into consideration. Furthermore, the cylinder (borehole) is proposed to be filled with the medium identical to that out of the borehole and the infinite domain is composed of a homogeneous medium. The spiral coil is not taken into account as a spiral, but it is simplified as a continuous cylindrical heat source, therefore the suggested model fails to distinguish the effect of the spiral pitches (Man et al., 2011).

Another model was developed by Cui et al. (2011) referred to as the "ring-coil source model" to overcome the issues presented in the first model by Man et al. (2010). The new proposed model takes into consideration the discontinuity of the heat source and the spiral pitches. It is based on the basis of the cylindrical model

and it considers the spiral coils as separated rings (Figure 2.7). This simplification, although an improvement on the earlier solid cylindrical model, still fails to meet the realistic conditions of the spiral pipe.

Further developments of the spiral models came from Man et al. (2011), where the proposed model referred to as "spiral heat source model" is based on the pre-mentioned ring-coil source model. In the described model (Figure 2.7) the coil is simplified into a spiral line heat source with pitch "b" and emits heat at intensity $q_l b$ for each pitch section (q_l is the heating intensity per length). This model is considered only with three-dimensional temperature distribution as it takes into account the asymmetry on the z-axis. The authors have shown that the finite length newly proposed model (spiral heat source) is desirable for thermal analysis of the spiral pile GHE. The authors did not provide any validation over experimental results.

Bezyan et al. (2015) performed heat transfer rate 3D simulations with a spiral coil configuration. The authors validated the U-tube configuration pipe model against experimental data comparing the outlet temperature with acceptable accuracy achieved. Furthermore, the authors compared three different configuration models (U-shaped, W-shaped and spiral-shaped) in terms of outlet temperature reduction. Their results indicated that the spiral-shaped configuration provided the highest efficiency in heat transfer rate and energy output. Additionally, the authors emphasized on the effect of the spiral pitch size to the outlet water temperature reduction.

The effect of the spiral coil pitch was also examined by Park et al. (2015). The authors compared a 500m and a 200m spiral coil pitch with 12.5m and 14m length respectively, using a new terminology of relative heat exchange efficiency introduced in their paper (efficiency pile and efficiency pipe). Their results indicated that the higher the pitch the higher the efficiency of the pipe but the lower the efficiency of the pile. This demonstrates that the pile efficiency is not be directly proportional to the installed pipe length, owing to the thermal interference between the spiral coils.

Furthermore, Park et al. (2015) conducted a comparison between the modified cylindrical source model, the ring-coil source model and experimental results. The

average temperatures of the inlet and outlet fluid were compared, with discontinuous temperature trend observed in the analytical models due to the mathematical convergence limitation due to the large diameter of energy piles. Their results indicated that when the spiral coil pitch was 200mm, both the modified cylindrical source model and the ring soil model are in good agreement with acceptable overestimation of the heat exchange capacity of the piles. These results were expected since the coil is denser and is close to the assumptions made by the cylindrical soil source model. When the pitch increased to 500mm, both analytical models failed to predict the correct temperature compared to the TRT results, with the ring-coil source model having a smaller discrepancy due to the prediction of the coil pitch interval.

2.5.2.6 Other Models

In addition to the models previously described above there are other models that are not so commonly used (Christodoulides et al., 2016).

For example, Lamarche and Beauchamp (2010) reviewed several procedures for sizing the boreholes for GSHP/GHE systems as this parameter can lead to inaccurate calculation of borehole depth or length that can result in the insufficient efficiency and high manufacturing costs. The authors observed and suggested that the best method for calculating the borehole resistance is the multipole method presented by Bennet et al. (1987) that is used in the software Earth Energy Designer (EED) (Hellstrom and Sanner, 1997). The multipole method can also be used for the internal resistance but not in the case where the grout and the soil thermal conductivities are very close.

Jaeger (1944) introduced the instantaneous line-source model for composite media. The strength of this theory is that it can be used to analyse transient heat conduction inside and outside boreholes and it offers the flexibility of being appropriate to model many GHE configurations. In this context, Hellstrom (1991) proposed a line-source model for composite region, as an approximation of the more general multipole method proposed by Bennet et al. (1987).

More recently, Li and Lai (2012) presented a new approach of composite-media line-source model. The model assumed both an infinite line as well as an infinite

composite cylinder (as in the case of the cylindrical model) obtaining temperature distributions around two boreholes and two pile GHEs.

Also, a short-time performance comparison of the composite-medium line-source model was performed by Yang and Li (2014). The authors compared the infinite line-source model, the multipole model and a Finite Volume (FV) numerical model. The results showed that the conventional models (infinite line-source and multipole model) failed to provide accurate results in the short time period (< 100min), but in the long-term time (< 10h) all models provided over-predicting results in relation to laboratory data. The FV method correctly predicted the solution in the shorter period of time (< 4min), where the authors noted that the parameters ignored (heat capacity of fluid and U-tube pipe) by the composite-medium line-source model were only influential in this short period of time. Different parameter inputs were compared with analytical and numerical models with the authors concluding that the difference of the models occurred only in the first 3 min, suggesting that the general minimum threshold of applying the composite-medium model should be 3 min.

Regarding numerical models, these are in general developed to represent the borehole geometry in more details than analytical models. Usually, three methods are implemented to such models in order to solve an energy balance equation (see for example Section 2.6 in the sequel): Finite Difference (FDM), Finite Element (FEM) and Finite Volume (FVM). Such approaches include the studies by Bennet et al. (1987), Hellstrom (1991), Rottmayer et al. (1997), Thornton et al. (1997), Shonder and Beck (1999) who all used FDM in the context of heat transfer models of U-tube GHEs. In the same direction, Bennet et al. (1987), Breger et al. (1996) and Muraya et al. (1996), all used FEM to model such heat transfer models (see also Section 2.6 in the sequel), while Li and Zheng (2009), Yavuzturk (1988) and Yavuzturk and Spitler (1999) constitute FVM applications on vertical GHE modelling.

In summary, the most important or indicative models used can be summarized as follows.

Long-term response with analytical solutions: (a) Infinite-length line-source by Lord Kelvin (1882), Ingersoll and Plass (1948), Hart and Couvillion (1986), (b)

Cylindrical-source by Carslaw and Jaeger (1959), Ingersoll et al. (1955), Kavanaugh (1985), Bernier (2001), (c) Finite- length line-source by Eskilson (1987), Zeng et al. (2002), Lamarche and Beauchamp (2007a).

Long-term response with numerical solutions by Mei and Emerson (1985), Eskilson (1987), a multipole method by Bennet et al. (1987), Hellstrom (1991), Breger et al. (1996), Muraya et al. (1996), Rottmayer et al. (1997), Thornton et al. (1997), Shonder and Beck (1999), Zeng et al. (2003), Li and Zheng (2009).

Short-term response: the Analytical Buried Electrical Cable Analogy by Young (2004), the Analytical Solutions for Composite Media by Li and Lai (2012) and Yang and Li (2014) (see also Hellstrom (1991), Lamarche and Beauchamp (2007b)), the Analytical Virtual Solid Model by Bandyopadhyay et al. (2008), the Implicit Numerical method by Yavuzturk and Yavuzturk, and Spitler (1988; 1999).

2.6 Discussion

In this study, the GHE/GSHP systems have been introduced through a particular analysis on the geometry and all related parameters, the materials used for a GHE and the modelling thereof.

The available options for GHE include the open or closed-loop systems, vertical or horizontal type (depending on the available land area), and finally the pipe network configuration. The configurations as described in Sections 2.2 and 2.3 for the horizontal type consist of the series connection, parallel connection, trench and overlapping loops, while for the vertical type are the U-tube pipe, multiple U-tube pipe, simple coaxial, complex coaxial and the spiral/helix configuration. The advantages and limitations for each system have been discussed, emphasizing more on the more conventional vertical type U-tube pipe GHE.

Additionally, to the conventional configuration types, there is also the spiral coil configuration, which has been given more attention in recent years due to the advantages offered when used with the buildings' foundations (also referred to as energy piles configuration). In specific applications, it is more effective to install a HGSHP system despite its complexity. The HGSHP system requires either a supplemental heat rejecter or a supplemental heater in order to balance the yearly

ground loads and consequently reduce the capital cost for the GHE since the depth will be reduced.

Future development is required to focus on the optimal operation control according to the ambient temperature, building loads and to balance the ground loads. One way to achieve the optimum operation of the systems is using forecasting techniques through Distributed Energy Systems. These are characterized as district load forecasting (DLF) models and a review of such models is presented by Ma et al. (2017). An upright first approach would be to distribute the GHE system into different controlled areas and apply an appropriate DLF model to the required area for the overall balance of the system. Another method was followed by Pu et al. (2017), where a multi-objective genetic algorithm combined with a Kriging response surface method was used to optimize the performance effecting the design parameters of a GSHP system.

The borehole materials have been presented with studies showing that the borehole backfill material (grout) thermal conductivity should be close to the ground thermal conductivity for the best efficiency results. Different materials are used with the most common to be the bentonite, while if thermal enhancement is required, graphite flakes are suggested to be added to the bentonite in order to increase its thermal conductivity. HDPE is the most commonly used material for the pipes and is recommended since it is durable and does not corrode.

Finally, the widely used available models have been presented, with more focus given to the line-source model, the cylindrical-source model and the spiral models. The models themselves can be separated into various sub-categories like, for instance, the long-term response and the short-term, and the finite-source and the infinite-source models.

Then a summary of experimental and/or mathematical models has been provided to the reader, showing a comparison of studies with regard to the design aspects of GHE systems. The important findings with respect to each study are highlighted, and this can lead to very useful conclusions for the engineer.

Further research and development is recommended to follow on the energy pile systems since the technology and the configuration provides high efficiency with

lower capital cost in comparison with a U-tube pipe configuration. The spiral coil configuration requires further attention and should be further used in areas where it can have the above-mentioned advantages. In addition, the groundwater can be used, but the configuration will no longer be acting as a support pile. Also, one needs to stress that the selection of the GSHP system is always dependent upon the available land area and the thermal characteristics of the ground.

Table 2.1 Experimental and mathematical studies of GHE systems

References / Year	*Backfill Material*	*Vertical*				*Varying factors*	*Method and/or Software*			*Comments*
		Single U-tube	**Multiple U-tube**	**Coaxial**	**Spiral**			*Numerical*	*Experimental*	
Daehoon et al. (2017)	cement based	✓				nine different water/cement and silica sand/cement ratios	lab experimental, numerical model	✓	✓	Increasing the s/c ration had greater influence on the thermal conductivity than by decreasing the w/c ratio
Baek et al. (2017)	bentonite	✓				heat extraction recovery time	TRT, new analytical model	✓		Importance of GHE recovery time to reduce borehole length
Sivasakthivel et al. (2017)	cement	✓	✓			thermal performance	TRT		✓	Double u-tube -better average effectiveness in heating and cooling modes
Qiang et al. (2016)	concrete	✓	✓			design type	COMSOL	✓	✓	Spiral best performance in terms of short and long-term thermal loads
Bezyan et al. (2015)	concrete	✓	✓		✓	design type	Gambit, Fluent	✓		spiral is best configuration inside pile
Sangwoo et al. (2015)	concrete				✓	spiral pitch, thermal performance	TRT		✓	heat exchange rate not directly proportional to pipe length

Beier et al. (2014)	not given			✓	new analytical model	new coaxial analytical model	✓	new model gives a more accurate estimate of the borehole thermal resistance
Borinaga-Trevino et al. (2013b)	cement & bentonite base	✓	✓		grout material	TRT	✓	cement-bentonite-graphite mix performs the best
Eslami-nejad and Bernier (2013)	PCM & sand	✓			PCM material	TRT, 1D numerical model	✓	✓	proposed configuration reduce borehole length by up to 9%
Florides et al. (2013)	bentonitic clay		✓		arrangement and connection	FlexPDE	✓	double U-tube superior to single by 26–29% in efficiency for parallel and 42–59% for series configuration
Florides et al. (2013)	bentonitic clay	✓	✓		centre-to-centre distance	FlexPDE	✓	✓	vertical GHE has lower mean temperature than horizontal GHE with same centre-to-centre distances
Luo et al. (2013)	enhanced cement	✓			drill-hole diameters	TRT	✓	thermal exchange rate of BHE increases with drillhole radius
Xiaohui et al. (2013)	medium-coarse sand	✓			ground thermal properties	ILST, ICST, Bland-Altman analysis, TRT	✓	✓	new method could help to properly choose the TRT duration and data interval
Delaleux et al. (2012)	bentonite-graphite				grout materials	thermal analysis, experimental	✓	✓	partial drying of the grouts induces significant decrease in thermal conductivity

	composite & additives								
Desmedt et al. (2012)	cement, bentonite, sand, drilling rests & TEG	✓	✓	✓		thermal conductivity, borehole resistance	TRT, ILST	✓	✓	cement-bentonite mixture gives high thermal borehole resistance; addition of sand leads to better performance
Lee et al. (2012)	cement, bentonite & additives: silica sand & graphite	✓				novel 3-pipe configuration	TRT		✓	cement grout better thermal conductivity than bentonite; graphite better than silica sand as thermal additive
Wood et al. (2012)	steel pile & glycol mixture	✓		✓		two-loop design	TRT		✓	coaxial loop in this form does not outperform U-tube
Chulho et al. (2011)	cement, bentonite & additives	✓				grout materials, novel design	TRT		✓	cement grout higher thermal conductivity than bentonite; graphite better than silica sand as thermal additive
Cui et al. (2011)	concrete				✓	solid CST, ring coil model	new ring coil source model	✓		ring-coil model shows better the heat transfer process of the PGHE with spiral coils
Man et al. (2011)	concrete				✓	new model	spiral heat source model	✓		finite spiral heat source model better than other spiral models

Acuna (2010)	groundwater	✓			ground thermal properties	distributed TRT		✓	suggests placing fiber-optic cable in the borehole to measure temperature
Lee et al. (2010)	bentonite base	✓			grout materials	XRD test, free swell test, viscosity test, volume reduction test		✓	select amount of silica sand and graphite considering not only thermal conductivity but also viscosity
Man et al. (2010)	concrete			✓	'hollow' and 'solid' CST	new 'solid' CST	✓		solid CST models adequate for simulating pile GHEs
Zanchini et al. (2010a)	ground		✓		coaxial design aspects	COMSOL	✓		annulus-in flow is more efficient than centre-in flow
Zanchini et al. (2010b)	custom grout		✓		pipes diameter	COMSOL	✓		performance of CBHE improves with diameter
Jun et al. (2009)	bentonitic clay	✓			design aspects	ILST, CST, TRT	✓	✓	gives guidelines for designing GHEs in GHP systems
Spitler el al. (2009)	bentonite	✓			commercial programs	EnergyPlus, eQuest, HVACSIM+, TRNSYS, EES	✓		Geostar and EnergyPlus predict 20% lower energy consumption than eQuest and GEOEASE II
Hamada et al. (2007)	reinforced concrete	✓	✓		thermal properties	SMASH	✓	✓	COP for heating was as high as 3.9

Kara et al. (2007)	sand	✓		backfill material	TRT	✓	suggests sand as low-cost grout and 1-2m thick surface plug of clay to improve COP
Lamarche and Beauchamp (2007a)	not given	✓		new analytical model	new analytical model	✓	new analytical model provides same values as ILST and is subject to the same constraints
Sekine et al. (2007)	reinforced concrete	✓		thermal properties	TRT	✓	COP for cooling 4.89, and 1.7 times more effective than typical ASHP systems
Laloui et al. (2005)	reinforced concrete	✓		thermo-mechanical loads	TRT, THM finite elements	✓ ✓	numerical model is able to reproduce the most significant thermo-mechanical effects
Gehlin and Nordell (2003)	groundwater	✓		temperature, groundwater borehole	temperature logging, TRT, flow temp method	✓	temperature logging provides the correct temperature of the ground
Pahud amd Matthey (2001)	bentonitic & quartz		✓	backfill material, TRT	TRT	✓	thermal resistance decreased by 30% when quartz sand used instead of bentonite
Pahud et al. (1999)	concrete	✓		thermal properties	TRNSYS, PILESIM	✓	Dock Midfield presents good conditions for optimal use of heat exchanger piles

Morino and Oka (1994)	steel pile, concrete & groundwater	✓		temperature and heat exchanged with the soil	TRT, 3D finite differences	✓	✓	calculation method could predict variations in the water temperature and the quantity of heat exchanged with the soil

Chapter 3*

3 Economic Evaluation of GSHP systems

Summary: The recent evolution of the Ground Source Heat Pumps (GSHPs) has initiated the debate whether it is economically feasible to install a GSHP as an alternative to an Air Source Heat Pump (ASHP). A typical house heating/cooling load for moderate climates is presented and discussed in this chapter for comparison purposes.

For this purpose, the thermal response of the Ground Heat Exchanger (GHE) and the estimated characteristics of the GSHP, based on existing experimental data and simulations in summer and winter through a CFD model are presented. The computed power rejected to the ground from the GSHP is discussed in relation to the HP characteristics at different operating temperatures, which affect the efficiency. More than one borehole for the GHE may be needed for the reduction of the temperature.

Finally, a cost analysis is presented for different length GSHP systems and a comparison of the total energy savings is obtained. ASHP systems with the specifically designed, inverter technology ducted series HP are proven to be highly competitive with GSHP systems, which fail to be a clear viable investment for energy saving.

3.1 Overview

The GHEs, compared to air-to-air heat exchanger systems, exhibit significantly higher performance (Yu et al., 2013), but are still not widely used due to their higher installation cost and their requiring of larger spaces. Hence, recent research has focused on the reduction of the cost along with the further advancement of the overall efficiency (Aresti et al., 2018). Large GSHP projects have since demonstrated significant advantages with regard to energy efficiency, CO2 emissions and may be economically beneficial over conventional heating and cooling systems.

* Material from published paper (Christodoulides et al., 2019)

For example, Chang et al. (2017) have presented a case with an economic analysis of a GSHP system in the Shandong Jiaotong University Sports Centre in China. The project cooling load was 2268 kW and the heating load was 1376 kW, both noticeably greater than those of a residential building. A payback period of 7.1 years was calculated upon comparison of the GSHP system with a water-cooling machine and matching gas furnace system, making the GSHP system economically favourable.

In smaller scale, conventional heating methods have been compared with a horizontal GSHP system for a test room based in Turkey (Esen et al., 2006), with heating and cooling loads of 2.5 kW and 3.1 kW respectively. The authors used an annualized life cycle cost method to determine the economic advantages of using the GSHP system. The results have indicated that the GSHP system is a cost-effective solution (although of higher initial cost) compared to electric resistance, fuel oil, liquid petrol gas, coal and diesel oil, with respective payback periods of 8.4, 23.2, 12.4, 20.8 and 10.3 years. The authors have also noted that the GSHP system is not a profitable economic alternative when compared to the natural gas furnace system as it would require a payback period of 35.7 years. Further studies have been conducted in Turkey with similar findings, see for example (Camdali and Tuncel, 2013) and (Esen et al., 2007).

Three different types of active systems for a passive house have been economically compared by Badescu (2007), namely conventional systems, GHEs combined with conventional systems, and GSHP systems. The conventional systems refer to gas-based heater, oil-based heater, electric heater and heat exchanger based on the district heating. The authors have considered different cases where the GHE was installed during construction, with part of the excavation costs saved, and have concluded that the GSHP system is a better solution compared with the other cases for a time longer that 3–10 years.

In a comprehensive economic analysis, using different economic methods, Lu et al. (2017) have presented previous studies detailing the limitations and the documented capital cost of GSHP systems. An average 3.8 heating coefficient of performance (COP) and 3.6 cooling COP was selected for the calculations in the economic feasibility study. Conclusions have been drawn that the GSHP systems would

provide an economic advantage compared to the ASHP systems in the long term (40 years), however the system is not favourable in the short to medium term (20 years).

In an older study, Healy and Ugursal (1997), compared the economic benefits of using GSHP systems with conventional systems in a residential building in Nova Scotia, Canada. The required yearly heating load was 22800 kWh and the yearly cooling load was only 2300 kWh, as the system was required for a cold climate. The authors reported that between the four different residential heating and cooling systems, namely GSHP, electric resistance heat, oil-fired furnace and ASHP systems, the GSHP system was the least expensive to own and operate.

Based on the literature presented above, it seems that GSHP may or may not be an economically favourable solution for heating and cooling a house. That depends on many parameters and factors. One such important factor is the ASHP efficiency that has considerably increased through technology in recent years. Other factors may be the house specific area, location and climate conditions, building materials, orientation, insulation, residents' behaviour, country's legislation, etc. (Tsagarakis, 2019). The current study aims at contributing in the debate whether it is economically feasible to replace or install a GHE/GHSP as an alternative to an ASHP. The study addresses two important factors. Firstly, a global factor, the efficiency of modern ASHPs is shown to play a crucial role. Secondly, a typical house heating and cooling load is considered in the moderate climate conditions – a novelty – of Cyprus, similar to a large area of the Mediterranean basin countries.

In Section 3.2 the design of such a typical house is presented along with its calculated heating and cooling loads. Also, in Section 3.2 the thermal response of the GHE and the estimated characteristics of the GSHP – based on existing actual experimental data and simulations in summer and winter through a Computational Fluid Dynamics model developed in the FLEXPDE software – are presented. Then, a system cost analysis is offered for different length GSHP systems in Section 3.3, where a comparison of the total energy savings is obtained. We conclude with Section 3.4.

3.2 Typical House Load and HP Selection of Operating Temperatures

To evaluate and compare the cost effectiveness of a GSHP system, a typical house in moderate climate in Cyprus is considered. The characteristics and the typical loads of the residential buildings in Cyprus have been presented by Panayiotou et al. (2012, 2010).

Shown in Figure 3.1 is the selected typical house load (Pouloupatis, 2014), a three-bedroom two storey house, with a total floor area of 190 m². The house is made of reinforced concrete pillars and beams with the walls made of red and sandy clay bricks. All parts of the house are thermally insulated with extruded polystyrene, while double glazed aluminium framed windows are used. In one side, the house is attached to another house. There is available land space of at least 4 m in the other three sides. This house is a high energy efficiency building (Type B in the scale between A–G) with low running cost.

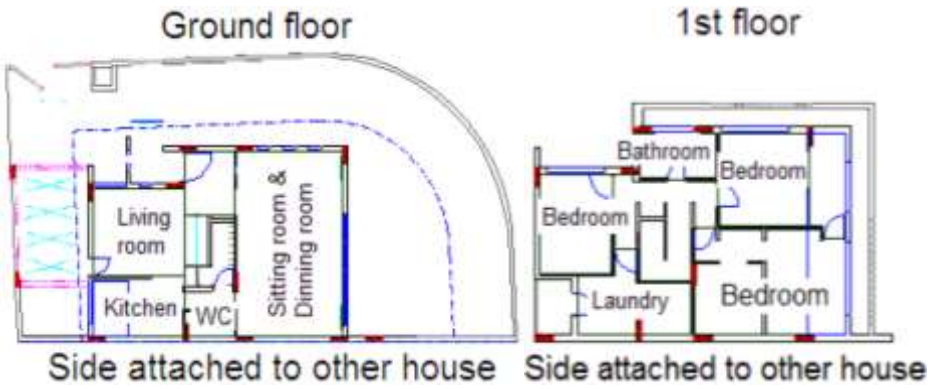

Figure 3.1 Plan views of the typical house used for the estimation of the heating and cooling load (Pouloupatis, 2014)

In a moderate climate (in the study case at Lakatamia, Cyprus) the estimated heating and cooling loads of the typical house, assuming typical values of thermal properties of the selected construction materials, are shown in Table 3.1. Note that for this type of house, Lakatamia represents the (rule of thumb) typical house considering the area's climate conditions and the population residing in such conditions. Although there are no data available for the whole Cyprus, according to

a small sample of 4 such areas (Pouloupatis, 2014), the mean total cooling load is 6100 kWh and the mean total heating load is 7400 kWh.

Table 3.1 Heating and cooling loads of the typical house used in the calculations

Month	***Cooling load (kWh)***	***Cooling peak load (kW)***	***Heating load (kWh)***	***Heating peak load (kW)***
January	0		2300	
February	0		2450	20.78
March	0		600	
April	150		0	
May	500		0	
June	1050		0	
July	1600	11.56	0	
August	1500		0	
September	1000		0	
October	300		0	
November	0		600	
December	0		1450	
Total	6100		7400	

Next, the thermal response of the GHE is examined for the maximum and the minimum load months of the year in Cyprus, i.e. July and February. In the presented case, a borehole study provides actual data for the design. Such a borehole may consist of three sublayers, a dry layer on top, a middle layer with high velocity water flowing in it and a bottom layer with low water flow. This arrangement, simulated using the FLEXPDE software by Stylianou et al. (2019), is used as a guide for the analysis in the sequel. The model was validated by following the geometry of an experimental set-up. The GHE exiting fluid temperature in summer operation and at steady input temperatures between 28–45°C, varies between 26–37°C. In summer operation the greater the difference between the input water temperature and the ground temperature, the greater the rejected heat to the ground.

Although the higher the temperature exiting the GHE the greater the heat rejected to the ground, one should consult the HP specifications to decide about the GHE design temperature.

Figure 3.2 shows typical pump characteristics, taken from Pouloupatis et al. (2017). The pump can operate with an entering fluid temperature between 20–44°C with a corresponding pump capacity over input power (COP) between 3–5.7. Lower temperatures correspond to greater pump efficiencies but also to a bigger number of boreholes and greater initial cost. Therefore, the designer should balance the advantage of a greater HP efficiency to the disadvantage of a greater initial cost.

The GHE exiting fluid temperature in winter operation, may vary between 9–21°C at a variety of steady input temperatures between 0–18°C. In winter operation the greater the difference between the input water temperature and the ground temperature, the greater the absorbed heat from the ground.

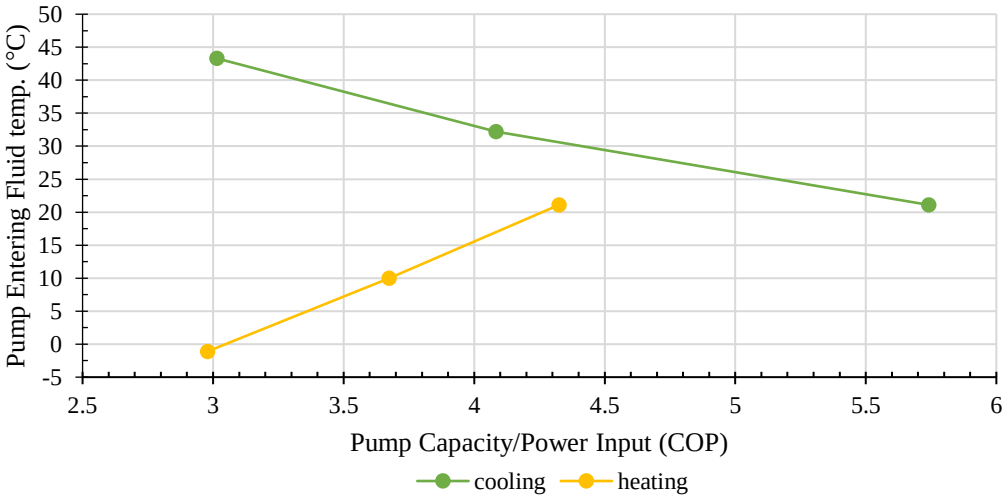

Figure 3.2 Characteristics of a typical heat pump, showing the pump entering fluid temperature against the ratio of pump capacity over power input, for cooling and heating mode of operation (Pouloupatis et al., 2017)

Referring again to Figure 3.2, to achieve higher temperatures and greater HP efficiency a larger number of boreholes are needed and therefore the initial cost will be greater. An exercise showing the characteristics for three different GHE lengths, of namely 800 m, 600 m and 400 m, is presented in Table 3.2. Of course care should be taken for the proper design of the system with the correct reflection of the

season and climate conditions, otherwise the ratio of pump capacity and power input will be lower (Luo et al., 2015a; Zhu et al., 2012).

Table 3.2 Estimated characteristics of the GSHP for various heat exchanger lengths

Season	***Max. load (kW)***	***GHE length (m)***	***GHE power/length (kW/m)***	***HP entering fluid temperature (°C)***	***Ratio of pump capacity to power input***
Summer	11.56	800	0.0145	26.2	4.9
		600	0.0193	27.5	4.7
		400	0.0289	29.5	4.4
Winter	20.78	800	0.0260	16.5	4.05
		600	0.3463	14.5	3.95
		400	0.0520	10.5	3.75

3.3 GHE Cost Analysis

Economic assessment and evaluation research of the GSHP system has been performed by several researchers (Chang et al., 2017; Cui et al., 2019, 2018; Esen et al., 2007, 2006; Guo et al., 2012; Healy and Ugursal, 1997; Lu et al., 2017; Luo et al., 2019; Morrone et al., 2014). Robert and Gosselin (Robert and Gosselin, 2014) demonstrate a good case of a techno-economic analysis of a GSHP system, where they have attempted to establish a mathematical connection between the GSHP system and the optimal cost design of the system. The total cost of any GSHP system consists of the initial capital invested and the operating costs. The capital invested initial costs is the sum of the costs of the GSHP, mechanical room installation, drilling, piping, ground loop installation, fittings, etc. The operating costs include cost due to electricity consumption by the HP, the heat transfer fluid circulation pump and the backup heating/cooling system.

The difference in the cost between an ASHP and a GSHP system lays in the GHE and the associated equipment, such as the borehole extraction, U-tube GHE, grout material, ground loop installation, header-flowmeter valves, horizontal pipe circuits, and some general expenses. Additionally, a specifically designed inverter technology for specific climates is used for the HP of ASHPs, which is of higher

value than the HP for the GSHPs (based on suppliers in Cyprus, €8500 versus €6500 respectively). Furthermore, the life span and the replacement cost of the HPs must be taken in account. It turns out that the lifespan of the GSHP is considered to be 20 years and 10 years for as ASHP (Lu et al., 2017).

Table 3.3 shows the difference in cost between a GSHP and an ASHP (common costs are not shown), based on the installation of three types of GHEs, able to satisfy the necessary building load, and the HP cost.

Table 3.3 Typical extra cost values for the installation of a GSHP

Item	***Current Cost***	***400m GHE Cost (€)***	***600m GHE Cost (€)***	***800m GHE Cost (€)***
Borehole extraction	13 €/m	5200	7800	10400
U-tube GHE Φ 32 mm	6 €/m	2400	3600	4800
Grout material	7.5 €/m	3000	4500	6000
Header-flowmeters-valves	900 €	900	900	900
Horizontal pipe circuits	600 €	600	800	1000
General expenses	500 €	500	600	700
Difference in the HP price	-2000 €	-2000	-2000	-2000
Total		10600	16200	21800

The costs presented in Table 3.3 are average prices taken in October 2018 from companies based in Cyprus. Note that, as stated by Rawlings and Sykulski (1999), direct comparison between different countries or regions cannot be established due to the socioeconomic scale. Additionally, other important issues that may affect the economic analysis comparison of technologies among different countries, include the macroeconomic indicators, the technology maturity, the energy prices, government incentives, etc. (Tsagarakis, 2019; Tsagarakis et al., 2018). For example, a comprehensive GSHP systems capital cost study performed in 2011 in Germany by Blum et al. (2011), with data taken from 1100 individual GSHP systems of average total length of GHE of 180 m, the average cost of the GHE was €11997 (including 61€/m for drilling).

A specifically designed inverter technology (for a specific climate) ducted series ASHP of similar capacity, can have a ratio of Pump Capacity/Power Input of

around 3.0 for cooling and around 3.7 for heating (taken from technical data of known brands). An estimation for the electrical power needed to cover the total heating and cooling load per year is shown in Table 3.4.

Different methods are used in the literature to examine the economic benefits of installing a GSHP system, and a good discussion with more references are reported by Lu et al. (2017). Such methods include the Present Worth (PW), the Annual Worth (AW), the Internal Rate of Return (IRR), the External Rate of Return (ERR), the Simple Payback Period (SPP), the Discounted Payback Period (DPP) (see (Tassou et al., 1986)), the Annualised Life Cycle Cost (ALCC) method, the Levelized Cost of Energy (LCOE) (Ouyang and Lin, 2014) and the equivalent Total Annual Economic Cost (TAEC) (Tsagarakis, 2007). It is beyond the scope of the current study to go in detail into all the above-mentioned methods, as the goal of comparing a single GSHP (with vertical GHEs) and an ASHP can be achieved through a comparison of different DPP scenarios explained below with adequate precision.

Simple and adequate methods for a comparable economic evaluation are the SPP and the DPP, where the years required to equal the inflow and the outflow cash are calculated, taking into account the inflation of electricity prices and the discounting future cash flow (Sullivan et al., 2014). They can be described by the following equations.

$$\text{SPP} = \sum_{k=1}^{\theta} (S_k \times EP - E_k) - I \geq 0 \qquad 3.1$$

$$\text{DPP} = \sum_{k=1}^{\theta} (S_k \times EP \times (1+i)^k - E_k) - I(1+r)^k \geq 0 \qquad 3.2$$

where θ is the years for either SPP or DPP, S_k is the savings for the k^{th} year (considered to be constant each year), E_k is the net expenditure for the k^{th} year (i.e. the replacement of the HP after its lifecycle), I is the capital investment, EP is the initial electricity price for year 0 per kWh, and i is the electricity price inflation and r is the loan interest rate.

The results presented in Table 3.4 describe the SPP and DPP for the cost difference required to upgrade from an ASHP system to a GSHP system. Also shown are the power savings per year for the 400 m GHE (673 kWh), the 600 m GHE (862 kWh)

and the 800 m GHE (961 kWh). Considering the current price for house holdings of 0.19€/kWh would result to the following savings per year: €128 for the 400m GHE, €164 for the 600m GHE, and €183 for the 800m GHE. Clearly, without considering any inflation of the electricity price, nor taking in account the maintenance cost (yearly expenses E_k), for all cases the payback period would be well over 50 years.

Table 3.4 Estimated Energy savings per year and SPP-DPP results for the typical house

Season / HE / length (m)	***Cooling/Heating load (kWh)***	***COP***	***Input electrical power (kWh)***	***Savings per year compared to ASHP (kWh)***	***SPP for GSHP vs ASHP (years)***	***DPP for GSHP vs ASHP with 2% EP inflation (years)***	***DPP for GSHP vs ASHP with 2% EP inflation and Loan with 3% interest rate (years)***
ASHP summer	6100	3.0	2033				
ASHP winter	7400	3.7	2000				
GSHP summer/400	6100	4.4	1386	647	16.2	15.5	21.2
GSHP winter/400	7400	3.75	1973	27			
GSHP summer/600	6100	4.7	1298	735	23.2	22.1	35.5
GSHP winter/600	7400	3.95	1873	127			
GSHP summer/800	6100	4.9	1245	788	30.5	28.2	>45
GSHP winter/800	7400	4.05	1827	173			

The SPP, although failing to examine the indicate project desirability, the inflation of the energy tariffs, and the interest of loan (when funds are bank financed), can be a simple and useful first indicator, giving a best scenario of payback of about 16 years for the 400 m GHE. Employing the more precise DPP yields similar results when the loan interest rate is not taken into consideration. Once the latter is considered, the best scenario of payback is about 21 years for the 400 m GHE.

In the case where there is uncertainty of the HP lifecycle, a sensitivity analysis should also be carried out (Tsagarakis, 2007), unless is it specified by the manufacturer for the specific region. A sensitivity analysis in such cases, could vary the SPP (Kljajić et al., 2018). Such a sensitivity analysis is presented in Figure 3.3, where the yearly savings are varied by ±(0→30)%. It is observed that reducing the savings by 30% the SPP is decreased by 6.28%, while in the case where the yearly savings are increased by 30% the SPP is increased by 5.87%.

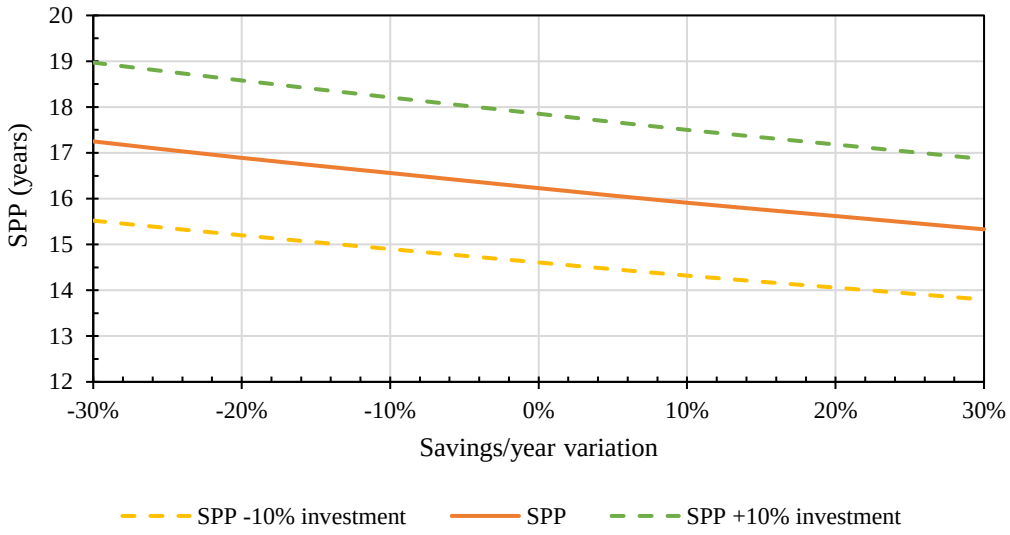

Figure 3.3 Sensitivity analysis on investment and savings

The obtained results show that the new specifically designed, inverter type ASHPs, have reached such a high stage of technology that can antagonize strongly GSHPs for residential use. The results in general are comparable with those of Lu et al. (2017), where similar cost and electricity prices are noticed, with the notable exception that the GSHP with the 400m GHE could be favourable in the short to medium term. Also, the results are in accordance with previous studies suggesting that GSHPs are not an obvious profitable economic alternative compared to other solutions (Camdali and Tuncel, 2013; Esen et al., 2007, 2006; Gabrielli and Bottarelli, 2016; Lu et al., 2017), but in contrast with other studies suggesting a small payback period with an economic advantage of the GSHP system (Anis Akrouch et al., 2020; Badescu, 2007; Healy and Ugursal, 1997; Kharseh et al., 2015; Kljajić et al., 2018). The difference in such estimations is based on the parameters and factors present for each specific case.

3.4 Discussion

A residential building in Cyprus has been presented as a case study with heating and cooling loads in moderate Mediterranean climate conditions. The 3-bedroom house of 190 m^2 has peak cooling and heating loads of 11.56 kW and 20.78 kW. A "typical" GHE simulated in FLEXPDE software for various circulating water input

temperatures for summer and winter yields Pump Capacity/Power Input ratios of 3.6–5.

Cost analyses and comparisons have been presented for the ASHP and GSHP systems. It can be concluded that the payback period of using GSHP systems over ASHPs would be in the range of 20 years at best, making it not an obvious economical solution in the specific case. Due to comparable ratios between the Pump Capacity/Power Input ratios of specifically designed inverted technology ducted series ASHPs and GSHPs, one can draw the conclusion that this technology can antagonize strongly GSHP technology for residential use. Another sound conclusion is that, although HP efficiency increases with GHE length, the initial cost is so high making such a solution not viable over a certain GHE length.

To overcome the above concern, further investigation is required on system parameters. To this end, the effect of groundwater is investigated in Chapter 4, and other geometries are studied in Chapter 5.

Chapter 4*

4 Computational Modelling of a Ground Heat Exchanger with groundwater flow

Summary: Multiple layers of ground and the flow of ground water in some layers have a significant effect on the cooling of vertical heat columns and heat exchangers. This chapter investigates the important implication on the design of the Ground Heat Exchanger with regard to their heating effect. For this reason, a thermal model is constructed in COMSOL Multiphysics software and the effect of various parameters such as thermal conductivity of the ground and the groundwater flow velocity is considered. The model parameters were adjusted to present actual (known) parameters of an installed column and were validated against experimental values. The key for an overall capital cost reduction is the borehole length, where the results indicate that by using the groundwater available, construction of shallower Ground Source Heat Pump systems can be achieved with an increase of the coefficient of performance (COP).

4.1 Overview

A reliable GSHP system depends on the proper design of the GHE, where is the key to reduce the overall capital cost of a vertical GSHP system. For designing a GHE the two most important parameters are (as already mentioned) the soil thermal conductivity as well as the borehole thermal resistance. The borehole thermal resistance depends upon borehole diameter, pipe size and configuration, pipe material and the backfill material. It is specified that for high soil thermal conductivity and a low borehole thermal resistance, the heat exchange rate will be higher for a given borehole (Zhang et al., 2014). Therefore, it is of high importance to determine the thermal characteristics of the ground prior to the system design. For larger installations borehole tests are carried out in a test borehole.

There are several methods in the literature for the determination of ground thermal characteristics (Zhang et al., 2014), such as soil and rock identification (Bose,

* Material from published paper (L. Aresti et al., 2016)

1989), experimental testing of drill cuttings (Sass et al., 1971), in situ probes (Choudhary, 1976), and inverse heat conduction models. However, the most commonly used is the Thermal Response Test. The TRT is a method to determine the ground thermal characteristics and it was first introduced by Mogensen (1983). TRT suggests heat injection in the borehole at constant power whereas the mean borehole temperature is defined on output. The recorded fluid temperature response is the temperature developed over time, which is evaluated to obtain the thermal characteristics of the borehole such as the thermal resistance, the volumetric specific heat capacity, and the soil conductivity by using inverse heat transfer analysis (Gehlin, 2002).

Throughout the years several analytical and numerical models have been developed to implement fast and reliable predictions of a GHE where all the models are based on the Fourier's law of heat conduction (Florides and Kalogirou, 2007) and do not account for groundwater flow. The models can be categorized with regard to the type of the 'source' heat (infinite or finite, linear or not). The most commonly used include the "infinite length line source method", developed by Lord Kelvin (1882), while later Ingersoll et al. (1950), (1955), applied it to model radial heat transfer, the "cylindrical heat source method", firstly described by Carslaw and Jaeger (1959) and "finite length line source method", Eskilson (1987) and Claesson and Eskilson (1988) were the first to develop an analytical g-function expression where the solution is determined using a line source with finite length (Javed et al., 2009).

Another important aspect to consider when designing a GSHP system is the groundwater flow where an aquifer is present. In-situ experiment performed in Minnesota (Chiasson et al., 2000) with groundwater flow have observed unusual high thermal conductivity values. Furthermore, the implementation of the groundwater flow is not supported by current model approaches where only heat conduction is considered and may overestimate the thermal conductivities.

The aim of this chapter is to study the effect of the groundwater flow on a GHE using the computational modelling approach. The geometry used is similar to the one in Florides et al. (2013) and has been reconstructed in COMSOL Multiphysics. v.5.1, which is a computational modelling software allowing the user to use general equations, but also add and edit equations manually. It also allows the user to create

a CAD model, construct the mesh, apply the physic parameters and post processes the results under the same user interface.

4.2 Mathematical model

The heat distribution over time is described by the general heat transfer equation based on the energy balance. For the current application the rate of energy accumulated in the system is equal to the rate of energy entering the system plus the rate of energy generated within the system minus the rate of energy leaving the system (Florides et al., 2013).

Thus, the three-dimensional conservation of the transient heat equation for an incompressible fluid is used (and applied in COMSOL Multiphysics) as follows:

$$\rho c_p \frac{\partial T}{\partial t} + \rho_w c_{pw} u \nabla T + \nabla \cdot q = Q \qquad 4.1$$

where T is the temperature, t is time, ρ is the density of the borehole/soil material, c_p is the specific heat capacity of the borehole/soil material at constant pressure, ρ_w is the density of the ground water, c_{pw} is the specific heat capacity of the ground water at constant pressure, u is the velocity of the groundwater, Q is the heat source and q is given by the Fourier's law of heat conduction that describes the relationship between the heat flux vector field and the temperature gradient:

$$q = -k \nabla T \qquad 4.2$$

where k is the thermal conductivity of the borehole/soil material.

In Equation 4.1, the first term represents the internal energy, the second term is the part of the heat carried away by the flow of water, the third term represents the net heat conducted (as described in Equation 4.2) and the fourth one is the heat source.

Since the problem will be solved in a transient mode and is time-dependent the first term is not ruled out as in the case of the steady-state solution. Note that in the case where the groundwater is absent, parameter u (velocity) is set to zero and the second term disappears.

The heat source term describes heat generation within the domain and is set as the heat transfer rate:

$$Q = \frac{P_0}{V} \tag{4.3}$$

where here V is the domain (borehole) volume and P_0 is the power per unit length, in the case of a single U-tube pipe described as:

$$P_0 = \dot{m}_w c_{p\,w} dT \tag{4.4}$$

where dT is the temperature difference from the outlet of the second tube to the inlet of the first one and $\dot{m}_w$ is the mass flow rate of the water in the tube, defined as:

$$\dot{m}_w = \rho_w A_p u_p \tag{4.5}$$

where A_p is the area of the tube and u_p is the flow velocity in the tubes.

At the extremities of the domain the boundaries were set as the COMSOL Multiphysics default "thermal insulation," where there is no heat flux across the boundaries. This setting does not affect the heat distribution along the examined area of the borehole as the domain is set to be significantly larger than the borehole itself.

When water is present in the ground layer, the heat transfer equation in porous media is applied (Bear and Yehuda, 2012) (being similar to Equation 4.1):

$$\rho_{eff} c_{p.eff} \frac{\partial T}{\partial t} + \rho_w c_{pw} u \nabla T + \nabla \cdot q = Q \tag{4.6}$$

where $\rho_{eff} c_{p.eff}$ is the volumetric heat capacity of the porous media at constant pressure (ρ_{eff} being the density and $c_{p.eff}$ the specific heat capacity) given by:

$$\rho_{eff} c_{p.eff} = \theta_s \rho_s c_{ps} + (1 - \theta_s) \rho_w c_{pw} \tag{4.7}$$

where θ_s is the soil material volume fraction given in a percentage from 0 to 1, $\rho_s c_{ps}$ is the volumetric heat capacity of the porosity soil material (ρ_s being the density and c_{ps} the specific heat capacity), and $\rho_w c_{pw}$ is the volumetric heat capacity of the fluid material (water) (ρ_w being the density and c_{pw} the specific heat capacity). The velocity u in the second term of Equation 4.6 represents the Darcy's velocity as specified in the following Section.

In Equation 4.6 the heat conduction q can be expressed as:

$$q = -k_{eff}\nabla T \quad (4.8)$$

where k_{eff} is the effective thermal conductivity that is present in three different models (Nield and Bejan, 2013). The first model, termed volume average, assumes that the heat conduction occurs in parallel between the solid material and the fluid and the effective thermal conductivity is expressed as:

$$k_{eff} = \theta_s k_s + (1-\theta_s) k_w \quad (4.9)$$

where k_s is the thermal conductivity of the porosity material and k_w is the thermal conductivity of the fluid material (water). In the case where the heat conduction occurs in series with heat flux through both materials, solid and fluid, the effective thermal conductivity is expressed as a reciprocal average law (model):

$$\frac{1}{k_{eff}} = \frac{\theta_s}{k_s} + \frac{(1-\theta_s)}{k_w} \quad (4.10)$$

The third model is an estimation of the weighted geometric mean of the thermal conductivity of both the solid and the fluid materials and the effective thermal conductivity is expressed as:

$$k_{eff} = k_s^{\theta_s} \cdot k_w^{(1-\theta_s)} \quad (4.11)$$

In the current model set up, the first method of determining the effective thermal conductivity (Equation 4.9) has been chosen as it was closer to the requirements of the specific application.

4.2.1 Darcy's velocity

In order to describe the flow through a porous medium, Darcy's law needs to be applied. The theory was firstly established by Henry Darcy based on experimental results (Darcy, 1856) and allows the estimation of the velocity or flow rate within an aquifer. In the case of the investigation of the groundwater effect on the GHE Darcy's velocity is used in the porous media heat transfer equation as stated in Equation 4.6.

Darcy's velocity (also called *Specific Discharge*) assumes that flow occurs across the entire cross-section of the soil (Chiasson et al., 2000) and is determined as:

$$V_D = -Ki = -K\frac{dh}{L} \quad (4.12)$$

where K is the hydraulic conductivity that measures the ability for the flow though porous media, i is the hydraulic gradient with dh being the head difference from a datum point and L the distance between the two heads (or boreholes). The minus sign indicates that the flow is moving away from the head. Darcy's velocity is accurately represented though experiments when laminar flow is observed with low Reynolds number (Harr, 1991).

To determine where the Darcy's velocity is applicable the Reynolds number, described below, should be examined:

$$\mathrm{Re} = \frac{vD\rho}{\mu} \quad (4.13)$$

where v is the discharge velocity, D is the average of diameters of soil particles, and μ is the viscosity. Experiments have shown that the transition flow (from laminar to turbulent) occurs approximately at $\mathrm{Re} \approx 10$, which is lower than the free flow conditions. The validity of Darcy's law is acceptable at $\mathrm{Re} \leq 1$ (Harr, 1991).

As stated in (Harr, 1991), the specific discharge does not predict accurately the flow through a porous media but instead through a pipe. In order to overcome this issue the seepage velocity was introduced representing the average fluid velocity within the pores and includes a porosity term as described below:

$$v_S = -K\frac{dh}{Ln} = \frac{V_D}{n} \quad (4.14)$$

where $n = A_v/A$ is the porosity term specified as the area of the void space (A_v) through which fluid can flow over the total area (A) of the ground though which fluid does not flow over the hydraulic thermal conductivity.

4.2.2 Coordinate scaling

When modelling a system, as in the present case, it is commonly observed that one of the dimensions may have an enormous difference in relation with the others, and by meshing the model with equilateral cells, high computational memory and time

will be required. The way to overcome this difficulty is to scale the large dimension and balance the coordinate sizes. Consider a coordinate transformation:

$$z = s \times w \tag{4.15}$$

where w is the physical coordinate, s is the scaling factor, z is the model coordinate. The general heat equation (Equation 4.1 combined with Equation 4.2) reads in expanded form:

$$\rho C_p \frac{\partial T}{\partial t} + \rho C_p u \nabla T + \frac{\partial}{\partial x}\left(k \frac{\partial T}{\partial x}\right) + \frac{\partial}{\partial y}\left(k \frac{\partial T}{\partial y}\right) + \frac{\partial}{\partial w}\left(k \frac{\partial T}{\partial w}\right) = Q \tag{4.16}$$

Regarding the vertical axis we have:

$$\partial w(q) = \frac{\partial q}{\partial w} = \left(\frac{dq}{dz}\right) \times \left(\frac{dz}{dw}\right) = s \times \frac{dq}{dz} \tag{4.17}$$

Incorporating Equation 4.17 into Equation 4.16 yields:

$$\rho C_p \frac{\partial T}{\partial t} + \rho C_p u \nabla T + \frac{\partial}{\partial x}\left(k \frac{\partial T}{\partial x}\right) + \frac{\partial}{\partial y}\left(k \frac{\partial T}{\partial y}\right) + s \frac{\partial}{\partial z}\left(s\, k \frac{\partial T}{\partial z}\right) = Q \tag{4.18}$$

The required physical model has a very large height, of 100m, in contrast with the length and width of the model, which is 10m × 5m. Therefore, the model was scaled down on the vertical axis (height). In order to achieve this reduction the geometry in the COMSOL Multiphysics was built with a scale factor of 0.1 using the thermal conductivity in the materials section (as described in Table 4.1). Since multilayer ground is considered here the *z*-direction thermal conductivity in each layer is scaled as follows:

$$k_z = k(s^2) \tag{4.19}$$

Refer to (PDE Solution, 2010) for the flux conservation and how to un-scale fluxes in scaled models.

4.3 Computational modelling

As already mentioned, following the required parameters the model was constructed using the COMSOL Multiphysics v.5.1. The geometry as seen in Figure 4.1 was set with two cylinders representing the boreholes. The multilayer ground was constructed with different material properties in order to achieve the required results

and the general model, as descripted in the Coordinate scaling section, was scaled down on the *z*-axis.

The material properties of each ground layer and the boreholes are described in the following Table 4.1 and were taken from the experimental results provided by Florides et al. (2013).

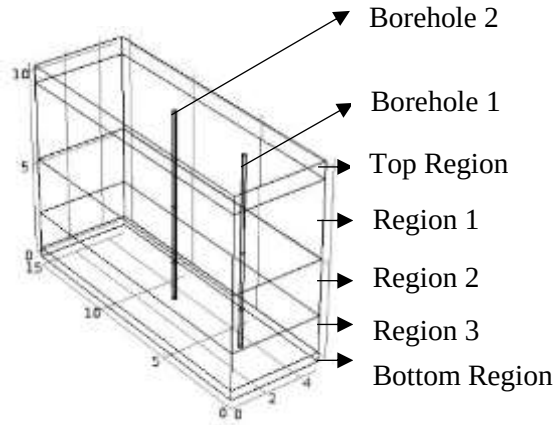

Figure 4.1 Model Geometry

Table 4.1 Material properties

Layer	*Height (m)*	*k (W m^{-1} K^{-1})*	*C_p (W kg^{-1} K^{-1})*	*ρ (kg m^{-3})*
Top (top)	9×zscale	1.64	2353	731
Region 1	41×zscale	1.73	2290	780
Region 2	30×zscale	1.94	2330	840
Region 3	20×zscale	1.94	2330	840
Bottom	5×zscale	1.94	2330	840
Boreholes	95×zscale	1	800	1500

The groundwater velocity was set using the seepage velocity as described in the previous section, where the hydraulic conductivity is considered for the minimum and maximum values from typical data presented in Domenico and Schwartz (1990).

The value of power used was the same as in Florides *et al.*(2013) and the boreholes were set as a heat source with a general source applied of 1273.2 W/m^3. The heat source was not constantly (24h) applied as this is not a realistic situation. It was chosen to reject heat for 12 hours, while for the next 12 hours it was chosen to remain idle and did not act as a heat source. To achieve this on COMSOL Multiphysics a rectangle function and an analytic function were selected. Moreover, a heat source applied time function was set (with lower limit 0 and upper limit 12 hours) within the rectangle function. Following on, an argument *t* (time) was introduced in the analytic function (expression of: comp1.rect1 (t[1/s]), where rect1 is the rectangle function and comp1 (component) is the location of the function), defining the overall length of 7 days (upper limit) and setting a period of 1 day (periodic extension). The analytic function is described graphically in Figure 4.2. It must be noted that *smoothing* is added by default in COMSOL Multiphysics in order to prevent the equations from shock, and hence produce valid results.

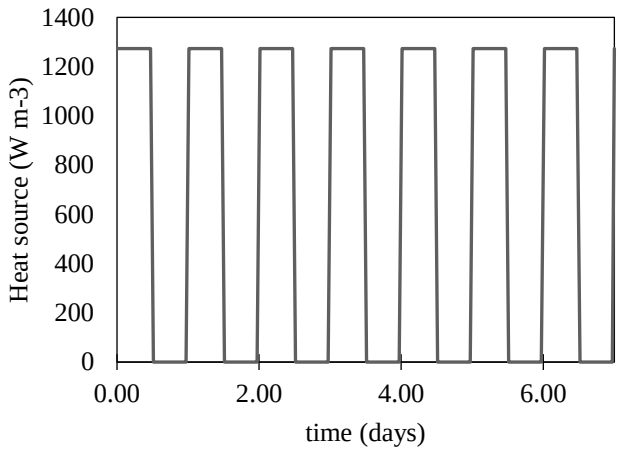

Figure 4.2 Heat Source analytic function

4.4 Results

After the computational model set-up, a set of runs were performed in order to confirm that the scale factor produced reasonable results within acceptable error. The scale comparison was run for the factors of 0.1, 0.2, 0.3 and 0.4. The quantity

analysed was the average temperature on the outer surface of both boreholes in region 3 ground layer (seen in Figure 4.1).

Between the scale factors, the results demonstrate a good agreement with less than 0.5 K in temperature difference (seen in Figure 4.3) ±0.5 K (professional equipment may exhibit a tolerance of usually ±0.2 K). It should be noted that all the parameter values are the same for all 4 cases considered, except the mesh density that had to be changed. The mesh density on the boreholes was maintained at a minimum of 10 to 12 points on the boreholes diameter with a growth rate of 1.2–1.4. As a consequence, the selected scale factor to proceed with the computational models was 0.1 as it required the least computational time and memory.

For presenting a nearly realistic model a pulse function was applied, by equating the heat source term to 1 for 12 hours and to zero for the next 12 hours, for 7 consecutive days as shown in Figure 4.2.

The values presented in all the figures are the average surface temperature on the outer wall on region 3 as shown in Figure 4.1.

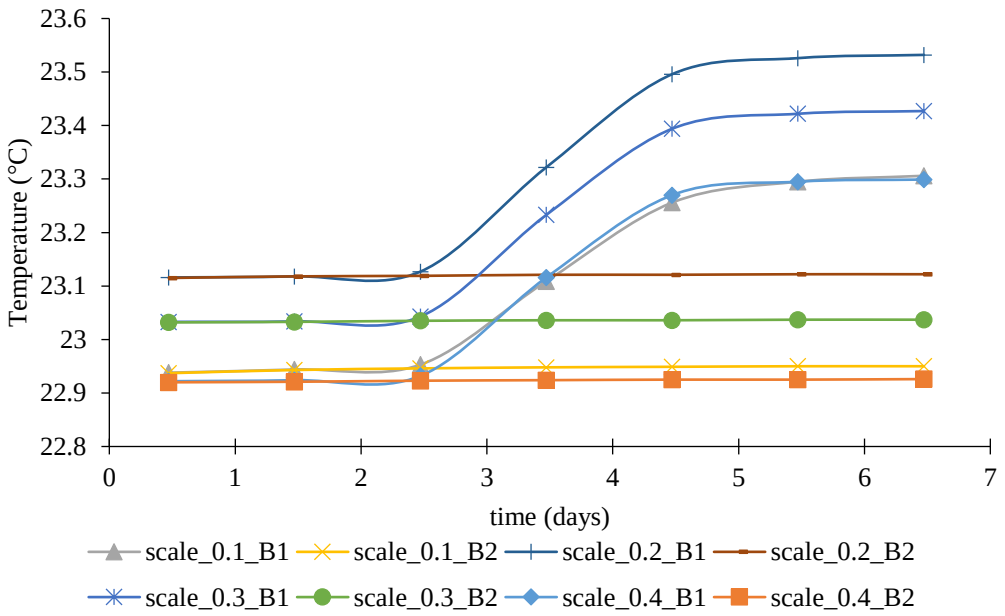

Figure 4.3 Scale comparison of the region 3 borehole surface showing average temperature over time

By analysing the boreholes individually and at different regions it is observed that the temperature increases with time except in the region of the groundwater (Figure

4.4). This is due to the fact that heat is carried away from the borehole section, where groundwater is present, while in the other sections heat is generated and maintained in the region. In addition, 7 peak points are noticeable due to the pulse function applied. The temperature reaches its peak point each day in the middle of the day after the 12 hours of continuous heat rejection.

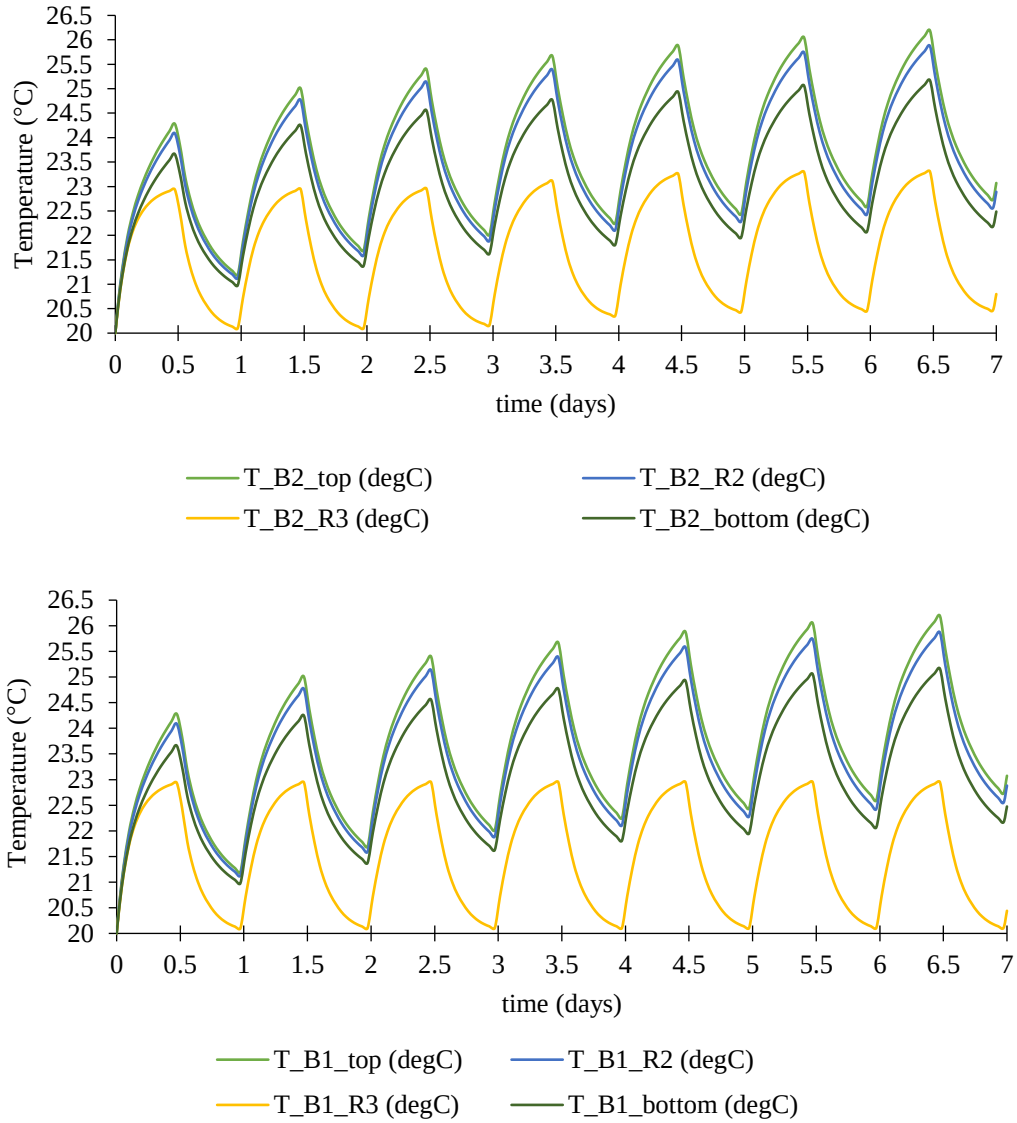

Figure 4.4 Temperature profiles versus time for a seepage velocity $v_S = 10^{-5}$ m s^{-1}

It is easier to examine the rise of the heat by plotting only the maximum points in each borehole (as seen in Figure 4.5 and Figure 4.6). In Figure 4.5 it can be observed that by increasing the groundwater velocity (seepage velocity as applied in the model) the average surface temperature on the groundwater region decreases. Note that it turns out that all the values with a low seepage velocity ($v_S =$

1.6667×10^{-9} and $v_S=10^{-9}$) applied produce the same temperature peak points (see plots). Thus it can be concluded that where seepage velocity smaller than 10^{-9} is applied there is not enough groundwater velocity to cool down the boreholes, whereas in the maximum seepage velocity regime the boreholes response with lower average temperature and, in addition, they are reaching steady state in a shorter time frame. It is also noticeable that in the case of the first borehole, the average temperature reaches a steady state from the first day peak point, whereas on the second borehole (on the downstream) there is an increase in temperature before it reaches steady state again.

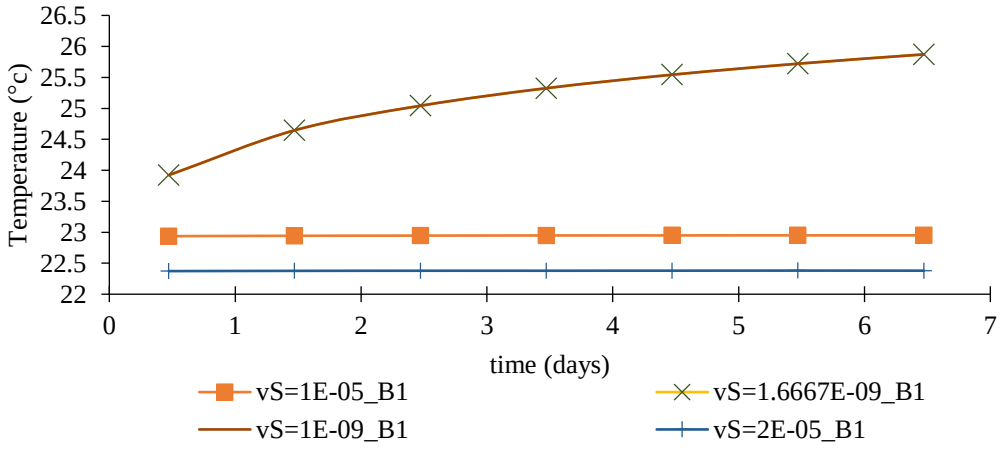

Figure 4.5 Temperature peak points versus time for borehole 1 (B1) in region 3 for various values of seepage velocity (v_S)

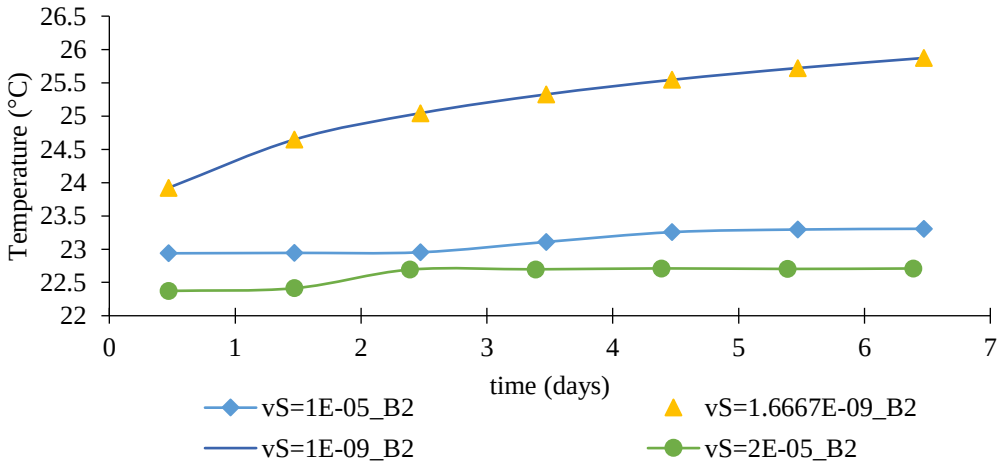

Figure 4.6 Temperature peak points versus time for borehole 2 (B2) in region 3 for various values of seepage velocity (v_S)

In order to further examine the conditions under which the temperature on the second borehole increases, a direct comparison under the same conditions between the two boreholes is shown in Figure 4.7. The heat carried away from the first borehole interferes with the second borehole when the groundwater velocity is high enough – like in the case of the maximum seepage velocity ($v_S = 10^{-5}$ m s^{-1}) – as can be observed in the plot of a 2D plane of the y-z axis and the x-y axis in Figure 4.8 and Figure 4.9.

This interference occurs after 60 hours and continues for another 3 days until the heat flow is steady and the average surface temperature on the second borehole reaches steady state.

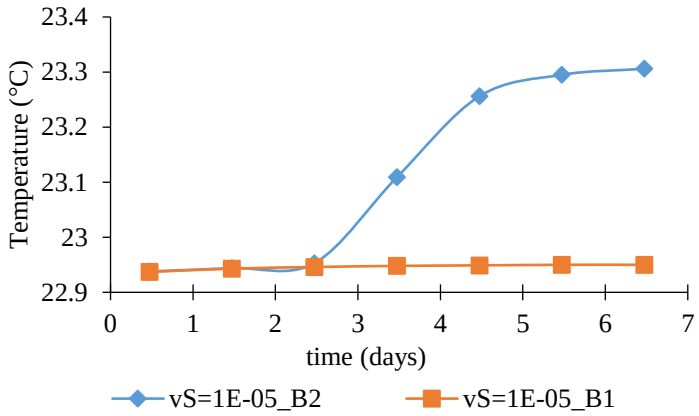

Figure 4.7 Temperature peak points at $v_S = 10^{-5}$ m s^{-1} versus time for both boreholes in region 3

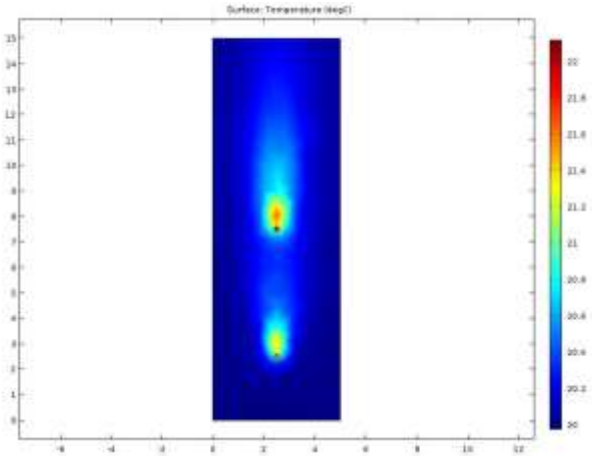

Figure 4.8 2D cut-plane on the x-y plane, $v_S = 10^{-5}$ m s^{-1}, $t = 7$ days, centre of region 3

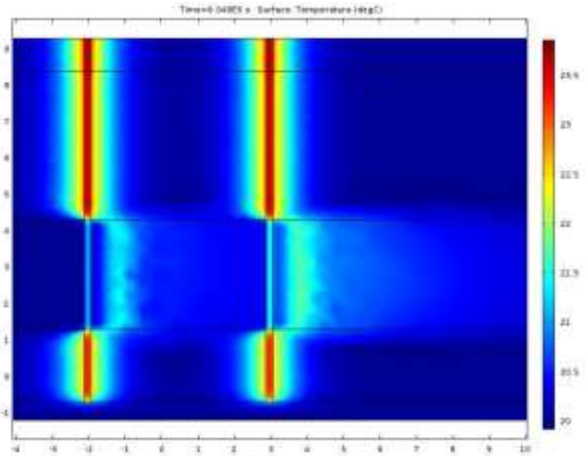

Figure 4.9 2D cut-plane on the y-z plane, $v_S = 10^{-5}$ m s^{-1}, $t = 7$ days, centre of boreholes

The effect of the interference, when the maximum hydraulic conductivity is applied, can also be noticed by plotting the isothermal contours. After a 2 days run the isothermal contours of the first borehole have not reached the second borehole, as can be seen in Figure 4.10. But after a 5 days run (Figure 4.11), the first borehole has reacted with the second borehole, whence the increased temperature detected.

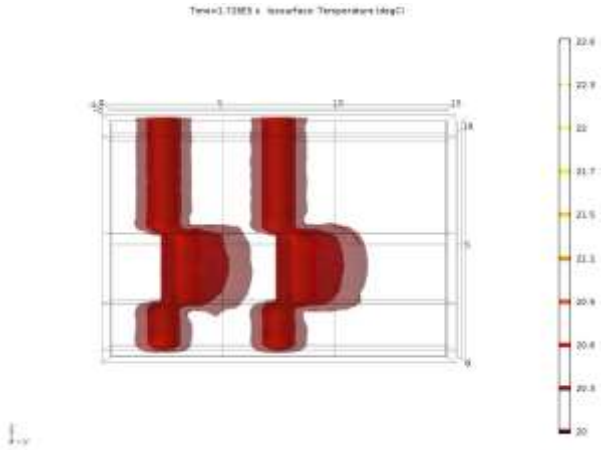

Figure 4.10 Isothermal contours, $v_S = 10^{-5}$ m s^{-1}, $t = 2$ days

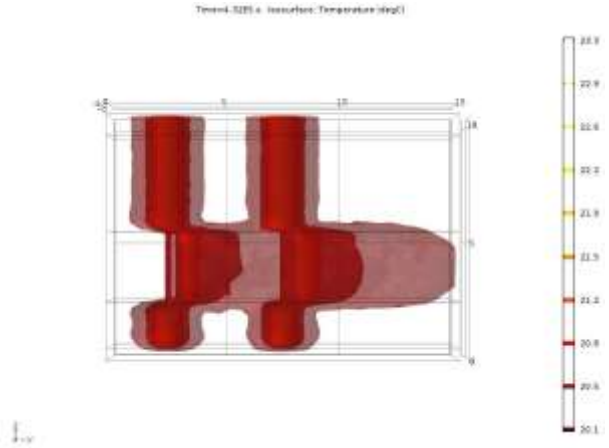

Figure 4.11 Isothermal contours, v_S = 10^{-5} m s^{-1}, t =5 days

The interference does not occur at lower velocities (e.g. v_S = 1.6667×10^{-9} m s^{-1} for minimum hydraulic conductivity applied) as can be clearly seen in Figure 4.12, as expected due to the low velocity in the groundwater region. Of course even this very low seepage velocity can still produce lower average surface temperature in region 3 that in the other regions (as seen in Figure 4.4). Note that steady state has not been reached after 7 days of computational run (Figure 4.5 and Figure 4.6), as in the case of the higher seepage velocity applied (v_S = 10^{-5} m s^{-1} for maximum hydraulic conductivity).

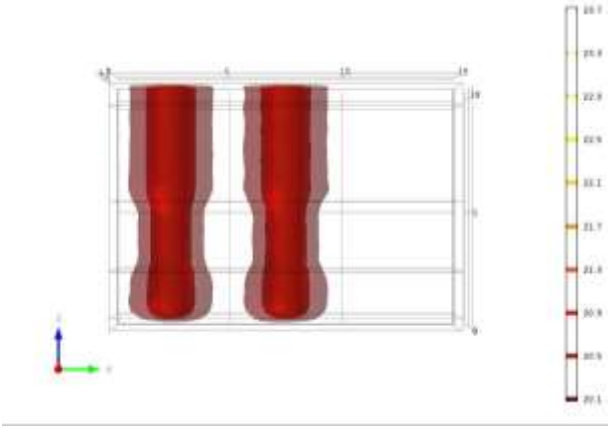

Figure 4.12 Isothermal contours, v_S = 1.6667×10^{-9} m s^{-1}, t = 7 days

4.5 Discussion

In this chapter the effect of the groundwater flow on a GHE in cooling mode has been examined through computational modelling using COMSOL Multiphysics software. Heat transfer in porous media, Darcy's velocity and seepage velocity were

introduced by taking typical values of hydraulic conductivity and were adapted in COMSOL Multiphysics. The coordinate scaling technique was employed in order to save valuable computational time and memory. The heat source was added to the model as a pulse function and it was activated 12 hours a day.

Moreover, the average borehole surface temperatures on every ground layer were presented for low and high seepage velocities. The results indicate that groundwater flow has an effect on the average surface temperature, and in the water-baring layer the average temperature decreases as opposed to the dry regions. It is also noticeable that the temperature of the affected ground layer reaches a steady state much sooner than in other regions. Additionally, when the groundwater flow velocity is high, the two boreholes are observed to interfere with each other. This interference has an effect on the downstream borehole that can reach a lower steady-state temperature. Therefore, it can be suggested that the underground flow should be taken in consideration when designing a GSHP system, as it could either enhance or diminish the efficiency of the system. The effects of groundwater flow are also examined by Stylianou et al. (2018), where a useful parametric analysis on the borehole GHEs is conducted.

Further examination of cooling and heating mode must be considered in the future and in addition, in-situ experiments could be conducted in order to validate directly the model using a groundwater flow GHE.

Chapter 5*

5 Residential buildings' foundations as a Ground Heat Exchanger and comparison among different types in a moderate climate country

Summary: Shallow Geothermal Energy Systems (SGESs) constitute Renewable Energy Systems (RES), which find application in the residential sector through the use of Ground Source Heat Pumps (GSHPs). GSHPs are associated with Ground Heat Exchangers (GHEs), whereby heat is gained/lost through a network of tubes into the ground. GSHPs have failed to flourish in the RES market due to their high initial costs and long payback periods. In this study, the use of Energy Geo-Structure (EGS) systems, namely the foundation (or energy) piles and the foundation bed of a residential building in Cyprus were computationally modelled in the COMSOL Multiphysics software. Firstly, the single-houses' trend in number of units and area in Cyprus was examined and a theoretically typical house with nearly Zero Energy Building (nZEB) characteristics was considered. The heating and cooling loads were estimated in the TRNSYS software environment and used as inputs to investigate the performance of the GSHP/GHE systems. Both systems were shown to exhibit steady performance and high COP (Coefficient of Performance) values, making them an alternative RES solution for residential building integration. Next, the systems were economically evaluated through a comparison with a conventional Air Source Heat Pump (ASHP) system. The economic analysis showed that the cost of the suggested conversions of the foundation elements into GHEs had short payback periods. Consequently, either using the foundation piles or bed as a GHE, is a profitable investment and an alternative to conventional RES.

5.1 Overview

Ground Heat Exchangers (GHEs) act essentially as conventional heat exchangers, with a network of tubes concealed underground, gaining or rejecting heat from/to

* Material from published paper (Aresti et al., 2020c)

the ground. There are two main categories of GHEs: the horizontal and the vertical (or borehole) types, with the vertical type requiring less ground surface area making it a conventional type compared to the horizontal type (Aresti et al., 2018). The U-tube and double U-tube constitute the typical vertical GHEs, with the spiral or helical type GHE gaining more ground in recent years. As with the rest of configurations, the spiral or helical type GHEs can be coupled with GSHP systems for heating and cooling a building. Owing to their high efficiency, the use of spiral GHEs can lead to a reduction of the required depth of the GHE, and consequently of the initial capital cost of the GSHP system, making them more attractive for investment than the other configurations.

The spiral coil GHE configuration was investigated by Bezyan et al. (2015) through a Computational Fluid Dynamics (CFD) package and, specifically the FLUENT software. The authors validated their model against a U-tube configuration by comparing the corresponding outlet temperatures. The single U-tube, the double U-tube in series (also known as W-shaped) and the spiral coil GHE configurations were examined and compared in terms of their performance, with the latter having the highest heat transfer rate efficiency and energy output. A similar comparison was also performed by Zhao et al. (2016), where the authors used the COMSOL Multiphysics software to perform computational investigations. Similar findings were reported, with the spiral GHE configuration outperforming the other GHE configurations in terms of thermal behaviour for long-term and short-term thermal loads. Further experimental and numerical studies have been conducted by other researchers with regard to maximization of efficiency and identification of the most accurate way for effective GHEs design (e.g., (Brandl, 2013; De Moel et al., 2010; Fadejev et al., 2017; Gao et al., 2008; Gashti et al., 2014; Suryatriyastuti et al., 2012; Yoon et al., 2015b)).

GSHP systems have been recently utilized in the buildings foundation as a form of so-called Thermo-Active Structure systems or Energy Geo-Structures, with applications such as energy piles, barrette piles, diaphragm walls (Sterpi et al., 2020), shallow foundations, retaining walls, embankments, and tunnel linings (Brandl, 2013). In particular, GHEs can be integrated into the foundation piles of a dwelling to form energy piles. Energy piles are reinforced concrete foundations

with geothermal pipes, whereby the buildings foundations are utilized to provide space heating and cooling. Typical sizes for energy piles are 10–40m in depth (Brandl, 2013) and 0.3–1.5m in diameter (Loveridge, 2012). As for borehole GHEs, different configurations can be used for an energy pile GHE, with the most common being the U-tube, the W-tube, the 3U-tube and the spiral/ helical tube. The spiral-shaped energy pile thermally outperforms the other types due to the longer pipeline (for the same depth) and the geometrical arrangement form, by at least 15% (but it can be much larger, depending on the case and parameters values) (Zhao et al., 2016).

Details on the design process, types and materials for energy piles are extensively discussed in Sani et al. (2019). A comparison between the three commonly used types (namely, W-tube, 3U-tube and spiral tube) were performed by Carotenuto et al. (2017), where the spiral coil provides the greatest temperature difference between inlet and outlet temperature and the best heat transfer performance. Similar results were obtained by Zarella et al. (2013) and Zhao et al. (2016), where a spiral pipe configuration was compared with a 3U-tube and a double W-tube configuration.

The conventional way for reducing the initial costs of a GSHP system is to limit the number or size of GHEs (boreholes) depending on the buildings load and avoid overestimation. Such a scenario is not feasible in the case of energy piles, since there is already a specific number of piles based on the structural buildings' requirements. Therefore, it is important to incorporate a spiral coil in a single pile with the correct length and pitch angle. In such a scenario the tube diameter and the spiral pitch angle are the parameters to vary. Many researches exist for experimental and numerical investigations of the effect of the spiral pitch angle on the outlet temperature or the heat transfer rate of the coil (Bezyan et al., 2015; Cui et al., 2011; Dehghan et al., 2016; Kim et al., 2018; Park et al., 2012, 2015; Saeidi et al., 2018; Zarrella et al., 2013; Zhao et al., 2017). In all cases, by increasing the spiral pitch there is a reduction of heat transfer rate, and on the contrary, by reducing the spiral pitch (and hence increasing the length of the tube), the heat transfer rate is increased. There is however a point, where the thermal interference of the coils increases and the further reduction of the spiral coil will have a negative

impact on the heat transfer rate (Park et al., 2016). Another important factor to account for, is the presence of groundwater. This state can contribute as an advantageous factor for the system and improve the heat exchanger rate between the GHE and the ground (L. Aresti et al., 2016; Lazaros Aresti et al., 2016; Fan et al., 2007; Stylianou et al., 2019).

Other novel-type energy-pile GHE systems have also been explored by researchers; see for instance the truncated cone helix energy pile suggested by Huang et al. (2018). The suggested geometry is proposed to overcome the thermal interferences in radial directions with the small axial pitch of the coil. Another suggested geometry is an all-round W-type energy pile, that is a six-U-tube pipe connected in series attached on the wall of the pile (Mehrizi et al., 2016). The proposed configuration was computationally compared by the authors with the U-tube and the W-tube configuration, with results showing a greater heat transfer rate on the all-round W-tube energy pile. A different approach was examined by Saeidi et al. (2018), where the authors incorporated an energy pile with special metal rods (fins) on each axial pitch of the spiral coil. The authors investigated 5 different attachment fins (aluminium rods) using computational modelling (with the COMSOL Multiphysics software) and concluded that the suggested additional geometry could increase the heat transfer rate.

An alternative to energy piles, is given by incorporating the building bed foundation, and not the foundation piles, as a GHE. While foundation piles are not required in all constructions, a building's foundation bed is mandatory. Residential buildings foundation were also investigated by Aresti et al. (2017, 2020b) as Thermal Energy Storage (TES) unit, for seasonal heating. This configuration cannot be called energy pile since there are no piles involved, but it is still based on the principles of the energy pile. Experimental and numerical studies have been performed by Kayaci and Demir (2020), with pipes buried in and under the building foundations of a 2400m^2 building.

Buildings foundation as a GHE (such as energy piles and foundation bed GHE) have yet to be applied in Cyprus, the moderate climate country in investigation here, and thus the potential of such systems should be considered. To this end, an initial investigation on energy piles and a preliminary assessment was performed by

Aresti et al. (2019a, 2019b). The aim of the current paper is to extensively expand these preliminary findings and, in addition, to study the potential of such GSHP systems by utilizing the foundation in a moderate climate (such as in Cyprus), in the framework of a Zero Energy Building. More specifically, this paper investigates the potential of utilizing the energy foundations, namely the foundation piles and/or the shallow foundation bed, of a residential building in the Mediterranean island of Cyprus.

The rest of the chapter is organized as follows. Section 5.2 presents the characteristics of residential dwellings of nearly zero energy in Cyprus. Section 5.3 accommodates a computational model in the COMSOL Multiphysics environment for the foundation piles and/or the shallow foundation bed of a typical dwelling, with the obtained results given in Section 5.4. An economic evaluation of the studied GSHP systems is performed in Section 5.5, based on a comparison with ASHP systems, using well established payback methods. We conclude with Section 5.6.

5.2 Residential Dwellings with Nearly Zero Energy Characteristics in Cyprus

In order to select the correct heat pump or HVAC (Heating, Ventilation, and Air Conditioning) system, it is essential to calculate the heating and cooling loads of a building/ house. The selected house, as a new building, should meet – as of 2020 – the specifications based on the EU derivative 2010/31/EU (EU Parliament, 2010) regarding nZEBs. The technical characteristics of nZEBs, as described by the European Commission and the Cypriot Ministry of Energy, Commerce, Industry and Tourism (2017), are shown in Table 5.1. Thermal transmittance, expressed as U-value, describes the heat transfer rate through materials, such as the heat required to rise the temperature by one Kelvin per square meter, with lower values indicating higher insulation. The values of primary energy consumption describes the direct use of the source to the user without undergoing any transformation, therefore a conversion factor is required, as provided by the Cyprus Energy Department for different types of fuels to primary energy units (Panayiotou et al., 2010).

Table 5.1 Requirements and technical characteristics that must be met by a nZEB according to Derivative 366/2014, modified from (Ministry of Commerce Industry and Energy Tourism, 2017)

Requirements	***Minimum value***
Energy performance certificate of a building	A
Maximum primary energy consumption in residential buildings	100 kWh per m^2 per year
Maximum energy demand for heating for residential buildings	15 kWh per m^2 per year
Renewable Energy Sources percentage of the total primary energy consumption	25%
Construction elements	***Maximum U-value***
External walls and load-carrying elements (pillars, beams and load-carrying walls) that are part of the building envelope	0.4 W m^{-2} K^{-1}
Horizontal building elements (floors in a pilotis, floors in a cantilever, terraces, roofs) and ceilings that are part of the building envelope	0.4 W m^{-2} K^{-1}
Door and Window frames that are part of the building envelope	2.25 W m^{-2} K^{-1}

As it would not be efficient to collect a large sample of dwellings in Cyprus based on the area, orientation, construction materials and type, it would be therefore sensible to examine the typical dwelling characteristics in the whole island of Cyprus. According to CyStat (2016), the average area per dwelling for the year 2016 was 212.3 m^2, while in the year 2015 it was 193.5m^2. By observing dwelling units over a period of more than 10 years, new residential buildings have hit a minimum in the year 2014, with numbers starting to increase thereafter, as seen in Figure 5.1. The single unit houses are for the last 10 years very close in numbers to the dwelling units of buildings with two or more housing units. It is also worth noting that all new dwellings (100%) have installed a solar water heater based on the report of CyStat (2016). A more in depth review of the dwellings in Cyprus can be found in the Panayiotou et al. (2010). As reported by the authors, single houses represented the dominant type of dwellings in Cyprus, with 68% over all residential buildings up to the year 2010, despite the increase of dwelling units per year for buildings with two or more houses, since more units are built per year.

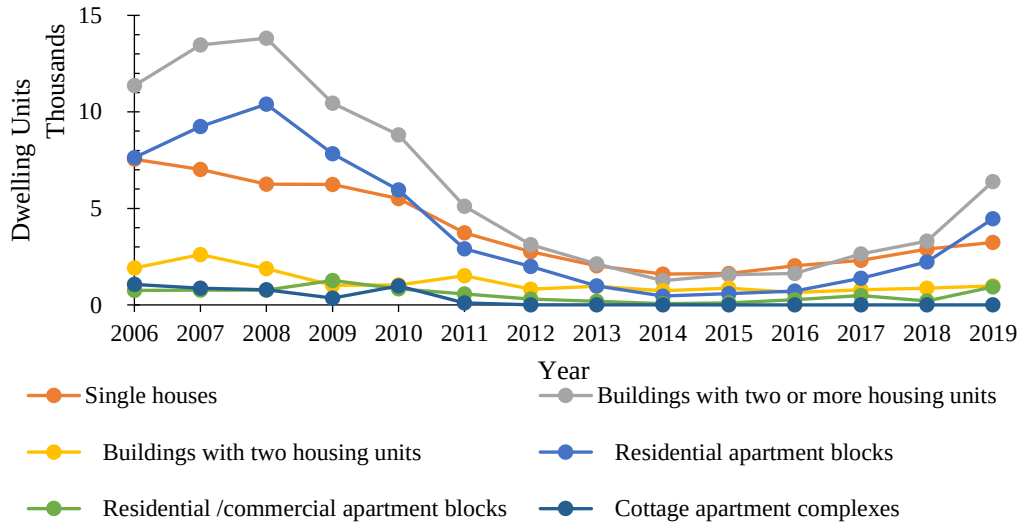

Figure 5.1 Residential buildings, dwelling units per year

Figure 5.2 presents the trend of the average area per single house up to the year 2019. It could be seen that although the single housing units were higher between 2006 and 2010 than after, the average area per single house was then smaller than now. This could potentially be explained through the status of the economic stability of Cyprus, but it is beyond the scope of this study to further examine this. Since the year 2012 the average area per single house has been between 260 m^2 and 270 m^2, with an average of 266m^2, one of the highest average areas per dwelling in the European Union (European, 2016), with an average household size of 2.7 people living in the same dwelling.

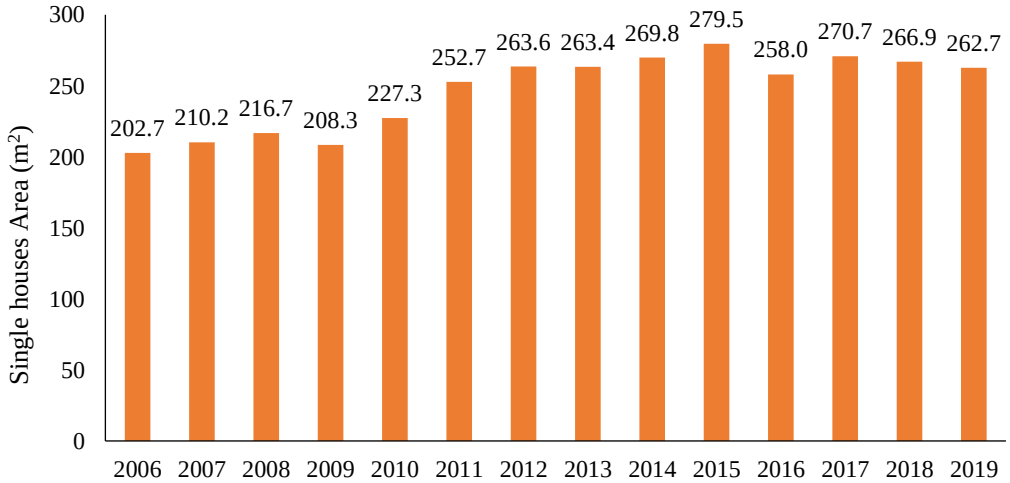

Figure 5.2 New residential dwellings, single houses average area per Year, derived from CyStat (2016)

5.2.1 Typical construction, with heating and cooling loads in Cyprus

Heating and cooling loads depend primarily on the climate of the area. Climate in Cyprus is characterized as intense Mediterranean with long dry summer of high temperatures (that can reach 40^{o}C or higher) between the mid-May to mid-September. Mild winter is noticeable from November to mid-March, between short autumn and spring seasons with rapid weather changes. The Cyprus Energy Service, for calculations reasons, has separated Cyprus into 4 climate zones: the coastal zone, the inland zone, the semi –mountains zone (up to 600m altitude), and the maintains zone (over 600m altitude) (Cyprus Energy Service, 2009).

The impact of the Energy Performance Building Derivative (EPBD) EU derivative 2010/31/EU has caused the typical masonry construction in Cyprus to change towards an improved thermal insulation for the dwellings. A typical masonry, roof and floor construction before and after the 2010/31/EU was presented by Fokaides et al. (2014). In the past, a typical external wall construction was comprised by a 200mm brick and 25mm plaster on each face, while with the new legislation two constructions can be found, with the use of perforated thermal brick and polystyrene as an insulating material (see Table 5.2 below).

Table 5.2 Typical Masonry and roof constructions in Cyprus, information derived from Fokaides et al. (2014)

	Material	***Thickness (mm)***	***U-values (W m^{-2} K^{-1})***
External wall			
Typical External wall Before EPBD	Plaster	25	1.388
	Brick	200	
	Plaster	25	
Typical External wall After EPBD – Configuration [1]	Plaster	25	0.581
	Perforated Thermal brick	300	
	Plaster	25	
Typical External wall After EPBD –	Plaster	25	0.318
	Insulation material (polystyrene)	50	

Configuration [2]	Perforated Thermal brick	250	
	Plaster	25	
Roof			
Typical roof ***Before EPBD***	Trowel	10	3.252
	Reinforced concrete	150	
	Screed	100	
	Waterproofing layer	5	
Typical roof ***After EPBD***	Trowel	10	0.274
	Reinforced concrete	150	
	Insulation material (polystyrene)	100	
	Screed	100	
	Waterproofing layer	5	

A residential building with an area of 190m^2, in moderate climate, was used in the study of Christodoulides el al. (2019), taking heating and cooling loads from Pouloupatis et al. (2014) and choosing a heat pump that matches the specific characteristics with its variable pump capacity over power input (Pouloupatis et al., 2017). The specific case, although an existing house and hence a realistic scenario, does not cover the scenario of any new buildings with nZEB characteristics, neither covers the new "trend" of multi storage/ multi-family buildings.

Although the nZEB construction would be a mandatory requirement, it comes with a high initial construction cost. Several incentives were endorsed from most EU countries, for encouragement to an upgrade of the current buildings into high energy efficient constructions. Serghides et al. (2015) have presented an investigation for converting an old single residential building into a nZEB with different scenarios in Cyprus. The results demonstrated that a roof insulation is the most cost-effective measurement, with a reported payback period of less than 2 years. The overall initial investment to a nZEB is noted at €9250 with a payback period of 7-8 years. Similar finding were observed in Greece by Alexandri and Androutsopoulos (2017), when investigating the payback period, of transforming an existing typical dwelling into a nZEB. Different materials and techniques were

considered by the authors with suggestions on the most effective selections. Payback periods for as low as 3 years are reported by the authors. An affordability assessment of Energy-Efficient Building Construction in Italy was addressed by Manganelli et al. (2019) with a different approach. The authors have viewed this investment from the angle of an entrepreneur in the building sector rather than the owners' side. The investigated cases have shown that retrofitting an existing building (increasing its energy efficiency) does not provide any benefits in the property value, which is in contrast with newly build buildings.

5.2.2 Selected dwelling with typical load for a nZEB

The selected case scenario here is a residential building in Lefkosia, Cyprus (Zone 2 – Low mainland area). The masonry and the roof of the building are in accordance to the nZEB characteristics (as described in Table 5.2) with U values of 0.318 and 0.274 respectively. The area of the residential building was chosen at 260m^2, based on the single houses trend discussed earlier in the section, and is occupied by a family of 4. The residential building was separated into 7 zones, consisting of three bedrooms, a kitchen, a living room, a bathroom, and a dining room. The heating and cooling load of the building were calculated using the TRNSYS software and, in specific, with type 56 – Multi-Zone building module. Figure 5.3 presents the heating (positive values) and cooling (negative values) loads of the investigated residential building. The peak heating load is estimated at 2.99 kW (i.e., 11.51 W m^{-2}, for the 260m^2 residential building under investigation), whereas the peak cooling load is at 7.22 kW (i.e., 27.78 W m^{-2}, for the 260m^2 residential building under investigation). It is clearly a higher cooling demand area with a total of 2150 kWh of heating load and a 11600 kWh of cooling load. The higher demand months are February for winter season, with 712 kWh heat demand, and July for summer season, with 2882 kWh cooling demand.

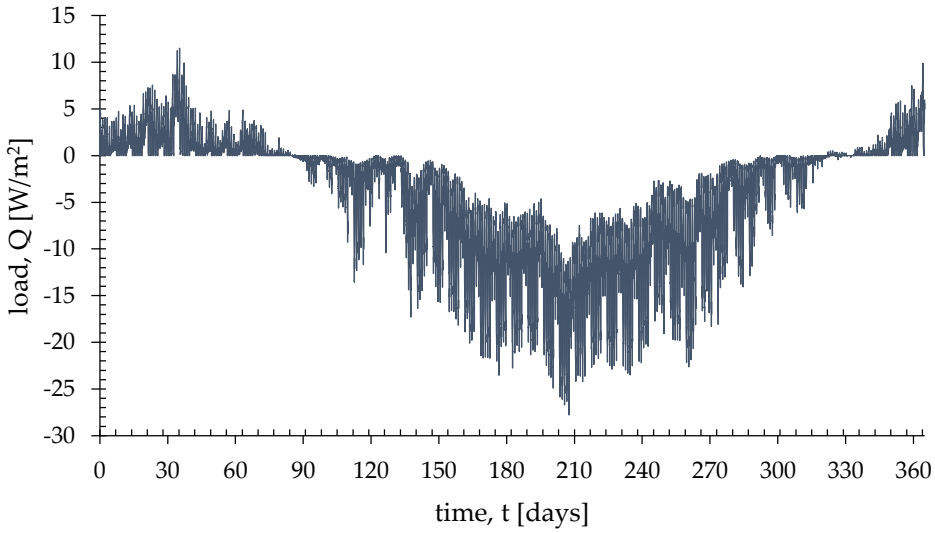

Figure 5.3 Heating and Cooling loads of a typical residential building with nZEB technical characteristics in Lefkosia, Cyprus, per square meter

5.3 Computational Modelling

To examine a GHE system, one can perform either physical experiments or computational investigations. In general, the sheer experimental set-up and testing of a GHE is expensive and time consuming, therefore a computational investigation is preferable. Here a numerical model using the COMSOL Multiphysics software based on the convection-diffusion equation (see Chapter 4) is introduced. The three-dimensional conservation of the transient heat equation for an incompressible fluid is used:

$$\rho c_p \frac{\partial T}{\partial t} + \rho c_p u \cdot \nabla T + \nabla q = Q \qquad 5.1$$

where ρ is the density, c_p is the specific heat capacity at constant pressure, T is the temperature, t is the time, u is the velocity, Q is the heat source, and q comes from the Fourier's law of heat conduction. The second term that includes velocity, is only referring to the domain where groundwater flow is present and does not apply to the rest of the domains.

Depending on the case, the three-dimensional model consists of the pipe domain, the reinforced concrete (either foundation pile of foundation bed) and the ground domain. Modelling and simulation of full-scale geometries for the GHEs can be

challenging, since there is a high scale difference between the depth (the *z*-axis) and the borehole and pipe diameter (*x*- and *y*-axes). Due to the high aspect ratio (i.e., the high scale difference between two dimensions as discussed above), meshing the model with equilateral cells will require high computational time and memory.

Existent computational methods could overcome this issue by either applying a coordinate scaling system (L. Aresti et al., 2016) or by applying parallel computational 1D running with a simplified version (see Equation 5.2) on the pipes and Equation 5.1 on the rest of the system:

$$\rho A c_p \frac{\partial T}{\partial t} + \rho A c_p u e_t \cdot \nabla_t T = \nabla_t \cdot (Ak\nabla_t T) + \frac{1}{2} f_D \frac{\rho A}{d_h} |u| u^2 + Q_{wall} \quad 5.2$$

where A is the area of the pipe, ue_t is the tangential velocity, f_D is the Darcy's friction factor based on Churchill friction model and d_h is the diameter of the pipe. Q_{wall} can be described with the heat conduction equation:

$$Q_{wall} = \left(h_p Z\right)_{eff} (T_{pipes} - T_{fluid}) \quad 5.3$$

where T_{pipes} is the temperature at the pipe wall, T_{fluid} is the fluid temperature in the pipes and $\left(h_p Z\right)_{eff}$ is the heat transfer coefficient; where Z is the pipes wall perimeter.

The following set of heat equations are used to evaluate the input heat on the GHE:

$$Q = \dot{m} c_p \Delta T, \;\; Q_{cond} = Q_{evap} + P_{comp}, \;\; COP = \frac{Q_{cond}}{P_{comp}}, \;\; Q_{evap} = Q_{cond}\left(1 - \frac{1}{COP}\right) \quad 5.4$$

where $\dot{m}$ is the mass flow rate, ΔT is the temperature difference between the outlet (T_{outlet}) and the inlet temperatures (T_{inlet}) of the GHE, Q_{cond} is the heat of the condenser, Q_{evap} is the heat of the evaporator, P_{comp} is the input work from the compressor and COP the Coefficient of Performance. The geometry models were constructed using the build-in environment of COMSOL Multiphysics with two different foundation types constructed.

5.3.1 Energy Pile

Figure 5.4 illustrates the geometry of the model serving as a study-case, where the spiral coil can be observed as a line in a 3D environment. As the computational processing power and memory are limited, one has to perform a computational investigation on different total mesh elements and different time-dependent solutions. By focusing on a less dense mesh (fewer mesh elements) the quality of the results is altered, therefore a combination of high-quality mesh cells with denser mesh on the study area is used to lower the computational time and memory. The configuration of the energy pile and the dimensional characteristics are defined in Table 5.3.

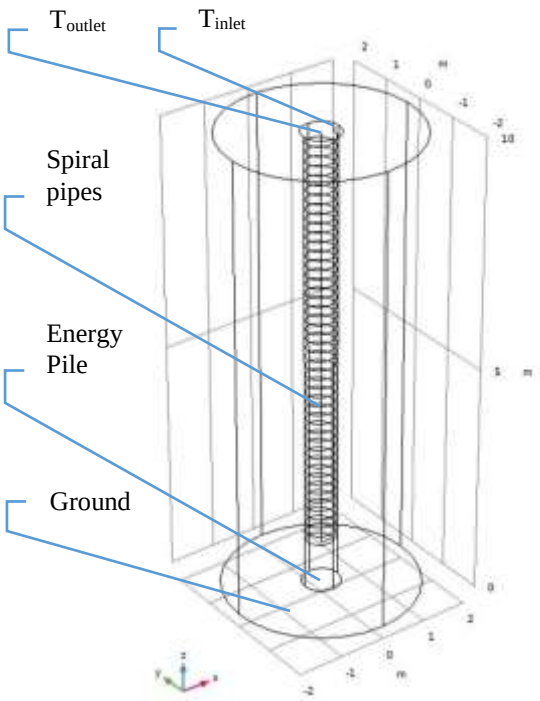

Figure 5.4 Model Geometry of Energy Pile

Table 5.3 Energy Pile model dimensional characteristics and operating parameters

Energy Pile Model Characteristics	
Energy Pile length	10 m
Energy Pile diameter	0.8 m
Spiral Coil diameter	0.6 m

Spiral Coil length	9 m
Spiral Coil pitch	0.2 m
Coil tube diameter	32 mm
Coil tube thickness	3 mm
Domain/ Ground diameter	4 m (5 × Energy Pile diameter)
Flow rate	10 L/min
Total Pipe length	85.3 m

5.3.2 Foundation bed GHE

Besides the foundation pile, the most-commonly used foundation element is the foundation bed, which can also be converted into a hybrid system and perform as a GHE. In almost all dwellings in Cyprus there is a foundation bed present, therefore making it an ideal element for conversion into a hybrid GHE system. As the foundation bed is not primarily designed as a GHE, it has to be constructed according to the geometry and the required strength characteristics set by the civil engineers. A further discussion of those effects of a hybrid foundation bed system was performed by Aresti et al. (2020b). Figure 5.5 demonstrates the geometry of such system. The material used are kept the same as in the case of the Energy Pile. The configuration of the foundation bed and the dimensional characteristics are defined in Table 5.4.

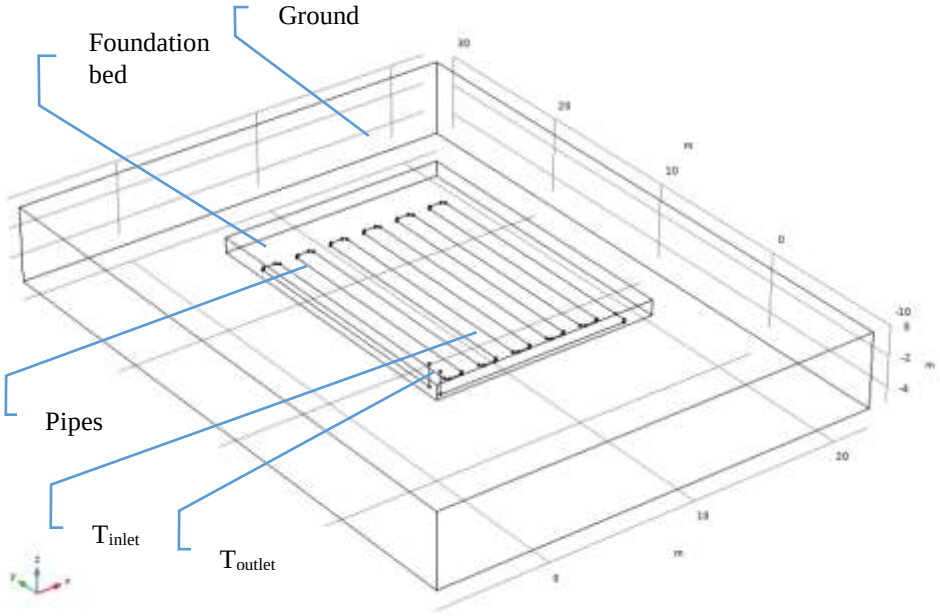

Figure 5.5 Foundation bed GHE geometry

Table 5.4 Foundation bed dimensional model characteristics

Foundation Bed Model Characteristics	
Foundation bed (length × width)	15 × 10 m
Foundation bed depth	1 m
Pipe diameter	32 mm
Pipe thickness	3 mm
Flow rate	10 L/min
Total pipe length	220 m

5.3.3 Computational Verification and Validation

In order to perform a computational investigation, it is of importance to provide a verification and a validation model with experimental results. COMSOL Multiphysics was used for a three-dimensional model consisting of the spiral pipe domain, the grout domain (borehole) and the ground domain with its sublayers. The same computational model with its boundary conditions for the energy pile of Sub-Section 5.3.1 is adapted to the actual parameters taken from experimental data by Dehghan (2017). The model constructed is based on the convection-diffusion

equation (described by Equations 5.1 and 5.2), with the following parameters/conditions: pipe radius of 0.014m, pipe thickness 0.003m, borehole depth 4m, borehole diameter 0.45m, spiral pitch 0.1m, volumetric flow rate 15 l/min, initial ground temperature 18°C, and the inlet temperature as fixed at 50.7°C. Experimental data were obtained using a Thermal Response Test (TRT), a conventional test for determining the ground thermal characteristics (Christodoulides et al., 2016). Figure 5.6 shows the validation of the model by comparing experimental and computational data. The overall validation indicates a very good agreement between the experimental and computational data, excepting the first 10 hours of the model run; this can be due to the lack of detailed information from the experimental data, as only average values were provided. All in all, it is safe to assume that the computational model is accurate enough to predict the outcome of the systems under investigation.

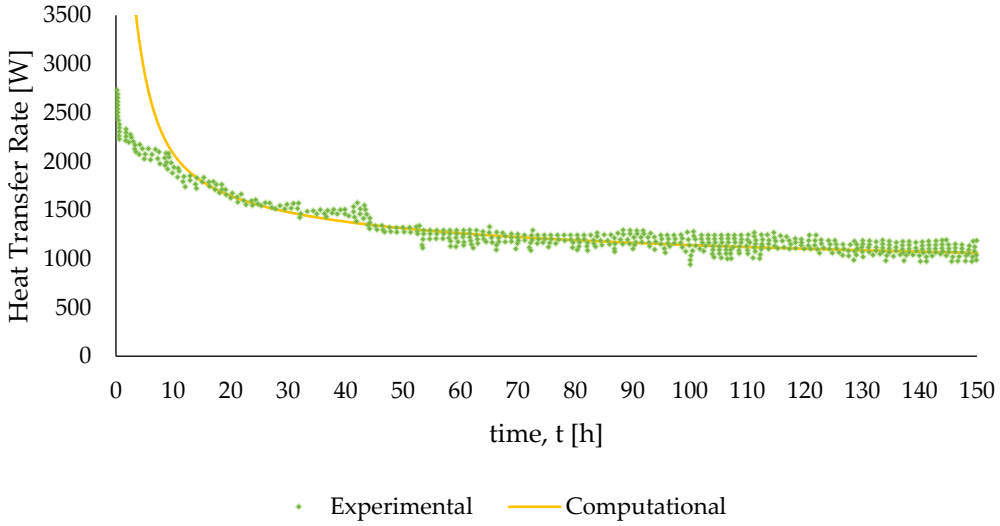

Figure 5.6 Experimental validation of computational model for a spiral GHE

5.4 Computational Results and Discussion

The computational models could be then modified to incorporate a theoretical case scenario of a foundation pile GHE and a foundation bed GHE installed in a residential building in Cyprus for moderate climate conditions. The validated models are subsequently adapted to match the Mediterranean conditions in Cyprus.

5.4.1 Energy piles

The energy pile model (seen in Figure 5.4) consists of a 10m depth foundation pile with reinforced concrete, a 0.8m pile diameter, a 9m depth spiral HDPE (High Density Poly Ethylene) coil contained in the foundation pile and an overall domain of a 4m diameter. Note that a similar configuration was installed at the new public university library in Lemesos, Cyprus, where the spiral coil GHE was incorporated in a well.

In order to obtain more accurate and realistic results, experimental ground temperature data were considered, where the temperature below a depth of 7m is constant at 22.7 ˚C (Pouloupatis et al., 2011; Stylianou et al., 2019). The same temperatures are observed in a similar case in Lemesos by Florides et al. (Florides et al., 2011). Additionally, based on the current calculated loads, a GSHP was selected (LM series by BOSCH) to calculate the COP of the system. The COP varies depending on the entering fluid temperature, as shown in Figure 5.7.

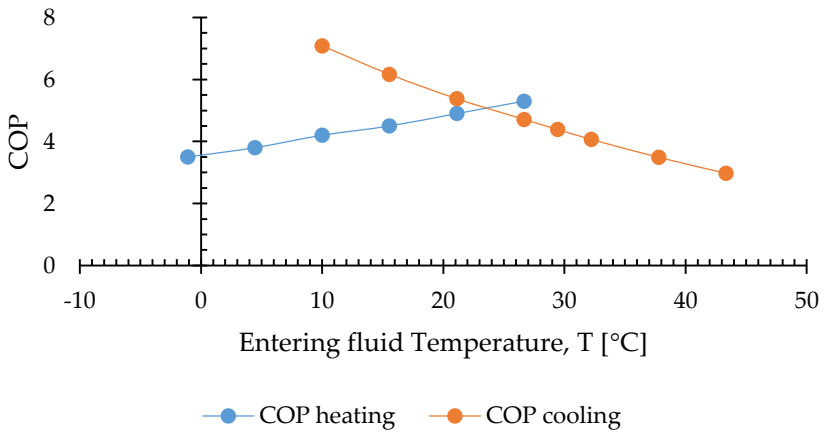

Figure 5.7 Heat pump COP in accordance to the entering fluid temperature, derived from manufacturers' catalogue

The equation of the undistributed ground temperature is used as input for the initial temperature in the computational model as presented by Stylianou et al. (2019). The case of summer was examined for the month of July, and of winter for the month of February. This selection is based on the fact that the highest loads are observed during those months. Furthermore, the ground characteristics of the case study in Lefkosia are considered (Ramos et al., 2019a, 2019b). The ground examined

consisted of marl, chalk and gravel, with the complete model material properties described in Table 5.5.

Table 5.5 Material properties

Material	***k*** ***W m^{-1} K^{-1}***	***ρ*** ***kg m^{-3}***	***c_p*** ***J Kg^{-1} K^{-1}***	***Description***
Ground	1.4	2300	950	Marl, chalk and gravel
Grout/ foundation	1.628	2500	837	Reinforced concrete
Pipes	0.42	1100	1465	HDPE
Circulating Fluid	0.6	998.2	4182	Water

A foundation pile system does however contain more than one pile, and this number is depended on the study of the civil engineer. For this specific case, 4 energy piles were incorporated into the system with all 4 working in parallel. The computational results of an energy piles system using COMSOL Multiphysics for the months of February and July are presented in Figures 5.8 and 5.9. The results of the outlet temperature are used to calculate the COP of the heat pump, where the lower the outlet temperature of the coil (entering the pump), the higher the pump efficiency (Pouloupatis et al., 2017).

It can be observed in Figure 5.8, that the operating outlet temperature is between 18°C and 21 °C, providing a high COP on the highest load month of winter at 4.8. The COP is, naturally, fluctuating depending on the required load, with a minimum COP of 4.7. It should be noted that, although the system is performing ideally, the peak load is at 3 kW and the total load of the month is only at 712 kWh. This change in the load can be observed in the summer months, and more specifically in the month of July, where a higher peak load is required, 7.22 kW, and a total month load of 2882 kWh. This is essentially 4 times the load of the highest winter month, February.

The results on the energy piles system with the summer month load is presented in Figure 5.9. During the initial test with the system of 4 energy piles, it can be seen that the temperature was nearly steady up to the 16th day, but with the higher load demand in the end of the month, the outlet temperature rose up to 30 °C.

Conventional outlet operating temperature ranges between 26°C and 28°C, as suggested by an existing conventional GHSP system in the public university Library in Lemesos. Therefore, the 4 energy piles system, although providing a higher outlet temperature, does maintain a high COP (4.4–4.7). Further examination was carried out by raising the number of energy piles in the system to investigate whether the additional piles could sustain the higher summer load. An increase of the piles to 6 or 8 does result in, as expected, a reduction in the outlet temperature and higher COP values (Figure 5.10). This is however a decision that is not depended on the buildings HVAC requirements but on structural reasons. Hence, if more foundation piles are used in the system, the GSHP system could maintain a higher COP values and higher loads.

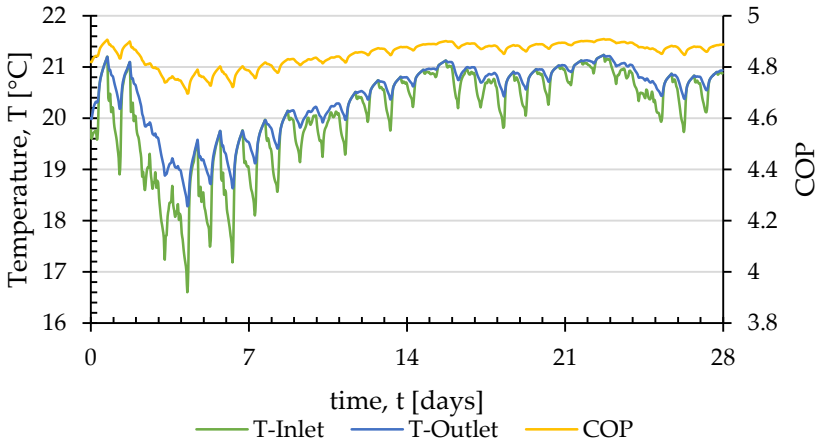

Figure 5.8 Energy pile temperatures and performance for the month of February

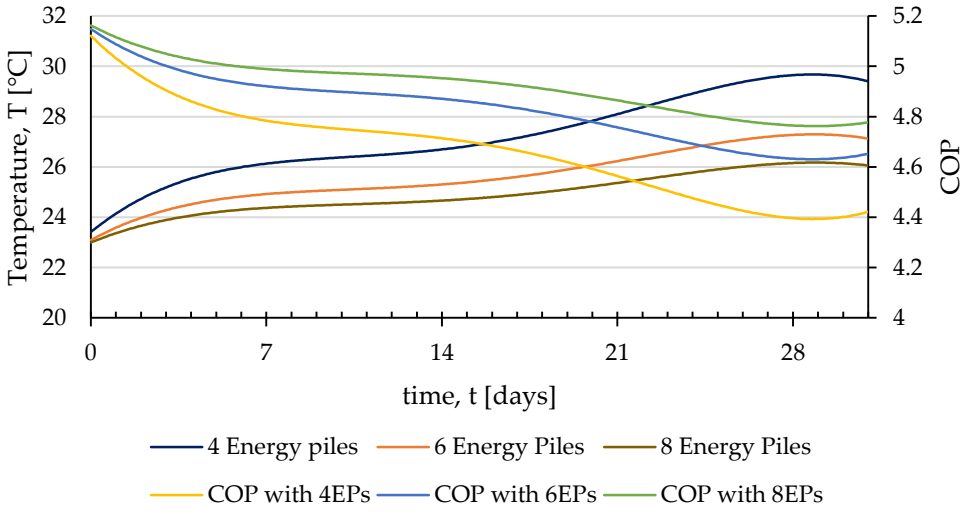

Figure 5.9 Outlet temperatures and COPs for 4, 6 and 8 Energy Piles for the month of July

Regarding the effect of parameters, out of several parameters, as mentioned above (e.g., borehole diameter, centre-to-centre distance, pipe diameter, etc), the spiral pitch is one that does not depend on the geo-structure. Decreasing the spiral pitch yields an increase in the outlet temperature of the pipe and a reduction in the heat transfer rate, as recorded by Carotenuto et al. (2017) and Park et al. (2016, 2015).

5.4.2 Foundation bed

In the case where the foundation piles are absent (not included in the design of the building), the foundation bed could eventually be used as a GHE. The foundation bed is a most common element in the residential buildings in Cyprus. The same heating and cooling loads and the same ground characteristics as for the energy pile system are used for the computational investigation of the foundation bed as a GHE. A major difference in this case, is the very shallow depth of the system (1m), making it liable to the ambient daily temperature. The ambient temperature was therefore applied as a boundary condition on the top surface of the ground domain with temperature data from the year 2019.

The results of the outlet temperature and COP of the foundation bed as a GHE are presented in Figure 5.10. In both cases, winter (February) and summer (July), the system appears to have a steady performance for the outlet temperature, providing a high COP; at 4.6 during winter, and 4.8 during the summer.

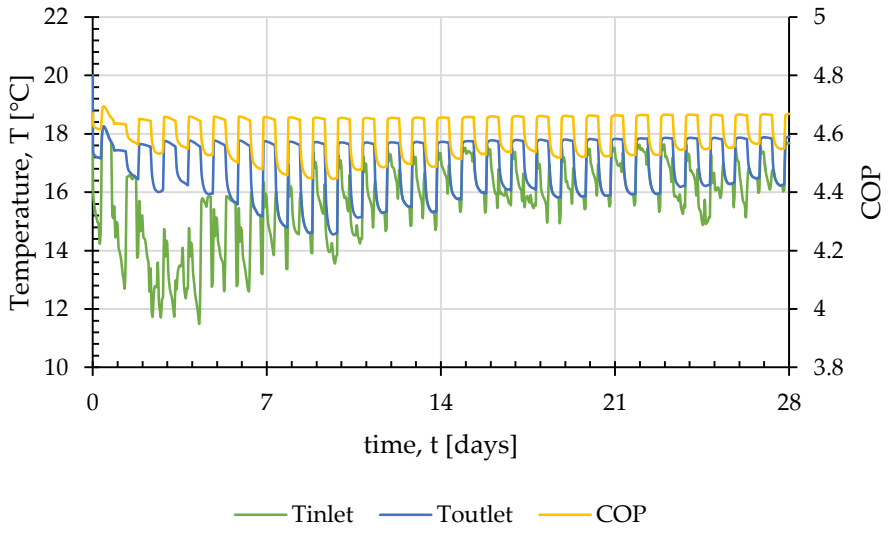

(a)

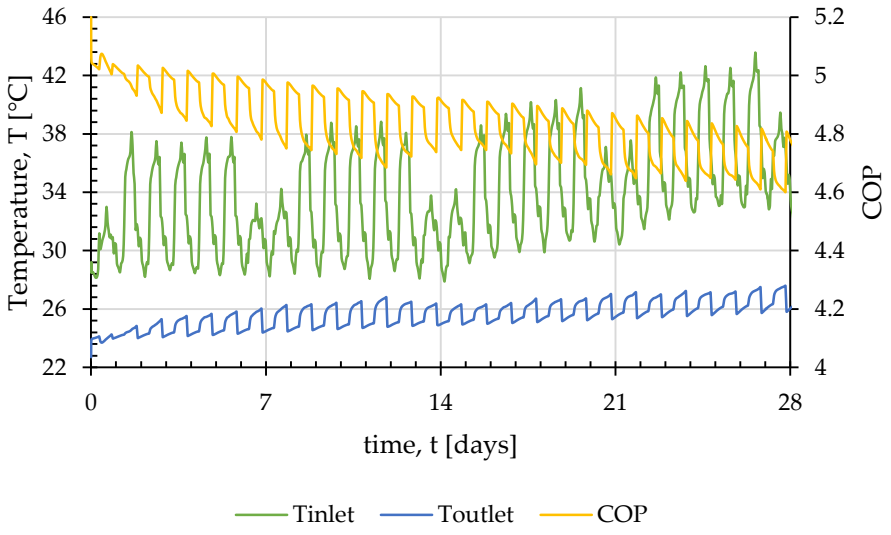

(b)

Figure 5.10 Foundation bed temperatures and performance for the months of (a) February and (b) July

An aspect that should be examined is the raise of the temperature of the surface in contact with the indoor space (on the house floor). A raise of the house contact surface temperature would have a negative impact of the cooling loads, since the heating energy rejected under the house would return through the foundation bed. This could be easily addressed with an insulation on the floor of the house, the same method applied on the roof.

A comparison on the performance of the foundation bed system with the energy piles system is presented in Figure 5.11 for both summer and winter conditions. The foundation bed as a GHE is observed to have a steady performance, something very desirable in a system. This however comes in a lower performance compared to the energy piles system, where higher COP values are provided during the winter, albeit failing to deliver the same efficiency during the summer.

This comparison however is not unbiased since one system (foundation bed) can be characterized as a horizontal system with larger area, and the other (energy piles) as a vertical system with limited depth. In reality, the main interest is not which system would perform best, but whether the systems could be used as hybrid element (GHE and buildings foundation) in a residential building, according to the

applied construction. In this respect, it is safe to say that both systems accomplish worthy performance as GHEs in a GSHP system.

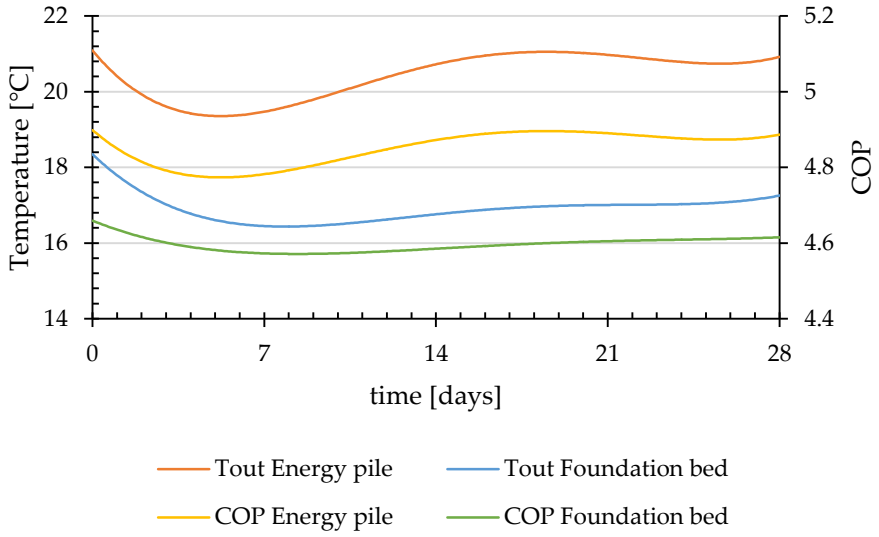

(a)

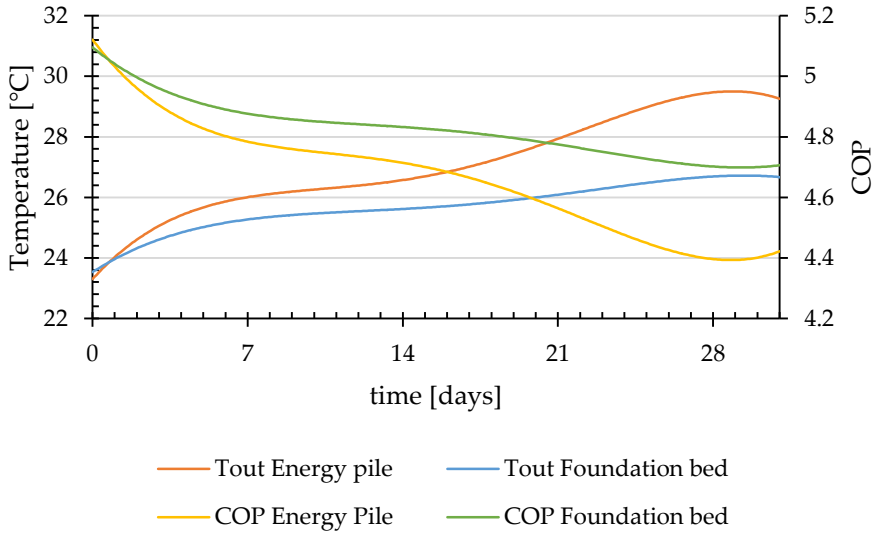

(b)

Figure 5.11 Performance comparison between the two types for the months of (a) February and (b) July

5.5 Economic Evaluation

Every (energy) system, even a RES, is only acceptable and widely applicable when the system is viable and economically beneficial for the user/ investor. It is therefore advisable to examine not only the performance of a GSHP system, but

also its economic sustainability and its optimal performance cost. Even though GSHPs have higher performance in comparison to the Air Source Heat Pumps (ASHPs), the systems high initial costs and long payback period have rendered them not so attractive as an investment (Blum et al., 2011; Christodoulides et al., 2019). It was reported by several authors that greater performance of a GSHP system could be achieved using spiral coil / energy piles in comparison with conventional ASHP systems (Cui et al., 2018; Park et al., 2015; Yoon et al., 2015b, 2015a; Zhang et al., 2017).

Yoon et al. (2015b) compared three different configurations, W type, 3U type and spiral coil type, for an energy pile system installation in terms of thermal characteristics and costs. The energy piles were considered to have the same load of 57kW, the same depth of 13.5m, and the same COP of 4.7. The results indicated that the coil type configuration required the least amount of piles to be installed, but at the same time the highest construction cost, approximately three times the cost of the W type heat exchanger. The authors mentioned that the 3U-tube and W type heat exchangers increase the number of piles by 20–30% in comparison with the spiral coil heat exchanger pile. It is however worth stating that the cost of the GHE is only 1% of the total cost of the construction.

To determine the optimal coil pitch, the long term heat exchanger rate and the economic feasibility were considered by Park et al. (2016). The authors varied the coil pitch as 100, 200, 350 and 500 mm, but kept the pile depth steady, hence decreasing the pipe length (475m, 240m, 160m, and 101m respectively). The authors found that the heat transfer rate of the pile increased with the reduction of the coil pitch, but at the same time the construction cost ratio (material cost and the installation) increased. The authors also accounted for the operating cost by considering an 8-hour daily operation time with 3 months heating operation and 3 months cooling operation. This resulted in payback periods of 2.00, 1.29, 1.14, and 1.09 years for the different coil pitches of 100, 200, 350 and 500mm respectively. Therefore, although the best configuration in terms of heat transfer rate is the minimum coil pitch (100mm) in terms of cost benefit it returns the highest payback period. The authors also noted that the optimum coil pitch should be considered with the ground conditions and the operation cost taken in account.

The initial cost comparison of two different GHEs, namely the double U-tube and the spiral tube, were investigated and presented by Suzuki et al. (2016), in accordance to the heat exchanging capacity. The authors studied depths of 10m and 20m for spiral GHEs and a 70m for the double U-tube. The results indicated a reduction of 30% in the initial cost per collected quantity of heat when the spiral tube was used over the double U-tube. Another economic study under cooling dominated condition was presented by Akroush et al. (2020). The authors presented the Present Value and reported a 13-year Simple Payback Period by comparing ASHP system with a GSHP system. This value, although less than the estimated lifespan of a GSHP (estimated at 25 years), did not make it attractive as an investment.

An economic evaluation of the sustainability of a typical GSHP system under moderate climate in Cyprus was explored and discussed by Michopoulos et al. (2016). The authors explored different dwelling cases (single-family building and multi-family building) in 5 different areas of Cyprus (Nicosia (Lefkosia), Larnaca, Limassol (Lemesos), Paphos and Saittas). European standards were used for the methodology to calculate the Net Present Value (NPV) with an economic lifetime of 15 years. The authors presented the results in comparison with an ASHP system with either LPG or oil-fired boiler and stated that in the case of a single house, a GSHP system is only economically profitable for the area of Saittas, the area with the highest heating demand. In the second case of a multi-family building, Saittas area was again a very favourable solution for GSHPs as were the cities of Nicosia and Larnaca. Similar findings were observed by Christodoulides et al. (2019) who studied a single family house with specific heating and cooling loads, with a selected case specific heap pump COP values. The authors presented different methods to evaluate the economic benefits of a GSHP system that resulted in long payback periods for all cases, making the GSHP system not economically favourable.

5.5.1 Economic evaluation of a residential building as a GHE results

The above-mentioned cases and related literature point to the initial cost as the main drawback of these (GSHPs) highly efficient systems. Therefore, the conversion to a

hybrid system of an existing element in the house, such as the foundation, would have a significant impact in lowering the initial costs. In order to verify this rationale, the initial and running costs of the foundation GSHP system studied in the current chapter were compared with a typical ASHP system.

Several methods could be used to evaluate the economic benefits of the system, such as the Present Worth (PW), the Annual Worth (AW), the Internal Rate of Return (IRR), the External Rate of Return (ERR), the Simple Payback Period (SPP), the Discounted Payback Period (DPP), the Annualised Life Cycle Cost (ALCC) method, the Levelized Cost of Energy (LCOE) [29] and the equivalent Total Annual Economic Cost (TAEC), with a brief explanation and application of the methods provided in the literature (Lu et al., 2017; Ouyang and Lin, 2014; Tassou et al., 1986; Tsagarakis, 2007).To simplify the study, only the difference in the costs of the two systems was used in the calculations.. The cost breakdown of the systems is described in Table 5.6. As it can be seen, the costs related to grout filling and for borehole extraction are not included since the building foundation would be constructed in any case, therefore no costs are added. The cost of the heat pumps (HPs) was estimated based on the local market (as of year 2020) at €8500 for a high-efficiency ASHP, €4500 for a low-efficiency ASHP and at €6500 for a GSHP.

Table 5.6 Typical extra cost values for the installation of a GSHP

Item	***Energy Pile single***	***Energy Pile ×4***	***Foundation bed***
U-tube GHE Φ 32mm (6 €/m)	341	1365	1320
Header-flowmeters-valve		400	
Horizontal pipe circuits		300	
Difference from a high-efficiency ASHP price (low-efficiency ASHP)		–2000 (+2000)	
General expenses / Labour	250	1000	1000
Total (€) compared to high-efficiency ASHP	-709	1065	1020
Total (€) compared to low-efficiency ASHP	3291	5065	5020

Furthermore, the cost difference was used as an input to evaluate the economic benefits of the system. The simple methods for computing the payback period require to equal the inflow and outflow cash per year, as described by the SPP and DPP (Christodoulides et al., 2019). The inflation of the electricity price, the maintenance and the discounting future cash flow (Sullivan et al., 2014) are incorporated, and the current household electricity price in Cyprus is considered as 0.19€/kWh. The COP values are estimated per hour for each month for one year and are presented in a polynomial form of order of 6 in Figure 5.12. Both systems exhibit similar behaviour, where it can be seen that in the high load months (as in the case of February and July) the COP values drop, and higher values are observed in the less demanding months (April and November). The lifespan of the HPs was assumed at 12 years for both the ASHPs and the GSHPs. Table 5.7 describes the average COP of each system per month and the total input electrical energy required per year for the modelled typical residential building. The overall yearly average COP for the foundation bed is 4.90, with an average of 4.73 during the winter and 5.00 during the summer. On the other hand, the energy pile system exhibits a higher COP, compared to the foundation bed system during winter with values of 4.84, and a lower one during the summer mode with a value of 4.97. An overall yearly average of 4.94 is estimated.

The GSHP systems are assumed to replace an ASHP system with either high or low efficiency. The high-efficient ASHP system is assumed to have a COP of 3.0 during heating mode (winter) and 3.7 during cooling mode (summer), whereas the low-efficient ASHP system is assumed to have a COP of 3.0 and 2.5 for summer and winter respectively. By considering the heating and cooling loads of the residential building under investigation (2150 kWh in winter and 11600 kWh in summer) the input electrical power required is 3852 kWh and 4727 kWh for the high- and low-efficient ASHP respectively. The difference between the required consumption of the ASHP system from the GSHP system characterizes the savings achieved per year. Savings of 1003 kWh and 967 kWh are estimated for the foundation bed and the energy pile GSHP systems respectively, compared to a high-efficient ASHP system. Savings of 1878 kWh and 1842 kWh are estimated for the foundation bed and energy pile GSHP system respectively, compared to a low-efficiency ASHP

system. Table 5.8 presents the energy savings as equivalent financial savings in order to allow one to investigate the systems as an investment. The initial cost to compensate are the values from Table 5.6, whereas the total savings per year column assumes the electricity savings with the current electricity unit price, and the savings for maintenance and end-of-life heat pump replacement. Two methods are presented, namely the SPP and the DPP with three further variations. The SPP has been varied with a 2% increase of the electricity price, whereas the DPP has been varied with a 2% and 5% electricity price inflation.

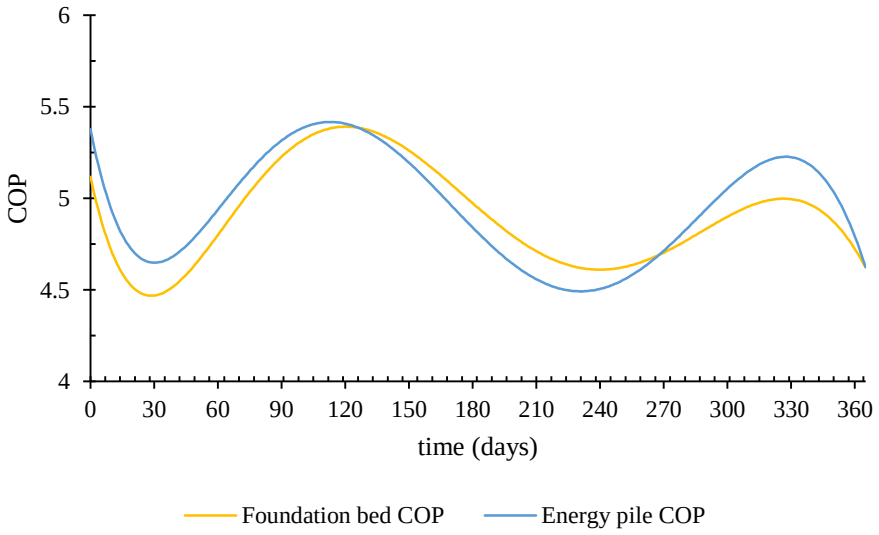

Figure 5.12 Estimated COP for the foundation bed and the energy pile systems

Table 5.7 Month and yearly, average COP and input electrical energy for the two GSHP systems

	Heating (kWh)	***Cooling (kWh)***	***Foundation bed COP (average)***	***Foundation bed input electrical energy (kWh)***	***Energy Pile COP (average)***	***Energy Pile Input electrical energy (kWh)***
January	709	0	4.71	151	4.91	144
February	712	0	4.60	155	4.76	150
March	205	7	4.75	43	4.73	43
April	0	376	5.63	67	5.67	66
May	0	809	5.33	152	5.45	148
June	0	2076	5.07	409	4.86	427
July	0	2882	4.83	597	4.66	618
August	0	2733	4.61	593	4.51	606

September	0	1909	4.64	411	4.56	419
October	0	687	4.88	141	5.06	136
November	9	121	4.96	24	5.19	23
December	514	0	4.85	106	4.96	104
Total (kWh)	**2150**	**11600**		**2849**		**2885**

Table 5.8 SPP-DPP results for the two GSHP systems compared to high and low efficient ASHP system

Type	***Cost to cover (€)***	***Total Savings per year (€)***	***SPP (years)***	***SPP with 2% EP inflation (years)***	***DPP 2% (years)***	***DPP 2%, with 2% EP inflation (years)***	***DPP 2%, with 5% EP inflation (years)***	***Cash flow Return Rate per year (%)***
Energy Piles GSHP system compared to ASHP with high COP (3852kWh)	1065	517	2.06	2.04	2.12	2.10	2.06	48.11
Foundation Bed GSHP system compared to ASHP with high COP (3852kWh)	1020	524	1.95	1.93	2.01	1.99	1.95	51.01
Energy Piles GSHP system compared to ASHP with low COP (4727kWh)	5065	683	7.41	6.97	8.10	7.56	6.89	8.31
Foundation Bed GSHP system compared to ASHP with low COP (4727kWh)	5020	690	7.27	6.85	7.94	7.42	6.77	8.69

By examining the results (seen in Table 5.8) for the SPP and the DPP, it can be clearly seen that the investment and risk is worth taking. A maximum SPP of 7.41 years was observed on the Energy Pile system with the worst overall case noticed at a 2%-DPP of 8.10 years. The SPP and DPP values of the conversion foundation bed into a GHE are even lower, with less than 8 years, in comparison with a low-cost low-efficiency ASHP and less than 2 years with an expensive high-efficiency ASHP. These results come in contrast with previous studies comparing GSHP systems with ASHP or other solutions (Christodoulides et al., 2019; Gabrielli and Bottarelli, 2016; Lu et al., 2017). The last column of Table 5.8 shows the yearly

cash flow return rate for the worst-case scenario for each system, which in all cases exceeds 8%, a figure pointing to a good investment.

The results above assume that the performance of the system will remain steady throughout the lifespan of the system. Although the loads seem unbalanced (higher cooling loads compared to heating loads), there are two months with insignificant loads (namely March and November), which can be considered as buffer months providing time for the ground to return to the natural undistributed temperature. However, with constant heat injection to the ground, the ground temperature might increase, thereby reducing the COP values during the summer mode. This ground temperature increase has been observed in long term simulations (Li et al., 2018) and experiments (Zhou et al., 2016), where depending on the case, the COP can be dramatically reduced (as far as 50% in a 15 year operation time (Li et al., 2018)). By examining the current case study, with the lifespan of the GSHP set to 12 years and a COP reduction of 25% assumed (an extreme figure for the current case study), there will still be a significantly low SPP (7.95 years in the worst case) and DPP (8.75 years in the worst case). This is due to the fact that the COP reduction is achieved gradually, which means only a 2% reduction per year, which will have an insignificant impact on the system and the investment. Even if one assumes a constant ASHP COP throughout the lifespan, the GSHP system will remain a sustainable investment if its COP is not reduced by more than 25%.

The described integration of the buildings foundations can undeniably lower the initial cost of the systems, providing a viable solution into a "greener" future. This green solution could be further explored through an environmental-impact comparison with existing GHE systems (Aresti et al., 2020a).

5.6 Discussion

The high initial cost of GSHP systems in comparison to the conventional ASHP systems has steered the researchers and engineers to convert existing dwelling elements into GHEs. Such hybrid elements, as addressed in the current study, can be the foundation bed and the foundation piles. The housing trend in Cyprus has been examined and a typical average residential building with ZEBs characteristics was theoretically investigated. With the use of the TRNSYS software the heating

and cooling loads were calculated in order to evaluate whether the buildings foundations could positively respond to the specific loads by maintaining a steady temperature.

A COMSOL Multiphysics computational model for both the energy pile system and the foundation bed system was constructed and simulated taking in account the site ground temperature characteristics and the local ambient temperature. The inlet and outlet temperatures were calculated hourly (based on the provided loads) for the two months of highest demand of summer (July) and winter (February). The obtained results have shown that both systems provide high COPs and nearly steady conditions, with COP values varying between 4.4 and 4.8. A further investigation on a yearly simulation have shown that the lowest COP values achieved by the systems, were 4.60 and 4.51 for the foundation bed and the energy piles system respectively. The two systems exhibit similar performance, with average heating (winter) and cooling (summer) COP values estimated at 4.73 and 5.00 for the foundation bed GSHP system, and, 4.84 and 4.97 for the energy pile GSHP system.

Finally, an economic evaluation of both systems has been performed using the simple SPP and DPP methods. The monthly loads and average monthly COP values of each system as well as the lifespan and the cost of the heat pump replacement were considered. The electricity price inflation was also considered for two scenarios, with a 2% inflation and an "extreme" 5% yearly inflation. Both systems have been demonstrated to be attractive investments as they exhibit short payback periods. Specifically, the best-case scenario for the energy pile systems is estimated to be 2.04 years and 1.93 years for the foundation bed system, whereas the "worst" cases are 6.97 years and 6.85 respectively. Regarding cash flow return, the worst-case scenario for all systems, results in a very satisfactory figure exceeding 8%.

Hence, the above-mentioned hybrid elements may offer a solution towards overcoming the barriers of high initial investments and long payback periods that have kept unpopular the GSHP systems hiding during the past years.

Chapter 6*

6 An investigation on the environmental impact of various Ground Heat Exchangers configurations

Summary: Ground Source Heat Pumps (GSHPs) are used for space heating and cooling, where the Ground Heat Exchangers (GHEs) are used to extract or reject heat from/to the ground. GHEs come in various configurations, vertical or horizontal. Compared to Air Source Heat Pumps (ASHPs), GSHPs, albeit having a higher installation cost, achieve a better coefficient of performance (COP) and, hence, electricity savings. This reduction in consumed energy is translated to a reduction in fossil fuels and environmental "harmful" gas emissions. As the environmental impact does not lie in a single aspect, it would be useful not to stop the discussion in terms of COP and cost, but to identify whether a GSHP system is indeed a sufficiently overall greener solution. Hence, a more comprehensive investigation on the environmental impact of different types of GHEs as part of a GSHP compared to an ASHP system is attempted in the current study. A case study of a residential building with a fixed heating and cooling load is considered for moderate climate conditions. Using GLD software, a GSHP system is studied for various GHE configurations. The system undergoes a Life Cycle Analysis (LCA), with the yearly heating and cooling load as functional unit, using two methods of the openLCA software, CML2001 and Eco-Indicator99, for a direct environmental impact comparison between the GHE configurations and an ASHP system. It is concluded that the ASHP system exhibits the highest impact, while among the GSHP systems the vertical coaxial configuration exhibits the highest impact and the horizontal GHEs the lowest, at times significantly below the ASHP impact.

6.1 Overview

Heating and cooling systems, in the recent past, used to be selected by the building's owners based on the capital and the energy costs (Alanne et al., 2007). Nowadays such decisions are more and more frequently based upon the life cycle

* Material from published paper (Aresti et al., 2020c)

costs, with the environmental issue also becoming of concern. Multiple-criteria decision analysis tools were used by several researches for the selection of either the best available renewable energy alternatives in a residential building (Seddiki and Bennadji, 2019), or the most appropriate technologies in a residential building considering environmental and economic criteria (D'Agostino et al., 2019). A sustainable selection of a hybrid renewable energy system has become a possibility even for low income households (Babatunde et al., 2019). The environmental impact of heating and cooling systems could play a decisive role in the selection of an appropriate energy system. The evaluation of the environmental impact is usually performed though the methods and tools of Life Cycle Analysis or Assessment (LCA). LCA can be divided into four steps: (i) the system boundaries, (ii) the life cycle inventory, (iii) the Life Cycle Impact Assessment (LCIA), and (iv) the analysis of the results.

Kristmanndottir and Armannsson (2003) argued that the main issues concerning environmental impact of geothermal energy exploitation are (i) the surface disturbances, (ii) the physical effects of fluid withdrawal, (iii) the noise, (iv) the thermal effects, (v) the chemical pollution, (vi) the biological effects, and (vii) the protection of nature features (Kristmannsdóttir and Ármannsson, 2003). Some of these effects occur where groundwater or hot springs are present (Arnórsson, 2004). However, in the case of space heating and cooling in residential areas, most of these effects would be neglected, while there may be other (mostly minor) effects, including CO_2 and atmospheric pollutant emissions (Lo Russo et al., 2009). In many studies the GSHP environmental impact effect is concentrated on one stage of the system, namely the operation stage. This can therefore be expressed as annual CO_2 savings (Bayer et al., 2012). Huang and Mauerhofer (2016) addressed the greenhouse gas emission reduction through three different environmental impact categories, namely (i) the global warming in all stages, (ii) the acidification and eutrophication in the manufacturing process, and (iii) the soil temperature change in the operation process.

Ren et al. (2018) evaluated a GSHP system using LCA for PE and steel pipes. The steps taken by the authors were (i) the determination of the system boundaries, (ii) the analysis of Life Cycle Inventory (LCI), and finally (iii) Life Cycle Energy

Consumption (LCEC) and Life Cycle Costing (LCC). The authors determined the LCI by using the production of the pipes, the transportation of the pipes, the transportation of the replacement soil, the transportation of the drilling machines, the tubes' drilling, the production of the GSHP, and the transportation of the GSHP. The results indicated a 44.9% reduction of CO_2 for the life cycle of the steel pipes, and a CO_2 reduction ratio of 0.45 against the PE pipes. The authors further examined and compared the LCEC and LCC of the two pipe materials, with results showing that steel pipes consume less energy and cost less in their life cycle.

Genchi et al. (2002) applied a different approach on a regional scale and investigated the CO_2 payback time of a GSHP, by calculating the CO_2 emissions during the construction phase over the annual CO_2 emissions reduction. Boreholes with bentonite as backfill material, and with U-tube PE pipes, were investigated. The authors reported that by replacing Air Source Heat Pumps (ASHPs) with GSHPs, a reduction of 54% of CO_2 emissions could be achieved, with a payback period of 1.7 years.

Greening and Azapagic (2012) conducted a LCA comparison between ASHPs, GSHPs, Water Source Heat Pumps (WSHPs) and gas boilers. The HPs with the highest and the lowest environmental impact were reported to be the ASHP and WSHP respectively. The authors examined individual environmental impacts including Abiotic Depletion Potential (ADP) elements and fossil, Acidification Potential (AP), Eutrophication Potential (EP), Fresh Water Aquatic Eco-Toxic Potential (FAETP), Global Warming Potential (GWP), Human Toxicity Potential (HTP), Marine Water Aquatic Eco-Toxicity Potential (MAETP), Ozone Layer Depletion Potential (ODP), Photochemical Oxidant Creation Potential (POCP), and Terrestrial Eco-Toxicity Potential (TETP). They concluded that the gas boiler provided a generally better impact compared to the ASHP, which only performed better in GWP, ADP fossil and POCP. By comparing the HPs only, the worst impact was provided by the ASHP, with the GSHP and the WSHP performing better in all categories. Operation had the main contribution on the impact, with 84%. The CO_2 savings of GSHPs during operation for a region were also investigated by Blum et al. (2010). The authors demonstrated that the use of a

GSHP system with German electricity mix, had a CO_2 saving ranging from 1800 to 4000 kg per year and 65 gCO_2/kWh.

Different results were demonstrated by Koroneos and Nanaki (2017), where the highest emissions were observed in the raw materials production. The authors presented an environmental assessment of a case study by investigating the impact on air emissions for a Town Hall in Greece. Five different GSHPs were considered through the SimaPro software, with the Eco-Indicator95 method, for a 25-year life cycle. The authors considered the production of the raw materials, the drilling, the operation, as well as the transportation. The results indicated that the raw material production covered the 79%, 81% and 45% for CO_2, SO_2 and NO_x emissions respectively. In the study, it was also noted that Greece and, also, Cyprus, were among the highest in EU in SO_2 emissions in 2004 (European Environmental Agency, 2004). This result was reconfirmed for the year 2008 (European Enviromental Agency, 2008).

There are uncertainties concerning the installation of a GSHP system, such as geological and hydrogeological features, such as artesian aquifers, swelling or soluble layers, landslide-prone areas, and groundwater quality, as raised by Casasso and Sethi (Casasso and Sethi, 2019). The authors investigated the GSHP systems from the groundwater quality protection perspective. Due to thermal interaction between GHEs and groundwater, in specific sites, an impact on the groundwater chemistry and the efficiency in close GSHP installations may occur. The authors made suggestions regarding the specific issues and stated that the GSHP systems are safe to be installed and a sustainable choice. Another hazard, which has caused local authorities to prohibit the installation of GSHP systems, is the usage of antifreeze solution in the GHEs and the possibility of leakage. The environmental impact of the antifreeze solution related to the GHEs was presented by Batrolini et al. (2020). The authors investigated four different heat carrier fluids, one of which is water. Water is a conventional fluid that offers a reduction of the lifetime carbon footprint, but its use could lead to an increase in the length of the borehole. Another environmental disorder is the thermal interference among systems, specifically in dense urban areas, which could though be resolved with the correct organization and planning from the local authorities (FascÌ et al., 2019).

A comparison between three different systems in the north of Europe, Sweden, was performed by Franzen et al. (2019). The authors examined a conventional type heating and cooling system (ASHP), a smart energy solution, and a GSHP, where the environmental impact was calculated using factors from previous LCAs. The results indicated a 20% reduction in greenhouse gas emissions and a 70% reduction in energy use. Kljajic et al. (2020) performed a comparison among a hot water condensing boiler system and a Ground Water Heat Pump (GWHP) system in central Europe, Serbia. The GWHP system exhibited a higher impact when compared to the hot water boiling system in most impact categories, except the terrestrial eco-toxicity, natural land transformation and fossil depletion. In the climate change impact category, an 82% increase was reported by the authors, justified by the current grid electricity mix in the Republic of Serbia. Regarding the south of Europe, Bartolozzi et al. (2017) examined a district heating, cooling and hot water system allocated for a residential neighborhood with a large sample of apartments (250 apartments) in Tuscany, Italy. A comparison between a GSHP system with vertical type GHEs, and a biomass system was performed using LCA software SimaPro and the Ecoinvent database. The highest impact contributor for the GSHP system is the operation process, contributing to the 95% for the climate change category. Compared to the base scenario of natural gas, GSHP exhibits at least a 20% impact reduction for the climate change category.

In the current study, LCA is performed for different GHEs types. A case study of a residential building in the island of Cyprus, under a moderate Mediterranean weather, is considered and evaluated based on the demand of heating and cooling loads. Specifically, a direct comparison based on the environmental impact assessment of GSHP and ASHP systems would point to the possible benefits of using a renewable energy system instead of a conventional system. The purpose is to identify whether the difference in the COP (coefficient of performance) between GSHPs and ASHPs is sufficiently large to make a GSHP system attractive as an overall greener solution. In Section 6.2, the heating and cooling loads of a residential building in Cyprus were considered, where a case study analysing the design and operation of several GSHP systems and their properties was conducted in the environment of the GLD software tool. Section 6.3 presents the LCA

methodology with all estimations performed in the OpenLCA software environment. The obtained results are discussed in Section 6.4. Finally, we conclude with Section 6.5.

6.2 Case study for GSHP systems in moderate climate

GSHP systems, as any HVAC (Heating Ventilation and Air-Conditioning) system, are evaluated according to the heating and cooling loads of a specific case, where the determined size is calculated for the peak values. Heating and cooling data from a load intensive previous study (Aresti et al., 2020b) are used as input to the GLD (Ground Loop Design) software. GLD software (Thermal Dynamics Inc., MN, USA) is a commercially available package for professionals in the industry of designing GSHP systems.

The examined case is a residential building, located in Lefkosia, the capital of the Mediterranean island of Cyprus. The soil thermal conductivity and diffusivity values, in addition to the undistributed ground temperature, are taken from literature (Pouloupatis et al., 2011; Stylianou et al., 2016). Ethylene Glycol is the selected antifreeze solution at 9.7% by weight with the freezing point being at –3.89°C.

In the case of vertical GHEs, the borehole diameter is 0.2m and the pipe diameter is 25mm, for an average pipe placement. Three (3) configurations are examined, namely the coaxial, the single- and the double-U-tube. Borehole spacing plays an important role, with the selected 4m separation providing a $16m^2$ area per borehole. In the case of horizontal GHEs, the pipe configurations examined are the single, the double, the triple, the slinky and the spiral pipe, all with a pipe diameter of 25mm.

In both cases, vertical and horizontal, the HP inlet fluid temperatures for heating and cooling are set at 4°C and 38°C respectively. The estimations provided by GLD are based on the cylindrical source heat transfer theory (Kavanaugh, 1985). For direct comparison between the borehole/ trench and piping length of the different configurations, the same HP is selected, corresponding to the same COP in all cases. Additionally, the same pipe (PE100-SDR11) diameter (32mm) is selected for all GHEs, while for the vertical configurations, the number of boreholes is fixed with the same borehole grid arrangement (3×3).

Depending on the case, the best available configuration will be considered by the mechanical engineer, depending on the heating and cooling loads, the available land area and the budget. In the case of a residential area, land area is one of the most important factors since it is limited and of high value. Table 6.1 shows the results provided by GLD, where the required area for the GHE can be observed. This is based on either the number of boreholes required or the trench length (width of trench is 500mm). A typical area of 500–600m^2 is considered as a single residential plot in the cities of Cyprus, with many cases of buildings constructed in half plots (250–300m^2). It follows that most horizontal GHEs configurations do not meet these restrictions (as seen in Table 6.1).

Table 6.1 GHE properties obtained by the GLD software

Vertical type	***Pipe length, m (weight, kg)***	***Borehole / Trench length, m (grout weight, kg)***	***Land area, m^2***
U-tube	2363.40 (670.25)	131.30 (71940.31)	144.00
Double U-tube	4514.40 (2559.64)	125.40 (68683.85)	144.00
Coaxial	1251.30 (7218.46)	139.00 (76164.58)	144.00
Horizontal type			
Single	1876.00 (531.94)	1876.00	938.00
Double	2545.00 (721.63)	1272.00	636.25
Triple	3066.70 (869.56)	1022.20	511.10
Slinky	5233.40 (1483.92)	390.30	355.17
Spiral	5452.00 (1545.9)	406.50	203.25

6.3 Methodology

The LCA method is used when one wishes to evaluate the environmental impact of a product or process. LCA investigates the potential environmental impact, by evaluating all the input and output material and processes for single or multiple products, processes and services. LCA is completed by considering (i) the extraction and processing of raw materials, (ii) the manufacturing process, (iii) transportation and distribution, (iv) product usage, and finally (v) recycling and disposal, though the lifetime of a product (see General LCA flow in Figure 6.1 and the flow diagram for the current LCA investigation in Figure 6.2).

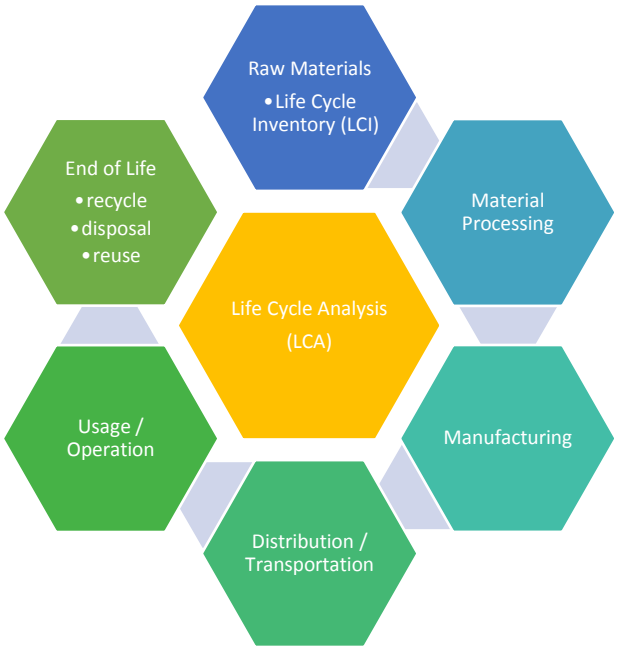

Figure 6.1 General Basic flow of LCA

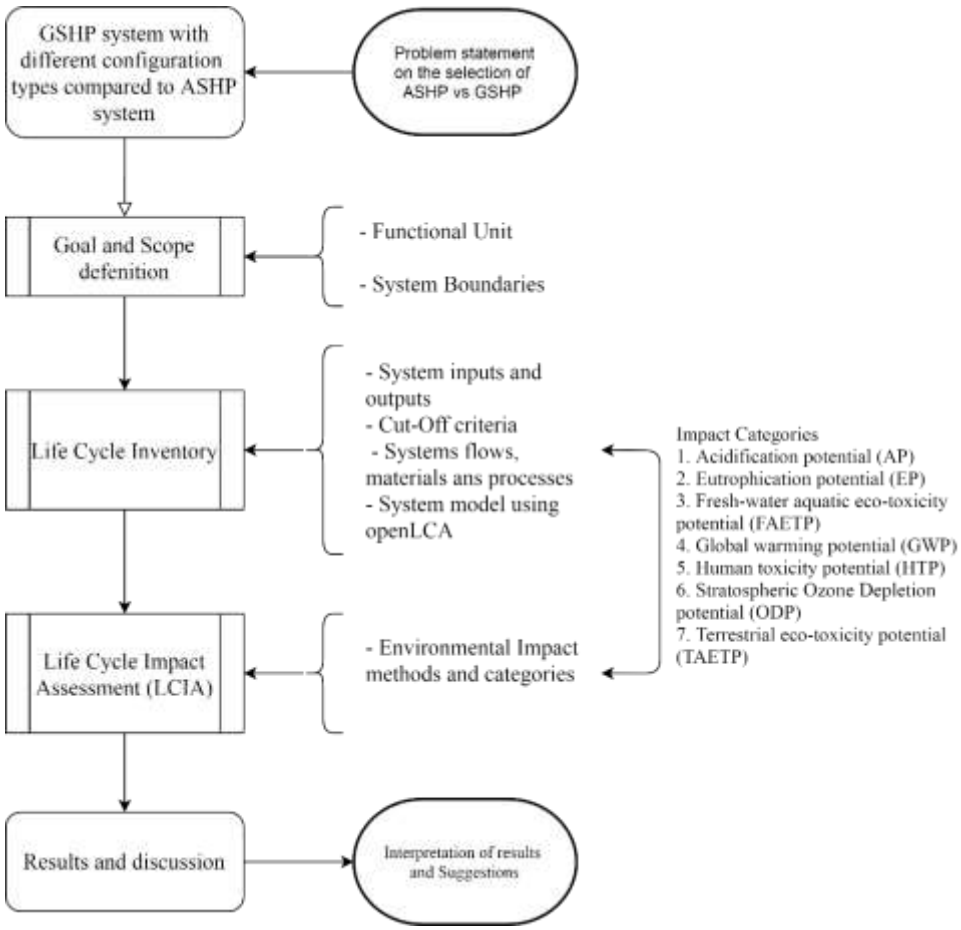

Figure 6.2 Methodology flow diagram of the current LCA investigation

The environmental LCA principles and framework, and requirements and guidelines are described by ISO 14040 (2006) and ISO 14044 (2006) respectively. The accurate estimation of the LCA of a specific product requires good knowledge of the raw materials quantity and processes used; such information can be extracted either from a manufacturing plant or from literature.

With several software available to assist in the estimation of the environmental impact, the reliable OpenLCA has been selected as the tool for the analysis of the current comparison case study. OpenLCA is a user-friendly open source software for Sustainability Assessment and LCA. It is widely used for its ability to perform at as high a performance as its commercially available competitors, such as SimaPro, GaBi and Umberto. It requires external databases and methods to be imported, which may be either commercial or for free use. For the current study, the Ecoinvent 3.6 database (Steubing et al., 2016) and methods with educational license were employed. The Ecoinvent 3.6 database is subject to three different system models: (i) the Cut-Off, (ii) the APOS (Allocation at the Point Of Substitution) and (iii) the Consequential system models (Wernet et al., 2016). For the scope of this study the Cut-Off method is considered for simplicity. The goal and scope definition, the System boundaries and the functional unit, LCI, and LCIA are addressed in the following subsections.

6.3.1 Goal and Scope definition

The objective of the current LCA study is to examine the primary resources, the energy consumption and the overall environmental load associated with different types of GHEs in comparison to an ASHP system used as a benchmark. The final goal is to identify whether the difference in the COP between the systems is sufficiently large for the GSHP system to be an attractive and an overall greener solution.

6.3.2 System Boundaries and Functional unit

The determination of the system boundaries is presented in Table 6.2 and illustrated in Figure 6.3 for the GHEs under consideration. The investigation excludes materials associated with the HPs, as the scope here is to examine the effect of

using different types of GHEs. It can be assumed that the HP used will be the same in all cases since the studied residential building will be the same. Included in the system boundaries are all materials and processes associated with the GHEs, including installation and operation.

In detail, the system boundaries flow is described in Figure 6.3. Firstly, the raw materials are extracted and processed into manufacturing. The fabricated products are then transferred to the construction site, where the installation will be performed. Following the construction and installation of both the GSHP and the GHE, the system is operated for a given amount of time. Electricity is assumed to be provided by the local grid, before the GHE is decommissioned. The flows and processes related to the HP and the maintenance of the system are not accounted for in the system boundaries under investigation. The system boundaries are focused solely on the additional materials and processes required when an ASHP system is compared to a GSHP system.

The functional unit provides the measurement of the function, upon which the inputs and the outputs of the system can be referenced to. Since each GHE has specific requirements and characteristics, each GHE scenario was studied as a single unit, where each unit represents the residential building's yearly heating and cooling loads. The functional unit in the case under investigation was set at 130 kW m^{-2} (per annum) or 28760 kWh for yearly heating and cooling.

Table 6.2 GHEs system boundaries

System boundaries	***GHEs***
Included	Extraction and process of raw materials
	Transportation
	Installation, including drilling for vertical GHEs and trenches for horizontal GHEs
	Operation
Excluded	Heat pumps and associated flows, processes, products, and wastes
	Maintenance of the system
	EoL, disposal or recycle

The life spam of a GSHP system can be considered either at 15 years (Christodoulides et al., 2019) or 20 years (Chiasson, 2006), whereas that of GHEs can be much higher. The maintenance of the GSHP system depends on the policy, preventive or when the system is broken down (Zhu et al., 2012). The maintenance of the GHEs is related to the circulating fluid, which can be considered similar in all cases, and is therefore excluded from the analysis. (Note that any other repair of a malfunction GHE would require a new installation process, therefore high cost.) For the End of Life (EoL) of the GSHP, refer to sub-section 6.3.4.

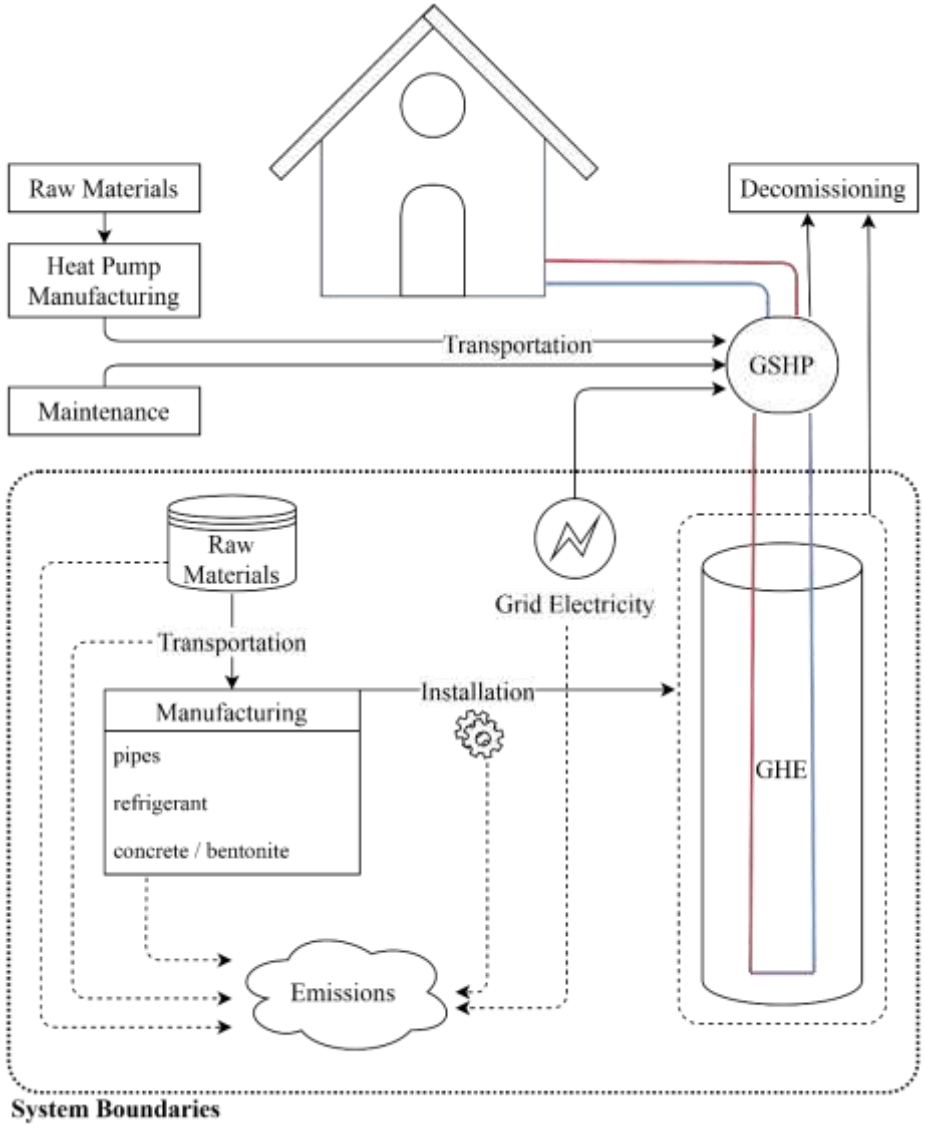

Figure 6.3 Flow diagram of LCA System boundaries

6.3.3 Life Cycle Inventory

The GHEs examined with the associated input flows (materials) are presented in the LCI as presented in Table 6.3. The background LCI data were included by the Ecoinvent 3.6 database. Most of the materials used are the same in all cases, but with different quantities. In each GHE type, the length of the pipes and the area required are varied according to the estimation of the GLD software, as presented in Table 6.1. The material or process column can be considered as the output of the system, whereas the column in the Vertical GHEs and the Horizontal GHEs can describe the material or process flow used as an input. For example, to produce the required HDPE pipes, the HDPE material with the desirable length (set as weight in the openLCA interface) was used from the Ecoinvent 3.6 database (process).

Table 6.3 Life Cycle Inventory of the considered GHEs as per functional unit

Material or Process / Life Cycle Stage	***Vertical GHEs***	***Horizontal GHEs***
Pipes	HDPE (weights defined in Table 6.1)	
Pipe insulation	LDPE (6 kg)	
Circulating fluid	Ethylene glycol 9.7% by weight (depending on the pipe length, Table 6.1)	
Manifold	Brass (6 kg)	
Grout	Bentonite (weights defined in Table 6.1)	None
Installation	Diesel (described in Section 6.3.3.1)	
Operation	CY Electricity, low voltage (described in Section 6.3.3.2)	
Transportation	Diesel (described in Section 6.3.3.3)	
Decommissioning	Ethylene glycol (9.7% of the total volume)	
	Bentonite and HDPE 100% landfill	HDPE 100% landfill

6.3.3.1 Installation

The installation materials are first manufactured and then transferred to the construction site. Although the manufacturing procedure is the same for the materials used, the installation of the system differs with each configuration. A GSHP system with horizontal GHEs mainly differs from one with vertical GHEs on

the excavation type and time. Specifically, more time is required for the horizontal GHE due to the longer trench. The additional process of removing dirt and bentonite filling is required for the vertical GHE. Both types of GHEs are connected to the GSHP unit by a manifold (brass) and 8m-length HDPE pipes insulated with LDPE (low density polyethylene).

The excavation machine for digging the trench is considered to burn 30 litres of diesel every working hour and 8 litres for every running meter excavated at 2 meters depth. A rotary drill is considered to burn 1.5 litre of diesel per drilling meter, for the vertical type BHEs (Greening and Azapagic, 2012). Specifically, the flows required for the vertical and horizontal type GHEs are presented in Table 6.4.

Table 6.4 Installation LCA flow parameters as per functional unit

	Diesel	***Remarks***
Vertical GHEs	1.5 L/m	Rotary drill machine
Horizontal GHEs	8 L/m	Excavation machine
	4 L/m	Excavation machine for covering and correcting the trench

6.3.3.2 Operation

The GSHP system is generally considered as a more efficient system than ASHP systems (Aresti et al., 2018; Christodoulides et al., 2020). This advantage relies on the steady temperature of the ground compared to the ambient temperature, providing higher COP for heating or cooling.

The results shown in Table 6.5 were obtained with set inlet fluid temperatures (see Section 6.2), which provided a heating COP of 6.1 and cooling COP of 4.4 for the GSHP, while the corresponding ones for the ASHP were chosen to be the typical (from manufacturers) 3.0 and 3.3 respectively. The lifetime for a GSHP system is conventionally 15 years, and the additional required electricity over the system's lifetime is estimated at 92725 kWh, or 6182 kWh per annum.

Table 6.5 GSHP annual and lifetime electricity demand

	Heating	***Cooling***	***Total***
Annual heating energy demand, kWh	5600	23160	28760
GSHP *(ASHP) COP*	6.1 (3.0)	4.4 (3.3)	

GSHP (ASHP) *Annual electricity demand, kWh*	918 (1867)	5264 (7018)	6182 (8885)
GSHP (ASHP) *Lifetime electricity demand, kWh*	13770 (28000)	78955 (105270)	92725 (133270)

The reason for the seemingly high COP for the heating period of the GSHP is that it is estimated on peak values. The peak value for the cooling period is higher than that for the heating period, therefore it is used for the calculations. With a ground temperature of 21.7°C, and the residential building indoor temperature set at 21°C during the heating period, the GSHP provides an unusually high efficiency (COP).

6.3.3.3 Transportation

The transportation impact only occurs during the installation process. Only the materials related to the GHEs are considered for transportation. It is however noticeable that other materials related to the GSHP system are group-transported with GHEs materials. The transportation can occur either to or from the construction site. The transportation impact is calculated using the transport type and the distance covered, as seen in Table 6.6.

Table 6.6 Transport LCI parameters

	Transport type	***Distance, km***
Raw materials	Freight, train	200
	Lorry > 32 tone EURO 5	100
To the construction site	Freight, container ship (materials imported)	1000
	Lorry 7.5-16 tone EURO 5 (equipment)	100
	Van < 3.5 tone (general)	100
	Lorry > 32 tone EURO 5 (bentonite)	100
From the construction site	Lorry > 32 tone EURO 5 (removal of dirt)	100

6.3.4 GSHP system End of Life

The End of Life (EoL) recycling process of the GSHP system is similar to that of the ASHP system, with the exception of the GHE that is not present in ASHP systems. The components containing metal (HPs) are processed though the recycle program in most cases, whereas the rest of the components are processed as waste for landfill (Greening and Azapagic, 2012). There are two main approaches in modeling the EoL in LCA: (i) the cut-off (recycled content approach) and (ii) the

EoL recycling (avoided burden approach) (Nordelöf et al., 2019). This does not apply in the case of the GHEs, where the GHE is not processed or recycled in any way, due to high costs. It is usually observed that when a GHE malfunctions or reaches its EoL, the GHE is abandoned or replaced at a nearby area.

6.3.5 Life Cycle Impact Assessment

Finally, the LCIA is examined. The LCIA is estimated based on the available methods, with the most common being the CML2001 and the Eco-indicator99. Other methods include the Cumulative Energy Demand, the Eco-Scarcity 2006, ILCD 2011, ReCiPe and the TRACI 2.1 (Acero et al., 2016). Previous studies compared different LCIA methods in order to evaluate which is the one to use either for a midpoint or an endpoint perspective (Dreyer et al., 2003; Weidema, 2015). LCIA can be distinguished as single and multi-category with either problem-oriented or damage-oriented methods.

CML2001 is a problem-oriented method, while the Eco-indicator99 is damage-oriented. These two methods have different approaches as regards their impact categories and their point impact. On one hand, CML2001, having a midpoint impact perspective, can limit the uncertainties, yielding a more transparent assessment at the early stages of the cause chain effect. On the other hand, the Eco-indicator99, having the endpoint evaluation of the cause effects, despite being case-specific simpler, in the sense that it uses a point system, it exhibits higher uncertainties than the midpoint methods (Monteiro and Freire, 2012). In order to avoid high uncertainties, the CML2001 method was initially used for the estimating the LCA, with the adaptation of the Eco-Indicator99 on second stage in this study.

The CML2001 includes 18 impact categories groups. Seven (7) of those are selected for the under investigation study: (i) the Acidification potential (AP), (ii) the Climate Change (or Global Warming) potential (GWP), (iii)-(iv) the Ecotoxicity potential (from which the Freshwater aquatic eco-toxicity (FAETP) and the Terrestrial eco-toxicity potential (TETP) were selected), (v) the Eutrophication potential (EP), (vi) the Human toxicity potential (HTP), and finally (vii) the Ozon layer depletion potential (ODP). On the other hand, the Eco-indicator99 follows a different strategy, weighing on the types of damages that are caused by the impact

categories. It is therefore assessed in three different categories: (i) the damage to human health, (ii) the damage to the ecosystem quality, and (iii) the damage to the resources. The above-mentioned categories (in both methods) were selected according to their relation on the materials and processes used in this application, complementing (the six of them) the self-evident climate change potential category. The investigation of the proposed "green" energy solutions (GSHP systems) will yield a more spherical image regarding their potential use.

6.4 Results

The LCI described in the previous section was implemented in the OpenLCA software to create flows, processes and products for each GHE for the GSHP and the ASHP as the baseline system. Results obtained by the CML2001 LCIA method are presented as percentages, for a better understanding of the comparison, in Figure 6.4 for the seven impact categories mentioned above. In all cases, the ASHP impact corresponds to the baseline of 100%.

6.4.1 Acidification and Eutrophication potential

Acidification potential (AP) describes the impact of acidifying substances to air emissions, which are the main cause of acid rain and forest decline, and it is expressed in kg SO_2 equivalents. This impact category is associated with air pollutants, caused – in the current application – mainly by fuel combustion either from electricity production or transportation. Fuel combustion could increase the acidity levels either on water or soil when observed from a midpoint perspective (such as in the CML2001 method) and can have a negative effect on flora, organism and buildings from an endpoint perspective (such as in the Eco-indicator99 method). Eutrophication potential (EP) describes the impact of high levels of macro-nutrients to the environment, caused by emissions to the air, water or soil. EP is expressed in kg PO_4 equivalents. The use of fossil fuel in the electricity generation (grid), transportation, and industry (such as in the construction of the pipes) is the major cause – in the current application – of eutrophication. From the midpoint perspective, excessive growth of biological organisms can lead to aquatic oxygen depletion, which has effects such as loss of biodiversity and toxicity to

humans. By examining the AP and the EP in Figure 6.4 (a) and (b), the ASHP exhibits the highest impact (of order 10^2 kg SO2-eq and 10^2 kg PO4-eq respectively). The result is as expected as ASHPs, owing to their lower COP, have higher operation process compared to GSHPs. The large quantities of HDPE raw material for the manufacturing process of the coaxial GHE renders it the configuration with the highest impact among the GHEs. The impact of all horizontal type GHEs is 23% lower than that of the ASHP system, while the impact of the vertical GHEs ranges between 16–18% lower than that of the ASHP system.

6.4.2 Climate Change potential

Climate change also referred to as Global warming potential (GWP) is a major effect associated with climate change and the greenhouse gases to air, and it could affect the ecosystem health, human health and material welfare. GWP is expressed in kg CO_2 equivalents. Global warming is mainly caused – in the current application – by fuel combustion either from electricity generation (grid), transportation or industrial processes. Figure 6.4 (g) shows the impact of the GWP category, which depends on the warming caused by CO_2 equivalent emissions, and it is of the order of 10^5 kg CO_2-eq. Since the operation time (15 years) has the highest duration compared to the other processes, it was anticipated that the highest impact would be provided by the operation process. With that in mind, and the better COP values given by the GSHP, the ASHP has the highest impact, even though only the operation process was considered. Compared to the ASHP system, a reduction on the impact of 22% (a value close to previous studies (Bartolozzi et al., 2017)) can be achieved by using the horizontal slinky tube, while the coaxial configuration corresponds to the lowest impact difference of 10%.

The obtained results are in line with previous studies (Bartolozzi et al., 2017; Koroneos and Nanaki, 2017), where the operation of the system determined the GWP. In countries (such as Switzerland, France and Norway) where the electricity mix (grid) has low carbon emissions, the impact is reduced for both GSHP and ASHP (Greening and Azapagic, 2012; Saner et al., 2010) and the difference between them is not as significant as in countries (such as Cyprus and Greece) with high carbon electricity mix emissions.

6.4.3 Eco-toxicity and Human toxicity potential

Fresh-water aquatic eco-toxicity potential (FAETP) refers to the impact on fresh-water ecosystems, from emissions of air toxic substances, water or soil, and is expressed in 1.4-dichlorobenzene equivalents. Terrestrial eco-toxicity potential (TETP) is similar to the FAETP and describes the impact of toxic substances on terrestrial ecosystems. Eco-toxicity potential main substances include the zinc, copper and organic chemicals. The degradation of the ecosystem could be considered as a midpoint impact, while the decrease of biodiversity as an endpoint impact. Human toxicity potential (HTP) describes the effect of toxic substances to the human health and is expressed in 1.4-dichlorobenzene equivalents. Freshwater and human (with impacts of order 10^4 kg 1.4-DCB-eq) and terrestrial (order 10^1) toxicities (Figure 6.4 (c), (d) and (e)) follow the same pattern as the previous results, where the operation and the manufacturing of the systems are the highest contributors.

More specifically for the FAETP, all GHE types exhibit a higher impact than the ASHP system, due to the higher manufacturing impact, with a minimum difference of 1% (single U-tube) and a maximum of 221% (coaxial configuration). A lower environmental impact is observed for the TETP, where all types, except the coaxial configuration (higher impact by 1%), outperform the ASHP system by 20%, despite their high manufacturing impact. This increase in the manufacturing impact is due to the use of the refrigerant solution in the circulation fluid and can be reduced to a minimum if pure water is used (Bartolini et al., 2020). The diesel consumed by the excavation machines during installation plays a role in the toxicity categories; this can mainly be seen mainly in the HTP category. For the HTP the impact of most horizontal type GHEs are lower than that of the ASHP system (by up to 8%), while the impact of the vertical GHEs ranges between 26–42% higher than that of the ASHP system.

It must be finally mentioned that by excluding the use of refrigerant as an antifreeze solution in the circulating fluid, as well as using alternative ecofriendly (mainly in the manufacturing process) materials for the pipes, the Eco-toxicity could potentially be adequately reduced to a minimum.

6.4.4 Ozone layer depletion

Finally, the Stratospheric Ozone Depletion potential (ODP) describes the impact of the ozone depletion of different gases, causing the thinning of the ozone layer in the upper atmosphere, and it is expressed in kg CFC-11 equivalents. Ozone depletion – in the current application – is majorly caused by the manufacturing of polymers (pipes) and the refrigerant, where the decrease in stratospheric ozone concentration could be considered as a midpoint impact. With the UV-B radiation passing unfiltered through the stratosphere, the potentially resulting skin cancer, agriculture damage and fauna damage could be considered as an endpoint impact. ODP (Figure 6.4 (f)) has an impact of order 10^{-3} CFC-11-eq. The manufacturing process and the fuel burned in the excavation and working machines have the greatest impact on ODP. The extra material and processes required for all GHEs can produce up to 240% higher impact than that of the ASHP systems. The coaxial GHE configuration has the highest impact due to its high manufacturing impact and installation. Even though there is a significant increase of the ODP in all GHE types, in reality the ODP impact is rather low, since – for the lifespan of the systems under consideration – the highest impact observed is at 0.0024 kg CFC-11 equivalent.

6.4.5 GHE types comparison

Comparing the vertical borehole GHEs, the single and double U-tube have a very similar impact, with the double U-tube having a slightly higher impact, and the coaxial GHE having the poorest performance. This can be observed in all the impact categories, where the coaxial has the highest impact out of all GHEs. The coaxial configuration has the highest weight of pipes (HDPE material) and, thus, the highest impact on the manufacturing process in all categories. The GHE configuration with the least impact is the slinky horizontal type. Comparison among the horizontal GHEs shows that the slinky and spiral (= vertical slinky) have the highest manufacturing impact, owing to the longer HDPE pipes required, with albeit a lower amount of land required.

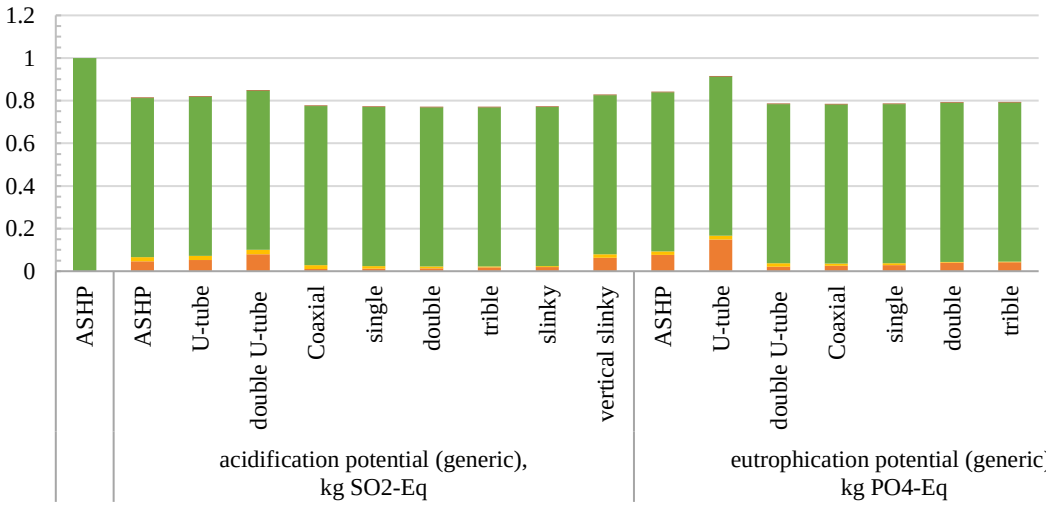
1.2
1
0.8
0.6
0.4
0.2
0
ASHP
ASHP
U-tube
double U-tube
Coaxial
single
double
trible
slinky
vertical slinky
ASHP
U-tube
double U-tube
Coaxial
single
double
trible
acidification potential (generic), kg SO2-Eq
eutrophication potential (generic), kg PO4-Eq

(a) (b)

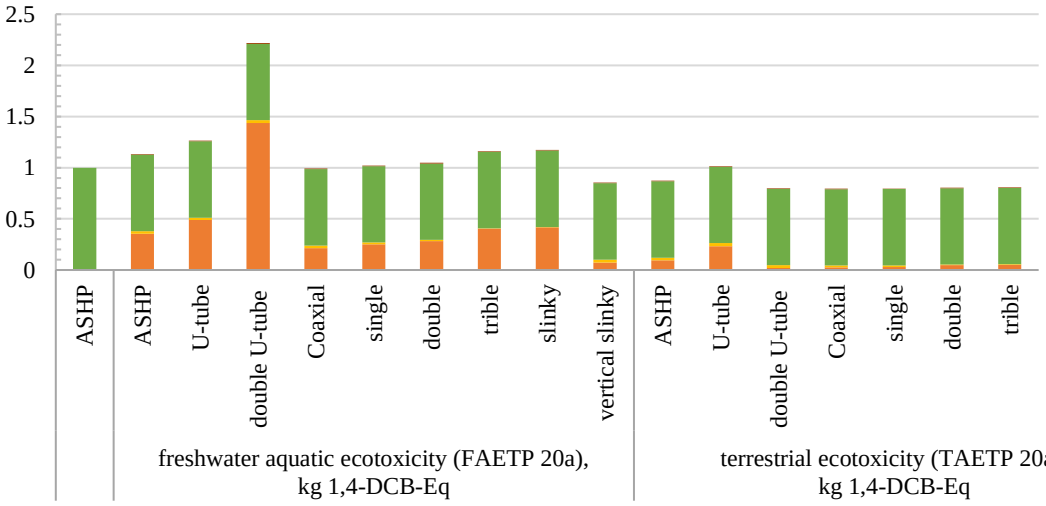
2.5
2
1.5
1
0.5
0
ASHP
ASHP
U-tube
double U-tube
Coaxial
single
double
trible
slinky
vertical slinky
ASHP
U-tube
double U-tube
Coaxial
single
double
trible
freshwater aquatic ecotoxicity (FAETP 20a), kg 1,4-DCB-Eq
terrestrial ecotoxicity (TAETP 20a), kg 1,4-DCB-Eq

(c) (d)

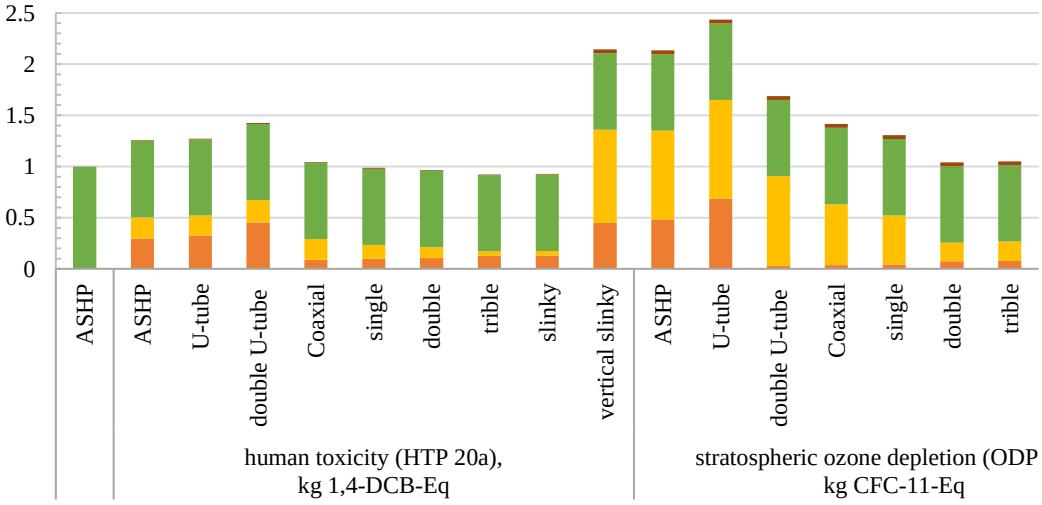
2.5
2
1.5
1
0.5
0
ASHP
ASHP
U-tube
double U-tube
Coaxial
single
double
trible
slinky
vertical slinky
ASHP
U-tube
double U-tube
Coaxial
single
double
trible
human toxicity (HTP 20a), kg 1,4-DCB-Eq
stratospheric ozone depletion (ODP 20 kg CFC-11-Eq

(e) (f)

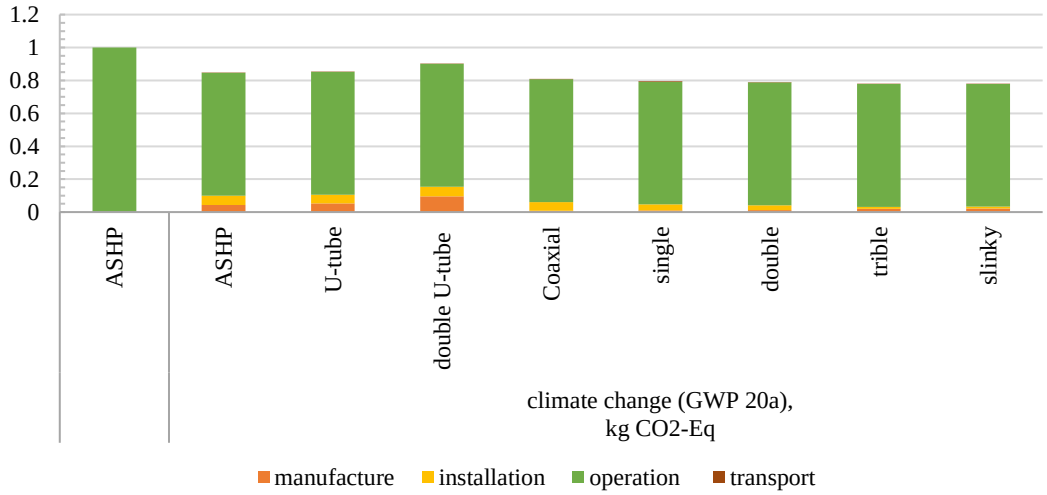

(g)

Figure 6.4 GHEs with different configuration LCIA results using CML2001 method. Vertical GHEs: single U-tube, double U-tube, coaxial; horizontal GHEs: single, double, triple, slinky, vertical slinky. (a) AP, (b) EP, (c) FAETP, (d) TETP, (e) HTP, (f) ODP, (g) GWP.

Focusing on GWP (the major impact category), it is worth noting that the major process contributor is the operation process at 83% and 88%, for the coaxial and the single U-tube GHE configuration respectively (seen in Figure 6.5). This is because the operation is performed during the lifetime of the system, while the other processes are only performed for a very short period of time. This result comes in agreement with the findings of Greening and Azapagic (2012), where the operation process was the main contributor at 84%. At the same time, the results here are lower than the results reported by Bartolozzi et al. (2017), due to a longer time period examined in that study. The above-mentioned operation process impact could be reduced with the use of renewable energy systems (RES) such as Photovoltaic systems. A hybrid system using RES for the operation process of both ASHP and GSHP may result in a lower impact for the hybrid ASHP system. Even though the use of RES would reduce the operation impact, at the same time it would increase the manufacturing impact and possibly the EoL impact of the associated processes/ materials. The transportation process, on the other hand, has the lowest impact contribution that corresponds to less than 1%. The transportation process

can be neglected when studied for a single GSHP unit, but at a larger scale, such as a district or country, it could be an impact worth noting.

Land occupation from GHEs, especially in a residential area (city) could be a very costly selection due to the high land area per m^2. This could be another downside of using horizontal GHEs, even though the environmental impact would be lower. The EoL of the GHE systems, as discussed in the previous section, would mean that the pipes and the grout would be left in the ground.

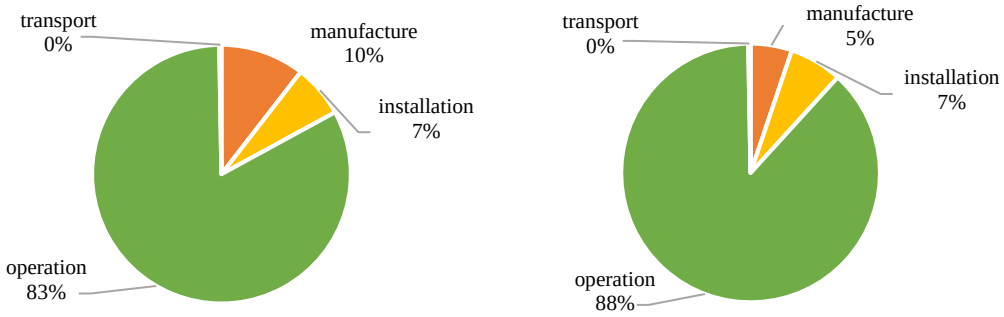

Figure 6.5 Different processes as a percentage with Coaxial GHE (left) and single U-tube GHE (right) for the GWP impact

6.4.6 Eco-indicator 99 LCIA method results

Furthermore, using the Eco-Indicator99 method with a point impact system can reveal a direct comparison on the overall performance of all the GHEs. This method provides a score on a point scale and represents the annual environmental load for an average European citizen. Results are presented in Figure 6.6 for 3 different categories: (i) the ecosystem quality, (ii) the human health and (iii) the resources point impact total. The ecosystem quality category takes in account the acidification and the eutrophication potential, the ecotoxicity potential and the land occupation potential. The human health is described by the carcinogenics, climate change, ionizing radiation, ozone layer depletion, and respiratory effects. The resources potential includes the fossil fuels and the mineral extraction. As observed from Figure 6.6, the highest impact in all categories is exhibited by the coaxial configuration, which has the highest manufacturing impact; observed also in Figure 6.4 for the CML2001 method.

The ASHP system has the second highest impact on the ecosystem quality category (seen in Figure 6.6), while the single horizontal configuration has the lowest impact due to lower manufacturing impact (less HDPE raw material). In the case of the resources impact category, the lowest impact is observed by the ASHP due to not having any additional raw materials as in the case of the GHEs. In the case of GHEs, the coaxial has a high manufacturing impact but the single horizontal has the highest impact on the installation process.

A further examination of the climate change impact category is seen in Figure 6.7. The ASHP has, as expected, the highest impact, since it has the highest CO2 emissions, as was verified in Figure 6.4. The conventional configurations, double U-tube and vertical slinky horizontal GHEs, have the lowest point impact; recall that these are the highest performance (better COP with lower depth/trench) GHEs (see Tables 6.1 and 6.5), but with the downside of being labour intensive during the installation process.

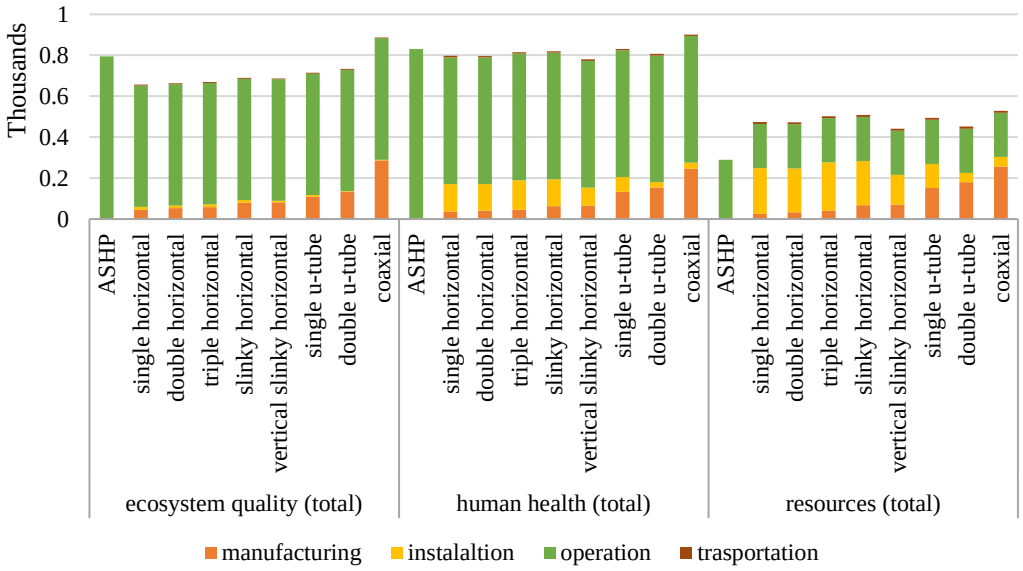

Figure 6.6 LCIA results using the point impact system of the Eco-Indicator99 impact category

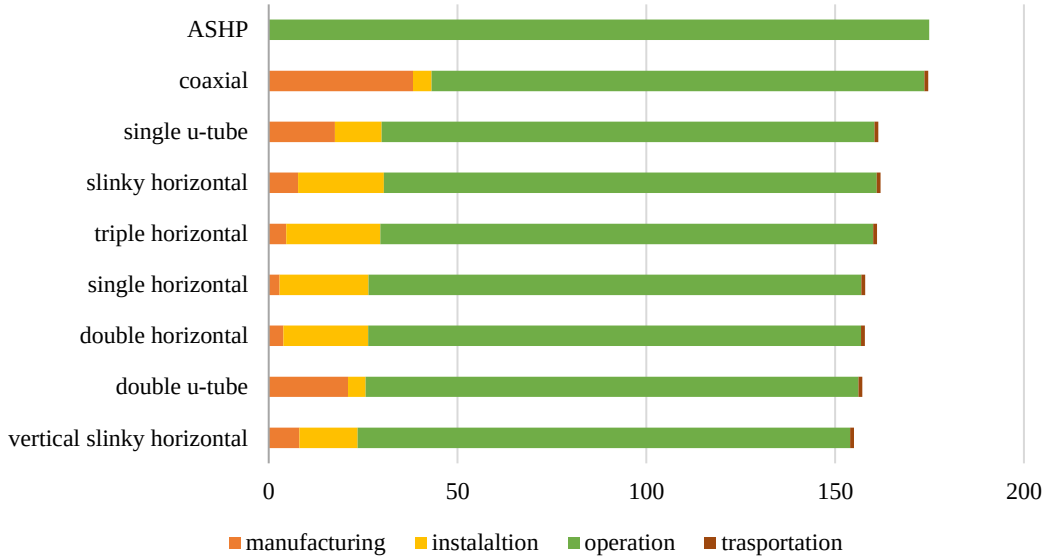

Figure 6.7 Climate change results for different GHEs configurations using the Eco-Indicator99 point impact method

6.5 Discussion

In this Chapter the environmental impact of different GHEs (as part of a GSHP) was considered and examined with the use of two different software programs. First, a case study of a residential building in the Mediterranean island of Cyprus was studied, with the different GHE parameters estimated by the GLD software. The length of the pipes and the boreholes or trenches were estimated based on set inlet fluid temperatures and GSHP characteristics.

The results were then used as inputs to the OpenLCA software for the different types of GHEs and an ASHP used as baseline for comparisons. The functional unit in the case under investigation was set at 130 kW m^{-2} for yearly heating/ cooling. The LCI was described with respect to processes divided as manufacturing, installation, operation and transportation. The flows for each process were determined for each GHE type and the LCIA was calculated using both the CML2001 method and the Eco-Indicator99 method. The impact categories evaluated were the AP, EP, GWP, FAETP, TETP, HTP and ODP.

The systems' operation process has the highest impact contribution (of at least 83%), and hence, the higher the efficiency of the system the lower the impact. Hence, the category with the highest impact is the GWP, in which the ASHP

provides the highest impact followed by the coaxial vertical GHE configuration. Compared to the ASHP impact, a 22% reduction was observed for the GSHP with the vertical slinky (horizontal GHE) configuration and a 10% decrease for the coaxial GHE. Note that a similar pattern is observed using the Eco-Indicator99 method, where the ASHP has the highest impact on the climate change score (the analog to GWP). The AP and the EP exhibit similar behaviour with the GWP, where the ASHP provides the highest impact and a 23% impact reduction is observed for the horizontal GHEs. A smaller reduction is observed for the vertical GHE types, where the coaxial GHE exhibits a 9% impact reduction on the EP and 15% on the AP. Of note is that the ASHP shows lower impact (in most cases) compared to the GHE/GSHP systems for the categories of FAEP, HTP and ODP. This is due to the increased use of the manufacturing and installation processes in these categories. It is also worth noting that the highest impact among all the GHEs configurations and all categories is provided by the coaxial GHE, with the horizontal type GHEs outperforming the vertical type GHEs in all impact categories.

Concluding, the direct comparison of different GHE types coupled to a GSHP with an ASHP system, studied in this chapter, has shown the need for a more sustainable choice when selecting a residential heating and cooling system. Even though all the GHE configurations outperform the ASHP in the GWP and climate change potential category, they remain higher in cost. This is of great importance for every energy system; hence, one should consider both aspects when switching to a "green" solution. Finally, note that, one way to reduce the operation process contribution and, hence, the impact of GWP, is through RES for electricity use (individual sourced or grid).

Chapter 7

7 Conclusions and Discussion

During the journey of this research, the question whether the geothermal energy could potentially offer a viable "green" solution, for heating and cooling a residential building in a moderate Mediterranean climate, is addressed.

Firstly, a literature review on the design aspects of the different GHEs and the modelling techniques were presented in Chapter 2. Available geometry options for GHEs such as orientation, pipe network configuration, borehole and pipe materials, and mathematical models were extensively reviewed. Suggestions and recommendations were discussed, but most importantly a summary table was provided that could be a useful tool for future researches and engineers.

The initial step towards achieving the goals of the stated problem in this research was to perform an economic evaluation of GSHP systems in the residential sector for a moderate Mediterranean climate, in Chapter 3. So, a residential building in the Mediterranean island of Cyprus was examined as a case study for heating and cooling loads. The case study was used for an economic evaluation between a high-efficient ASHP with a "typical" GSHP system. The results indicated payback periods in the range of 20 years, by using the simple methods of SPP and DPP. This is due to the high COP provided by the newly developed ASHP, which are highly antagonizing against the GSHPs. Even with an increased efficiency (using increased length of pipes) of the GSHPs, the high initial costs yield high payback period, leaving the system as a not viable solution. This issue is addressed throughout the current research.

The groundwater flow is an aspect examined in Chapter 4, towards reducing the GHEs length, and therefore the costs of the GSHP system. A case study with multi-layer ground was computationally investigated in the COMSOL Multiphysics environment considering Darcy's and seepage velocity in a convection-diffusion model. It was observed that the ground layer with the groundwater flow, reaches a steady state much sooner than in other regions and, therefore, a reduction in the outlet temperature is achieved. The groundwater flow should be taken into account for the design of the GHEs. In specific, the direction of the flow should be

considered so as to prevent the interference between the boreholes could have a negative impact on the system's performance. However, as the groundwater flow is not always present, an alternative system that may decrease initial and operation costs should further be considered.

Following on, Chapter 5 describes such alternative systems for the reduction of the system's costs. The use of a building's structural elements as GHEs leads to so-called EGS, where the residential buildings' foundations as GHEs are examined as such GSHP solutions. Typical masonry and single houses average area are investigated for the inland of Cyprus, with a typical building case study obtained. The use of the building's foundation piles and foundation bed as GHEs, are investigated for the heating and cooling loads of a typical residential building in the capital of Cyprus, with nZEBs characteristics. The foundation piles (also referred to as energy piles when used as GHEs) and the foundation bed cases were computationally investigated in COMSOL Multiphysics, with undistributed ground temperature and ambient temperatures taken into account. The efficiency of the systems was addressed for the first year of use, and it was used as an input for the economic evaluation and comparison against an ASHP system. This solution (the use of foundation piles or foundation bed as GHEs) at a residential building indicated a different and much more optimistic image than the first one produced in Chapter 3 of this research. Both systems exhibit low values of SPP (about 2 years at best) and DPP (about 7 years at best) with at least an 8% cash flow return on the investment. These hybrid elements are a viable heating and cooling alternative with the use of RES.

Finally, Chapter 6 investigated whether the use of GSHPs as a RES solution is also a "green" solution. The use of RES does not necessarily imply that the system is sufficiently environmentally friendly. This hypothesis is examined with the use of the Life Cycle Analysis method using openLCA as software tool. A residential building's yearly cooling and cooling load was considered as a functional unit with the system boundaries including all processes related to GHEs, but excluding the processes and flows associated with heat pumps. The baseline model was set as an ASHP system and the impact categories investigated were the Acidification Potential (AP), the Eutrophication potential (EP), the Climate Change (or Global

Warming) potential (GWP), the Ecotoxicity potential (from which the Freshwater aquatic eco-toxicity (FAETP) and the Terrestrial eco-toxicity potential (TETP) were selected), the Human toxicity potential (HTP), and finally the Ozon layer depletion potential (ODP). Two methods were considered, namely the CML 2001 and the Eco-Indicator99. The operation process was revealed as the main impact process in all cases with at least 83% contribution, with the transportation being the least impact process with less than 1%. All GHEs cases demonstrated a lower impact compared to an ASHP system in the GWP category, which is the main impact category. The worst configuration observed among the GHEs was the vertical coaxial type, where the increase in pipe weight affected its impact. Due to increased manufacturing and installation processes, the GSHP systems exhibit higher impact in the FAEP, HTP and ODP categories than the ASHP system. Overall, the GSHP systems outperform the ASHP system, providing a lower impact and a "greener" solution.

Conclusively, the use of Shallow Geothermal Energy systems as heating and cooling alternatives in residential buildings can be classified as a viable solution, but a comprehensive and careful parametric, economic and LCA study must be performed according to case.

7.1 Future work and Recommendations

The possible room for advancement in the sector of shallow geothermal energy systems consists not only of mathematical, physical and technical aspects, but mainly of innovative solutions and applications. How will the future of geothermal heating and cooling be shaped? To answer this, one must firstly consider the advancement of technology in the energy sector. Despite the continuous development of new RES and/or hybrid systems consisting of more reliant material and adaptable to nZEB environment, most of these technologies exhibit long payback periods. There is a need for smart monitoring and control of the systems, in addition to retrofit the current systems for improving their efficiency and reduction in costs. Requiring energy to be produced where and when needed, the smart micro-grids might shape the future in the energy sector, with neighbourhoods ("island grids") sharing energy (heating/cooling or electricity) with one another. The future

of Geothermal Energy holds many surprises as the “race” for the best value-and-performance technology available in the market has still a long way to go.

References

Acero, A.P., Rodríguez, C., Ciroth, A., 2016. LCIA methods: Impact assessment methods in Life Cycle Assessment and their impact categories, GreenDelta GmbH. Berlin, DE.

Acuña, J., 2010. Improvements of U-pipe Borehole Heat Exchangers, KTH Royal Institute of Technology.

Alanne, K., Salo, A., Saari, A., Gustafsson, S.I., 2007. Multi-criteria evaluation of residential energy supply systems. Energy Build. 39, 1218–1226. https://doi.org/10.1016/j.enbuild.2007.01.009

Alexandri, E., Androutsopoulos, A., 2017. Energy Upgrade of Existing Dwellings in Greece; Embodied Energy Issues. Procedia Environ. Sci. 38, 196–203. https://doi.org/10.1016/J.PROENV.2017.03.106

Anis Akrouch, G., Sánchez, M., Briaud, J.-L., 2020. Thermal performance and economic study of an energy piles system under cooling dominated conditions. Renew. Energy 147, 2736–2747. https://doi.org/10.1016/J.RENENE.2018.11.101

Antics, M., Bertani, R., Sanner, B., 2013. Summary of EGC 2013 country update reports on geothermal energy in Europe. Proc. EGC2013 3.

Aresti, L., Christodoulides, P., Florides, G., 2020a. An investigation on the environmental impact of various Ground Heat Exchangers configurations. Renew. Energy under review.

Aresti, L., Christodoulides, P., Florides, G., 2018. A review of the design aspects of ground heat exchangers. Renew. Sustain. Energy Rev. 92, 757–773. https://doi.org/10.1016/j.rser.2018.04.053

Aresti, Lazaros, Christodoulides, P., Florides, G., Messaritis, V., 2016. Computational modelling of a ground heat exchanger with groundwater flow, in: XXIV International Congress of Theoretical and Applied Mechanics. Montreal, Canada.

Aresti, L., Christodoulides, P., Lazari, L., Florides, G., 2019a. Computational

investigation on the effect of various parameters of a spiral Ground Heat Exchanger, in: 12th International Workshop on Applied Modeling & Simulation, WAMS. Liophant, 30-31 October, Singapore.

Aresti, L., Christodoulides, P., Messaritis, V., Florides, G., 2019b. Ground Source Heat Pumps costs analysis in moderate climate, in: 12th International Workshop on Applied Modeling & Simulation, WAMS. Liophant, 30-31 October, Singapore.

Aresti, L., Christodoulides, P., Panayiotou, G., Theophanous, E., Kalogirou, S.A., Florides, G., 2017. Passive Solar Floor Heating in Buildings utilizing the Heat from an Integrated Solar Flat Plate Collector Lazaros Aresti, Paul Christodoulides, Gregoris Panayiotou, Elisavet Theophanous, Soteris A. Kalogirou and Georgios Florides, in: First International Conference on Building Integrated Renewable Energy Systems. Dublin, Ireland, pp. 6-9 March.

Aresti, L., Christodoulides, P., Panayiotou, G.P., Florides, G., 2020b. The Potential of Utilizing Buildings' Foundations as Thermal Energy Storage (TES) Units from Solar Plate Collectors. Energies 13, 1–14. https://doi.org/10.3390/en13112695

Aresti, L., Christodoulides, P., Panayiotou, G.P., Florides, G., 2020c. Residential Buildings' Foundations as a Ground Heat Exchanger and Comparison among Different Types in a Moderate Climate Country. Energies 13, 6287. https://doi.org/10.3390/en13236287

Aresti, L., Florides, G.A., Christodoulides, P., 2016. Computational modelling of a ground heat exchanger with groundwater flow. Bulg. Chem. Commun. 48, 55–63.

Arnórsson, S., 2004. Environmental impact of geothermal energy utilization. Geol. Soc. Spec. Publ. 236, 297–336. https://doi.org/10.1144/GSL.SP.2004.236.01.18

ASHRAE, 2007. HVAC Applications: Geothermal Energy, in: ASHRAE Handbook. American Society of Heating, Refrigerating and Air-Conditioning Engineers, Inc., Atlanta, pp. 32.1-32.2.

ASHRAE, 1996. 96/01978 Commercial/Institutional ground-source heat pump engineering manual. Fuel Energy Abstr. 37, 134. https://doi.org/10.1016/0140-6701(96)87998-7

Austin, W., Yavuzturk, C., 2000. Development of an in-situ system and analysis procedure for measuring ground thermal properties. ASHRAE Trans. 106, 365–379.

Babatunde, O.M., Munda, J.L., Hamam, Y., 2019. Selection of a hybrid renewable energy systems for a low-income household. Sustain. 11, 1–24. https://doi.org/10.3390/su11164282

Badescu, V., 2007. Economic aspects of using ground thermal energy for passive house heating. Renew. Energy 32, 895–903. https://doi.org/10.1016/J.RENENE.2006.04.006

Baek, S.H., Yeo, M.S., Kim, K.W., 2017. Effects of the geothermal load on the ground temperature recovery in a ground heat exchanger. Energy Build. 136, 63–72. https://doi.org/10.1016/j.enbuild.2016.11.056

Ball, D., Fischer, R., Hodgett, D., 1983. Design methods for ground-source heat pumps. ASHRAE Trans. 89, 416–440.

Bandyopadhyay, G., Gosnold, W., Mann, M., 2008. Analytical and semi-analytical solutions for short-time transient response of ground heat exchangers. Energy Build. 40, 1816–1824. https://doi.org/10.1016/j.enbuild.2008.04.005

Bartolini, N., Casasso, A., Bianco, C., Sethi, R., 2020. Environmental and Economic Impact of the Antifreeze Agents in Geothermal Heat Exchangers. Energies 13, 5653. https://doi.org/10.3390/en13215653

Bartolozzi, I., Rizzi, F., Frey, M., 2017. Are district heating systems and renewable energy sources always an environmental win-win solution? A life cycle assessment case study in Tuscany, Italy. Renew. Sustain. Energy Rev. 80, 408–420. https://doi.org/10.1016/j.rser.2017.05.231

Bayer, P., Saner, D., Bolay, S., Rybach, L., Blum, P., 2012. Greenhouse gas emission savings of ground source heat pump systems in Europe: A review. Renew. Sustain. Energy Rev. 16, 1256–1267.

https://doi.org/10.1016/j.rser.2011.09.027

Bear, J., Yehuda, B., 2012. Introduction to modeling of transport phenomena in porous media, Fourth ed. ed. Springer Science & Business Media.

Beier, R.., Smith, M.., 2003. Minimum duration of in-situ tests on vertical boreholes. ASHRAE Trans 109, 475–486.

Beier, R.A., 2014. Transient heat transfer in a U-tube borehole heat exchanger. Appl. Therm. Eng. 62, 256–266. https://doi.org/10.1016/j.applthermaleng.2013.09.014

Beier, R.A., Acuña, J., Mogensen, P., Palm, B., 2014. Transient heat transfer in a coaxial borehole heat exchanger. Geothermics 51, 470–482. https://doi.org/10.1016/j.geothermics.2014.02.006

Bennet, J., Claesson, J., Hellstrom, G., 1987. Multipole Method to Compute the Conductive Heat Transfer to and between Pipes in a Composite Cylinder, in: Notes on Heat Transfer 3. Department of Building Physics, Lund Institute of Technology, Lund, Sweden.

Bernier, M.A., 2001. Ground-coupled heat pump system simulation. ASHRAE Trans. 106, 605–616.

Bernier Michel, Eslami-nejad, P., 2013. A Preliminary Assessment on the Use of Phase Change Materials around Geothermal Boreholes. ASHRAE Trans. 119, 312.

Bezyan, B., Porkhial, S., Mehrizi, A.A., 2015. 3-D simulation of heat transfer rate in geothermal pile-foundation heat exchangers with spiral pipe configuration. Appl. Therm. Eng. 87, 655–668. https://doi.org/10.1016/j.applthermaleng.2015.05.051

Birsen, E., 2010. The effect of soil type on sizing of vertical single U-tube ground heat exchanger for Ground Source Heat Pump, in: International Scientific Conference.

Blum, P., Campillo, G., Kölbel, T., 2011. Techno-economic and spatial analysis of vertical ground source heat pump systems in Germany. Energy 36, 3002–3011. https://doi.org/10.1016/J.ENERGY.2011.02.044

Blum, P., Campillo, G., Münch, W., Kölbel, T., 2010. CO2 savings of ground source heat pump systems – A regional analysis. Renew. Energy 35, 122–127. https://doi.org/https://doi.org/10.1016/j.renene.2009.03.034

Borinaga-Treviño, R., Pascual-Muñoz, P., Castro-Fresno, D., Blanco-Fernandez, E., 2013a. Borehole thermal response and thermal resistance of four different grouting materials measured with a TRT. Appl. Therm. Eng. 53, 13–20. https://doi.org/10.1016/j.applthermaleng.2012.12.036

Borinaga-Treviño, R., Pascual-Muñoz, P., Castro-Fresno, D., Del Coz-Diaz, J.J., 2013b. Study of different grouting materials used in vertical geothermal closed-loop heat exchangers. Appl. Therm. Eng. 50, 159–167. https://doi.org/10.1016/j.applthermaleng.2012.05.029

Bose, J., 1989. Soil and rock classification for design of ground coupled heat pump systems-field manual.

Bozzoli, F., Pagliarini, G., Rainieri, S., Schiavi, L., 2011. Estimation of soil and grout thermal properties through a TSPEP (two-step parameter estimation procedure) applied to TRT (thermal response test) data. Energy 36, 839–846. https://doi.org/10.1016/j.energy.2010.12.031

Brandl, H., 2013. Thermo-active Ground-Source Structures for Heating and Cooling. Procedia Eng. 57, 9–18. https://doi.org/10.1016/J.PROENG.2013.04.005

Breger, D.S., Hubbell, J.E., Hasnaoui, H. El, Sunderland, J.E., 1996. Thermal energy storage in the ground: Comparative analysis of heat transfer modeling using U-tubes and boreholes. Sol. Energy 56, 493–503. https://doi.org/10.1016/0038-092x(96)00013-8

Camdali, U., Tuncel, E., 2013. An economic analysis of horizontal Ground Source Heat Pumps (GSHPs) for use in heating and cooling in Bolu, Turkey. Energy Sources, Part B Econ. Plan. Policy 8, 290–303. https://doi.org/10.1080/15567240903452097

Carotenuto, A., Marotta, P., Massarotti, N., Mauro, A., Normino, G., 2017. Energy piles for ground source heat pump applications: Comparison of heat transfer

performance for different design and operating parameters. Appl. Therm. Eng. 124, 1492–1504. https://doi.org/10.1016/J.APPLTHERMALENG.2017.06.038

Carslaw, H., Jaeger, J., 1959. Conduction of heat in solids, 2nd ed. Oxford University Press, Oxford, UK.

Casasso, A., Sethi, R., 2019. Assessment and minimization of potential environmental impacts of ground source heat pump (GSHP) systems. Water (Switzerland) 11, 1–19. https://doi.org/10.3390/w11081573

Chang, J., Liu, H., Wang, C., Liu, M., 2017. The applications and economic analysis of Ground Source Heat Pump (GSHP) in certain national games sports centre. Procedia Eng. 205, 863–870. https://doi.org/10.1016/j.proeng.2017.10.029

Chiasson, A., 2006. Life-Cycle Cost Study of a Geothermal Heat Pump System.

Chiasson, A.D., Rees, S.J., Spitler, J.D., 2000. Preliminary assessment of the effects of groundwater flow on closed-loop ground-source heat pump systems. ASHRAE Trans. 106, 380–393.

Choudhary, A., 1976. An approach to determine the termal conductivity and diffusivity of a rock in situ. Oklahoma State, USA.

Christodoulides, P., Aresti, L., Florides, G., 2019. Air-conditioning of a typical house in moderate climates with Ground Source Heat Pumps and cost comparison with Air Source Heat Pumps. Appl. Therm. Eng. 158, 113772. https://doi.org/10.1016/J.APPLTHERMALENG.2019.113772

Christodoulides, P., Florides, G., Pouloupatis, P., 2016. A practical method for computing the thermal properties of a Ground Heat Exchanger. Renew. Energy 94, 81–89. https://doi.org/10.1016/j.renene.2016.03.035

Christodoulides, P., Vieira, A., Lenart, S., Maranha, J., Vidmar, G., Popov, R., Georgiev, A., Aresti, L., Florides, G., 2020. Reviewing the Modeling Aspects and Practices of Shallow Geothermal Energy Systems. Energies 13, 4273. https://doi.org/10.3390/en13164273

Chulho, L., Moonseo, P., Sunhong, M., Shin-Hyung, K., Byonghu, S., Hangseok, C., Lee, C., Park, M., Min, S., Kang, S.-H., Sohn, B., Choi, H., 2011.

Comparison of effective thermal conductivity in closed-loop vertical ground heat exchangers. Appl. Therm. Eng. 31, 3669–3676. https://doi.org/10.1016/j.applthermaleng.2011.01.016

Claesson, J., Eskilson, P., 1988. Conductive heat extraction by a deep borehole. Sweden.

Congedo, P.M., Colangelo, G., Starace, G., 2012. CFD simulations of horizontal ground heat exchangers: A comparison among different configurations. Appl. Therm. Eng. 33–34, 24–32. https://doi.org/10.1016/j.applthermaleng.2011.09.005

Cui, P., Li, X., Man, Y., Fang, Z., 2011. Heat transfer analysis of pile geothermal heat exchangers with spiral coils. Appl. Energy 88, 4113–4119. https://doi.org/10.1016/j.apenergy.2011.03.045

Cui, Y., Zhu, J., Meng, F., 2018. Techno-economic evaluation of multiple energy piles for a ground-coupled heat pump system. Energy Convers. Manag. 178, 200–216. https://doi.org/10.1016/J.ENCONMAN.2018.10.042

Cui, Y., Zhu, J., Twaha, S., Chu, J., Bai, H., Huang, K., Chen, X., Zoras, S., Soleimani, Z., 2019. Techno-economic assessment of the horizontal geothermal heat pump systems: A comprehensive review. Energy Convers. Manag. 191, 208–236. https://doi.org/10.1016/J.ENCONMAN.2019.04.018

Cyprus Energy Service, 2009. Thermal Insulation Guide (2nd edition). Ministry of Energy Commerce Industry and Tourism, Nicosia.

CYSTAT, 2016. Construction and Housing Statistics.

D'Agostino, D., Parker, D., Melià, P., 2019. Environmental and economic implications of energy efficiency in new residential buildings: A multi-criteria selection approach. Energy Strateg. Rev. 26. https://doi.org/10.1016/j.esr.2019.100412

Daehoon, K., Gyoungman, K., Donghui, K., Hwanjo, B., 2017. Experimental and numerical investigation of thermal properties of cement-based grouts used for vertical ground heat exchanger. Renew. Energy 112, 260–267. https://doi.org/10.1016/j.renene.2017.05.045

Darcy, H., 1856. Les fontaines publiques de la ville de Dijon. Victor Dalmont.

De Moel, M., Bach, P.M., Bouazza, A., Singh, R.M., Sun, J.O., 2010. Technological advances and applications of geothermal energy pile foundations and their feasibility in Australia. Renew. Sustain. Energy Rev. 14, 2683–2696. https://doi.org/10.1016/J.RSER.2010.07.027

Dehghan B., B., 2017. Experimental and computational investigation of the spiral ground heat exchangers for ground source heat pump applications. Appl. Therm. Eng. 121, 908–921. https://doi.org/10.1016/J.APPLTHERMALENG.2017.05.002

Dehghan, B., Sisman, A., Aydin, M., 2016. Parametric investigation of helical ground heat exchangers for heat pump applications. Energy Build. 127, 999–1007. https://doi.org/10.1016/J.ENBUILD.2016.06.064

Delaleux, F., Py, X., Olives, R., Dominguez, A., 2012. Enhancement of geothermal borehole heat exchangers performances by improvement of bentonite grouts conductivity. Appl. Therm. Eng. 33–34, 92–99. https://doi.org/10.1016/j.applthermaleng.2011.09.017

Desmedt, J., Van Bael, J., Hoes, H., Robeyn, N., 2012. Experimental performance of borehole heat exchangers and grouting materials for ground source heat pumps. Int. J. Energy Res. 36, 1238–1246. https://doi.org/10.1002/er

DiPippo, R., 1980. Geothermal energy as a source of electricity. A worldwide survey of the design and operation of geothermal power plants. Office of Scientific and Technical Information (OSTI). https://doi.org/10.2172/5165898

Domenico, P.A.., Schwartz, F.W., 1990. Physical and chemical hydrogeology. John Wiely and Sons, New York.

Dreyer, L.C., Niemann, A.L., Hauschild, M.Z., 2003. Comparison of Three Different LCIA Methods: EDIP97, CML2001 and Eco-indicator 99. Int. J. Life Cycle Assess. 8, 191–200. https://doi.org/10.1007/bf02978471

Esen, H., Inalli, M., Esen, M., 2007. A techno-economic comparison of ground-coupled and air-coupled heat pump system for space cooling. Build. Environ. 42, 1955–1965. https://doi.org/10.1016/J.BUILDENV.2006.04.007

Esen, H., Inalli, M., Esen, M., 2006. Technoeconomic appraisal of a ground source heat pump system for a heating season in eastern Turkey. Energy Convers. Manag. 47, 1281–1297. https://doi.org/10.1016/j.enconman.2005.06.024

Eskilson, P., 1987. Thermal analysis of heat extraction boreholes. Lund, Sweden.

EU Parliament, 2010. Directive 2010/31/EU of the European Parliment and of the Council of 19 May 2010 on the energy performance of buildings, Official Journal of the European Union.

European, C., 2016. Eurostat Database.

European Enviromental Agency, 2008. Emission intensity of public conventional thermal power.

European Environmental Agency, 2004. EN08 Emissions (CO2, SO2 and NOx) intensity of public conventional thermal power (electricity and heat) production.

Fadejev, J., Simson, R., Kurnitski, J., Haghighat, F., 2017. A review on energy piles design, sizing and modelling. Energy 122, 390–407. https://doi.org/10.1016/J.ENERGY.2017.01.097

Fan, R., Jiang, Y., Yao, Y., Shiming, D., Ma, Z., 2007. A study on the performance of a geothermal heat exchanger under coupled heat conduction and groundwater advection. Energy 32, 2199–2209. https://doi.org/10.1016/J.ENERGY.2007.05.001

FascÌ, M.L., Lazzarotto, A., Acuna, J., Claesson, J., 2019. Analysis of the thermal interference between ground source heat pump systems in dense neighborhoods. Sci. Technol. Built Environ. 25, 1069–1080. https://doi.org/10.1080/23744731.2019.1648130

Florides, G., Kalogirou, S., 2007. Ground heat exchangers—A review of systems, models and applications. Renew. Energy 32, 2461–2478. https://doi.org/10.1016/j.renene.2006.12.014

Florides, Georgios, Pouloupatis, P.D., Kalogirou, S., Messaritis, V., Panayides, I., Zomeni, Z., Partasides, G., Lizides, A., Sophocleous, E., Koutsoumpas, K., 2013. Geothermal properties of the ground in Cyprus and their effect on the

efficiency of ground coupled heat pumps. Renew. Energy 49, 85–89. https://doi.org/10.1016/j.renene.2012.01.059

Florides, G., Theofanous, E., Stylianou, I.I., Tassou, S., Christodoulides, P., Zomeni, Z., Tsiolakis, E., Kalogirou, S., Messaritis, V., Pouloupatis, P., Panayiotou, G., 2013. Modeling and assessment of the efficiency of horizontal and vertical ground heat exchangers. Energy 58, 655–663. https://doi.org/10.1016/j.energy.2013.05.053

Florides, G.A., Christodoulides, P., Pouloupatis, P., 2013. Single and double U-tube ground heat exchangers in multiple-layer substrates. Appl. Energy 102, 364–373. https://doi.org/10.1016/j.apenergy.2012.07.035

Florides, G.A.A., Pouloupatis, P.D.D., Kalogirou, S., Messaritis, V., Panayides, I., Zomeni, Z., Partasides, G., Lizides, A., Sophocleous, E., Koutsoumpas, K., 2011. The geothermal characteristics of the ground and the potential of using ground coupled heat pumps in Cyprus. Energy 36, 5027–5036. https://doi.org/10.1016/j.energy.2011.05.048

Fokaides, P.A., Christoforou, E.A., Kalogirou, S.A., 2014. Legislation driven scenarios based on recent construction advancements towards the achievement of nearly zero energy dwellings in the southern European country of Cyprus. Energy 66, 588–597. https://doi.org/10.1016/J.ENERGY.2013.12.073

Franzén, I., Nedar, L., Andersson, M., 2019. Environmental Comparison of Energy Solutions for Heating and Cooling. Sustain. 11. https://doi.org/10.3390/su11247051

Gabrielli, L., Bottarelli, M., 2016. Financial and economic analysis for ground-coupled heat pumps using shallow ground heat exchangers. Sustain. Cities Soc. 20, 71–80. https://doi.org/10.1016/J.SCS.2015.09.008

Gao, J., Zhang, X., Liu, J., Li, K., Yang, J., 2008. Numerical and experimental assessment of thermal performance of vertical energy piles: An application. Appl. Energy 85, 901–910. https://doi.org/10.1016/J.APENERGY.2008.02.010

Gashti, E.H.N., Uotinen, V.-M., Kujala, K., 2014. Numerical modelling of thermal

regimes in steel energy pile foundations: A case study. Energy Build. 69, 165–174. https://doi.org/10.1016/J.ENBUILD.2013.10.028

Gehlin, S., 2002. Thermal response test: method development and evaluation. Luleå tekniska universitet, Sweden.

Gehlin, S., Hellstrom, G., 2000. Recent status of in-situ thermal response tests for BETES applications in Sweden, in: Proceeding of the Terrastock. Stuttgart, Germany.

Gehlin, S., Nordell, B., 2003. Determination undisturbed ground temperature for thermal response test. Ashrae 4614, 151–156.

Genchi, Y., Kikegawa, Y., Inaba, A., 2002. CO2 payback–time assessment of a regional-scale heating and cooling system using a ground source heat–pump in a high energy–consumption area in Tokyo. Appl. Energy 71, 147–160. https://doi.org/10.1016/S0306-2619(02)00010-7

Gilbreath, C.S., 1996. Hybrid ground-source heat pump systems for commercial applications. Tuscaloosa, Alabama.

Greening, B., Azapagic, A., 2012. Domestic heat pumps: Life cycle environmental impacts and potential implications for the UK. Energy 39, 205–217. https://doi.org/10.1016/j.energy.2012.01.028

Guo, Y., Zhang, G., Zhou, J., Wu, J., Shen, W., 2012. A techno-economic comparison of a direct expansion ground-source and a secondary loop ground-coupled heat pump system for cooling in a residential building. Appl. Therm. Eng. 35, 29–39. https://doi.org/10.1016/J.APPLTHERMALENG.2011.09.032

Hamada, Y., Hisashi, S., Makoto, N., Hideki, K., Ochifuji, K., 2007. Field performance of a pile GHE system for space heating. Energy Build. 39, 517–524.

Harr, M.., 1991. Groundwater and Seepage.

Hart, D., Couvillion, R., 1986. Earth coupled heat transfer. National Water Well Association.

Healy, P.F., Ugursal, V.I., 1997. Performance and economic feasibility of ground source heat pumps in cold climate. Int. J. Energy Res. 21, 857–870.

https://doi.org/10.1002/(SICI)1099-114X(199708)21:10<857::AID-ER279>3.0.CO;2-1

Hellstrom, G., 1991. Ground heat storage: Thermal analyses of duct storage systems. University of Lung.

Hellstrom, G., Sanner, B., 1997. EED – Earth Energy Designer,Version 1.0, User's Manual. Wetzlar, Germany.

Huang, B., Mauerhofer, V., 2016. Life cycle sustainability assessment of ground source heat pump in Shanghai, China. J. Clean. Prod. 119, 207–214. https://doi.org/10.1016/j.jclepro.2015.08.048

Huang, G., Yang, X., Liu, Y., Zhuang, C., Zhang, H., Lu, J., 2018. A novel truncated cone helix energy pile: Modelling and investigations of thermal performance. Energy Build. 158, 1241–1256. https://doi.org/10.1016/J.ENBUILD.2017.11.020

IGSHPA, 2013. Closed-loop/geothermal heat pump systems: design and installation standards, 2013 edition. International Ground Source Heat Pump Association, Oklahoma State University.

Incropera, F., Dewitt, D., 1985. Introduction to heat transfer. John Wiley and Sons Inc., New York.

Ingersoll, L., Adler, F., Plass, H., Ingersoll, A., 1950. Theory of earth heat exchangers for the heat pump. ASHVE Trans 56, 167–188.

Ingersoll, L., Zobel, O., Ingersoll, A., 1954. Heat. McGraw-Hill, New York.

Ingersoll, L.R., Plass, H.J., 1948. Theory of the groung pipe heat source for the heat pump. Heating, Pip. Air Contitioning 20, 119–122.

Ingersoll, L.R., Zobel, O.J., Ingersoll, A.C., 1955. Heat Conduction with Engineering, Geological, and Other Applications. Phys. Today 8, 17. https://doi.org/10.1063/1.3061951

ISO 14040, 2006. Environmental management — Life cycle assessment — Principles and framework.

ISO 14044, 2006. Environmental management — Life cycle assessment —

Requirements and guidelines.

Jaeger, J.G., 1944. Some problems involving line sources in conduction of heat. London, Edinburgh, Dublin Philos. Mag. J. Sci. 35, 169–179. https://doi.org/10.1080/14786444408521476

Javed, S., Fahlén, P., Claesson, J., 2009. Vertical Ground Heat Exchangers: A review of heat flow models, in: Proceedings of Effstock 2009: The 11th International Conference on Thermal Energy Storages. Stockholm, Sweden, pp. 53–78. https://doi.org/10.1017/CBO9780511974885.006

Javed, S., Fahlen, P., Fahlén, P., 2011. Thermal response testing of a multiple borehole ground heat exchanger. Int. J. Low-Carbon Technol. 6, 141–148. https://doi.org/10.1093/ijlct/ctr004

Jensen, D.A., Kaminski, M.K., 2005. Introduction to thermal and fluids engineering. John Wiley & Sons Inc.

Jobmann, M., Buntebarth, G., 2009. Influence of graphite and quartz addition on the thermal-physical properties of bentonite for sealing heat-generating radial-active waste. Appl. Clay Sci. 44, 206–210.

Jun, L., Xu, Z., Jun, G., Jie, Y., 2009. Evaluation of heat exchange rate of GHE in geothermal heat pump systems. Renew. Energy 34, 2898–2904. https://doi.org/10.1016/j.renene.2009.04.009

Kara, Y.A., 2007. Experimental performance evaluation of a closed-loop vertical ground source heat pump in the heating mode using energy analysis method. Int. J. Energy Res. 31, 1504–1516. https://doi.org/10.1002/er.1316

Kavanaugh, S.P., 1998. A Design Method for Hybrid Ground-Source Heat Pumps. ASHRAE Annu. Meet. 691–698.

Kavanaugh, S.P., 1985. Simulation and experimental verification of vertical ground-coupled heat pump systems. Oklahoma State Univ. Stillwater, USA, PhD Thesis 194.

Kavanaugh, S.P., Rafferty, K., 1997. Ground-source heat pumps, design of geothermal systems for commercial and institutional buildings. Atlanta.

Kayaci, N., Demir, H., 2020. Comparative performance analysis of building

foundation Ground heat exchanger. Geothermics 83, 101710. https://doi.org/10.1016/J.GEOTHERMICS.2019.101710

Kelvin, T.., 1882. Mathematical and physical papers. Cambridge University Press, London.

Kharseh, M., Al-Khawaja, M., Suleiman, M.T., 2015. Potential of ground source heat pump systems in cooling-dominated environments: Residential buildings. Geothermics 57, 104–110. https://doi.org/10.1016/J.GEOTHERMICS.2015.06.009

Kim, M.-J., Lee, S.-R., Yoon, S., Go, G.-H., 2016. Thermal performance evaluation and parametric study of a horizontal ground heat exchanger. Geothermics 60, 134–143. https://doi.org/10.1016/j.geothermics.2015.12.009

Kim, M.-J., Lee, S.-R., Yoon, S., Jeon, J.-S., 2018. Evaluation of geometric factors influencing thermal performance of horizontal spiral-coil ground heat exchangers. Appl. Therm. Eng. 144, 788–796. https://doi.org/10.1016/J.APPLTHERMALENG.2018.08.084

Kljajić, M. V., Anđelković, A.S., Hasik, V., Munćan, V.M., Bilec, M., 2020. Shallow geothermal energy integration in district heating system: An example from Serbia. Renew. Energy 147, 2791–2800. https://doi.org/10.1016/j.renene.2018.11.103

Kljajić, M. V., Anđelković, A.S., Hasik, V., Munćan, V.M., Bilec, M., 2018. Shallow geothermal energy integration in district heating system: An example from Serbia. Renew. Energy. https://doi.org/10.1016/J.RENENE.2018.11.103

Koroneos, C.J., Nanaki, E.A., 2017. Environmental impact assessment of a ground source heat pump system in Greece. Geothermics 65, 1–9. https://doi.org/10.1016/j.geothermics.2016.08.005

Kristmannsdóttir, H., Ármannsson, H., 2003. Environmental aspects of geothermal energy utilization. Geothermics 32, 451–461. https://doi.org/10.1016/S0375-6505(03)00052-X

Laloui, L., Nuth, M., Vulliet, L., 2005. Chapter 37 Experimental and numerical investigations of the behaviour of a heat exchanger pile. Elsevier Geo-

Engineering B. Ser. 3, 1065–1084. https://doi.org/10.1016/S1571-9960(05)80040-0

Lamarche, L., Beauchamp, B., 2007a. A new contribution to the finite line-source model for geothermal boreholes. Energy Build. 39, 188–198. https://doi.org/10.1016/j.enbuild.2006.06.003

Lamarche, L., Beauchamp, B., 2007b. New solutions for the short-time analysis of geothermal vertical boreholes. Int. J. Heat Mass Transf. 50, 1408–1419. https://doi.org/10.1016/j.ijheatmasstransfer.2006.09.007

Lamarche, L., Kajl, S., Beauchamp, B., 2010. A review of methods to evaluate borehole thermal resistances in geothermal heat-pump systems. Geothermics 39, 187–200. https://doi.org/10.1016/j.geothermics.2010.03.003

Lanini, S., Delaleux, F., Py, X., R.Olivès, Nguyen, D., 2014. Improvement of borehole thermal energy storage design based on experimental and modelling results. Energy Build. 77, 393–400. https://doi.org/10.1016/j.enbuild.2014.03.056

Lee, C., Lee, K., Choi, H.H.-P., Choi, H.H.-P., Chulho, L., Kangja, L., Hangseok, C., Hyo-Pum, C., 2010. Characteristics of thermally-enhanced bentonite grouts for geothermal heat exchanger in South Korea. Sci. China Ser. E Technol. Sci. 53, 123–128. https://doi.org/10.1007/s11431-009-0413-9

Lee, C., Park, M., Nguyen, T.B., Sohn, B., Choi, J.M., Choi, H., 2012. Performance evaluation of closed-loop vertical ground heat exchangers by conducting in-situ thermal response tests. Renew. Energy 42, 77–83. https://doi.org/10.1016/j.renene.2011.09.013

Li, M., Lai, A.C.K., 2012. New temperature response functions (G functions) for pile and borehole ground heat exchangers based on composite-medium line-source theory. Energy 38, 255–263. https://doi.org/10.1016/j.energy.2011.12.004

Li, W., Li, X., Wang, Y., Tu, J., 2018. An integrated predictive model of the long-term performance of ground source heat pump (GSHP) systems. Energy Build. 159, 309–318. https://doi.org/10.1016/j.enbuild.2017.11.012

Li, Z., Zheng, M., 2009. Development of a numerical model for the simulation of vertical U-tube ground heat exchangers. Appl. Therm. Eng. 29, 920–924. https://doi.org/10.1016/j.applthermaleng.2008.04.024

Lo Russo, S., Boffa, C., Civita, M. V., 2009. Low-enthalpy geothermal energy: An opportunity to meet increasing energy needs and reduce CO2 and atmospheric pollutant emissions in Piemonte, Italy. Geothermics 38, 254–262. https://doi.org/10.1016/j.geothermics.2008.07.005

Lok Do, S., Haberl, J.S., 2010. A review on ground coupled heat pump models used in whole-building computer simulation programs. Proceedings of the 17th Symposium for Improving Building Systems in Hot and Humid Climates, Autin, Texas.

Loveridge, F., 2012. The Thermal Performance of Foundation Piles used as Heat Exchangers in Ground Energy Systems. Univ. Southhampt. 206.

Lu, Q., Narsilio, G.A., Aditya, G.R., Johnston, I.W., 2017. Economic analysis of vertical ground source heat pump systems in Melbourne. Energy 125, 107–117. https://doi.org/10.1016/j.energy.2017.02.082

Luo, J., Rohn, J., Bayer, M., Priess, A., 2013. Thermal Efficiency Comparison of Borehole Heat Exchangers with Different Drillhole Diameters. Energies 6, 4187–4206. https://doi.org/10.3390/en6084187

Luo, J., Rohn, J., Bayer, M., Priess, A., Wilkmann, L., Xiang, W., 2015a. Heating and cooling performance analysis of a ground source heat pump system in Southern Germany. Geothermics 53, 57–66. https://doi.org/10.1016/J.GEOTHERMICS.2014.04.004

Luo, J., Rohn, J., Xiang, W., Bayer, M., Priess, A., Wilkmann, L., Steger, H., Zorn, R., 2015b. Experimental investigation of a borehole field by enhanced geothermal response test and numerical analysis of performance of the borehole heat exchangers. Energy 84, 473–484. https://doi.org/10.1016/j.energy.2015.03.013

Luo, J., Xue, W., Hu, T., Xiang, W., Rohn, J., 2019. Thermo-economic analysis of borehole heat exchangers (BHE) grouted using drilling cuttings in a dolomite

area. Appl. Therm. Eng. 150, 305–315. https://doi.org/10.1016/J.APPLTHERMALENG.2018.12.130

Ma, W., Fang, S., Liu, G., Zhou, R., 2017. Modeling of district load forecasting for distributed energy system. Appl. Energy 204, 181–205. https://doi.org/10.1016/j.apenergy.2017.07.009

Man, Y., Yang, H., Diao, N., Cui, P., Lu, L., Fang, Z., 2011. Development of spiral heat source model for novel pile ground heat exchangers. HVAC&R Res. 17, 1075–1088. https://doi.org/10.1080/10789669.2011.610281

Man, Y., Yang, H., Diao, N., Liu, J., Fang, Z., 2010. A new model and analytical solutions for borehole and pile ground heat exchangers. Int. J. Heat Mass Transf. 53, 2593–2601. https://doi.org/10.1016/j.ijheatmasstransfer.2010.03.001

Manganelli, B., Morano, P., Tajani, F., Salvo, F., 2019. Affordability assessment of energy-efficient building construction in Italy. Sustain. 11. https://doi.org/10.3390/su11010249

Marcotte, D., Pasquier, P., 2008. On the estimation of thermal resistance in borehole thermal conductivity test. Renew. Energy 33, 2407–2415. https://doi.org/10.1016/j.renene.2008.01.021

Mazyar, S., Moghaddam, H., 2015. First step towards development of Distributed thermal response test using heating cables. Stockholm, Sweden.

Mehrizi, A.A., Porkhial, S., Bezyan, B., Lotfizadeh, H., 2016. Energy pile foundation simulation for different configurations of ground source heat exchanger. Int. Commun. Heat Mass Transf. 70, 105–114. https://doi.org/10.1016/J.ICHEATMASSTRANSFER.2015.12.001

Mei, V., Emerson, C., 1985. New approach for analysis of ground-coil design for applied heat pump systems. ASHRAE Trans. 91, 1216–1224.

Michopoulos, A., Voulgari, V., Tsikaloudaki, A., Zachariadis, T., 2016. Evaluation of ground source heat pump systems for residential buildings in warm Mediterranean regions: the example of Cyprus. Energy Effic. 9, 1421–1436. https://doi.org/10.1007/s12053-016-9431-1

Ministry of Commerce Industry and Energy Tourism, C., 2017. 2nd National plan fo increasing the number of Nearly Zero-Energy Buildings (NZEBs), Press and Information Office.

Mogensen, P., 1983. Fluid to Duct Wall Heat Transfer in Duct System Heat Storage, in: Proceedings of the International Conference on Subsurface Heat Storage in Theory and Practice. Stockholm, Sweden.

Monteiro, H., Freire, F., 2012. Life-cycle assessment of a house with alternative exterior walls: Comparison of three impact assessment methods. Energy Build. 47, 572–583. https://doi.org/10.1016/j.enbuild.2011.12.032

Monzo, P., 2011. Comparison of different Line Source Model approaches for analysis of Thermal Response Test in a U-pipe Borehole Heat Exchanger.

Morino, K., Oka, T., 1994. Study on heat exchanged in soil by circulating water in a steel pile. Energy Build. 21, 65–78. https://doi.org/10.1016/0378-7788(94)90017-5

Morrone, B., Coppola, G., Raucci, V., 2014. Energy and economic savings using geothermal heat pumps in different climates. Energy Convers. Manag. 88, 189–198. https://doi.org/10.1016/J.ENCONMAN.2014.08.007

Muraya, N., O'Neal, D., Heffington, W., 1996. Thermal interference of adjacent legs in a vertical U-tube heat exchanger for a ground-coupled heat pump. ASHRAE Trans. 102, 12–21.

Nguyen, A., Pasquier, P., Marcotte, D., 2015. Influence of groundwater flow in fractured aquifers on standing column wells performance. Geothermics 58, 39–48. https://doi.org/10.1016/j.geothermics.2015.08.005

Nield, D.A., Bejan, A., 2013. Convection in Porous Media, in: Convection Heat Transfer. John Wiley & Sons, Inc., Hoboken, NJ, USA.

Nordelöf, A., Poulikidou, S., Chordia, M., de Oliveira, F.B., Tivander, J., Arvidsson, R., 2019. Methodological approaches to end-of-life modelling in life cycle assessments of lithium-ion batteries. Batteries 5. https://doi.org/10.3390/batteries5030051

Omer, A.M., 2008. Ground-source heat pumps systems and applications. Renew.

Sustain. Energy Rev. 12, 344–371. https://doi.org/10.1016/j.rser.2006.10.003

Ouyang, X., Lin, B., 2014. Levelized cost of electricity (LCOE) of renewable energies and required subsidies in China. Energy Policy 70, 64–73. https://doi.org/10.1016/J.ENPOL.2014.03.030

Pahud, D., Fromentin, A., Hadorn, J.C., 1996. The duct ground heat storage model (DST) for TRNSYS used for the simu- lation of heat exchanger piles, in: Proceedings of DGC-LASEN Conference. France.

Pahud, D., Fromentin, A., Hubbuch, M., 1999. Heat exchanger pile system for heating and cooling at Zurich Airport. IEA Heat Pump Cent. 17.

Pahud, D., Matthey, B., 2001. Comparison of the thermal performance of double U-pipe borehole heat exchangers measured in situ. Energy Build. 33, 503–507. https://doi.org/10.1016/s0378-7788(00)00106-7

Panayiotou, G., Kalogirou, S., Tassou, S., 2012. Design and simulation of a PV and a PV–Wind standalone energy system to power a household application. Renew. Energy 37, 355–363. https://doi.org/10.1016/J.RENENE.2011.06.038

Panayiotou, G.P., Kalogirou, S.A., Florides, G.A., Maxoulis, C.N., Papadopoulos, A.M., Neophytou, M., Fokaides, P., Georgiou, G., Symeou, A., Georgakis, G., 2010. The characteristics and the energy behaviour of the residential building stock of Cyprus in view of Directive 2002/91/EC. Energy Build. 42, 2083–2089. https://doi.org/10.1016/J.ENBUILD.2010.06.018

Park, H., Yoon, S., Shin, H., Lee, D.-S., 2012. Case study of heat transfer behavior of helical ground heat exchanger. Energy Build. https://doi.org/10.1016/j.enbuild.2012.06.019

Park, S., Lee, D., Choi, H.H.-J., Jung, K., Choi, H.H.-J., 2015. Relative constructability and thermal performance of cast-in-place concrete energy pile: Coil-type GHEX (ground heat exchanger). Energy 81, 56–66.

Park, S., Lee, S., Lee, D., Lee, S.S., Choi, H., 2016. Influence of coil pitch on thermal performance of coil-type cast-in-place energy piles. Energy Build. 129, 344–356. https://doi.org/10.1016/J.ENBUILD.2016.08.005

Pasquier, P., Nguyen, A., Eppner, F., Marcotte, D., Baudron, P., 2016. Standing

column wells, in: Advances in Ground-Source Heat Pump Systems. Elsevier, pp. 269–294. https://doi.org/10.1016/b978-0-08-100311-4.00010-8

PDE Solution, I., 2010. FlexPDE user guide [WWW Document]. URL http://www.pdesolutions.com/help/index.html?coordinatescaling.html

Ping, C., Yi, M., Zhaohong, F., 2015. Geothermal Heat Pumps, in: Handbook of Clean Energy Systems. JohnWiley & Sons, Ltd.

Pouloupatis, P.D.., 2014. Determination of the Thermal Characteristics of the Ground in Cyprus and Their Effect on Ground Heat. Brunel University.

Pouloupatis, P.D., Florides, G., Tassou, S., 2011. Measurements of ground temperatures in Cyprus for ground thermal applications. Renew. Energy 36, 804–814. https://doi.org/10.1016/j.renene.2010.07.029

Pouloupatis, P.D., Tassou, S.A., Christodoulides, P., Florides, G.A., 2017. Parametric analysis of the factors affecting the efficiency of ground heat exchangers and design application aspects in Cyprus. Renew. Energy 103, 721–728. https://doi.org/10.1016/j.renene.2016.11.006

Pu, L., Qi, D., Xu, L., Li, Y., 2017. Optimization on the performance of ground heat exchangers for GSHP using Kriging model based on MOGA. Appl. Therm. Eng. 118, 480–489. https://doi.org/10.1016/j.applthermaleng.2017.02.114

Ramos, R., Aresti, L., Christodoulides, P., Vieira, A., Florides, G., 2019a. Assessment and Comparison of Soil Thermal Characteristics by Laboratory Measurements, in: Ferrari A., Laloui L. (Eds) Energy Geotechnics. SEG 2018. Springer Series in Geomechanics and Geoengineering. Springer, Cham, pp. 155–162. https://doi.org/10.1007/978-3-319-99670-7_20

Ramos, R., Aresti, L., Yiannoukos, L., Tsiolakis, E., Pekris, J., Vieira, A., Florides, G., Christodoulides, P., 2019b. Thermal and physical characteristics of soils in Cyprus for use in shallow geothermal energy applications. Energy, Ecol. Environ. 4, 300–309. https://doi.org/10.1007/s40974-019-00137-2

Rawlings, R.H.D., Sykulski, J.R., 1999. Ground source heat pumps : A technology review. Build. Serv. Eng. Res. Technol. 20, 119–129.

Raymond, J., Robert, G., Therrien, R., Gosselin, L., 2010. A Novel Thermal

Response Test Using Heating Cables. Proc. World Geotherm. Congr. 1–8.

Ren, C., Deng, Y., Cao, S.J., 2018. Evaluation of polyethylene and steel heat exchangers of ground source heat pump systems based on seasonal performance comparison and life cycle assessment. Energy Build. 162, 54–64. https://doi.org/10.1016/j.enbuild.2017.12.037

Robert, F., Gosselin, L., 2014. New methodology to design ground coupled heat pump systems based on total cost minimization. Appl. Therm. Eng. 62, 481–491. https://doi.org/10.1016/J.APPLTHERMALENG.2013.08.003

Rottmayer, S., Beckman, W., Mitchell, J., 1997. Simulation of a single vertical U-tube ground heat exchanger in an infinite medium. ASHRAE Trans. 103, 651–659.

Ruiz-Calvo, F., De Rosa, M., Acuña, J., Corberán, J.M.M., Montagud, C., Rosa, M. De, Acuña, J., Corberán, J.M.M., Montagud, C., 2015. Experimental validation of a short-term Borehole-to-Ground (B2G) dynamic model. Appl. Energy 140, 210–223. https://doi.org/10.1016/j.apenergy.2014.12.002

Saeidi, R., Noorollahi, Y., Esfahanian, V., 2018. Numerical simulation of a novel spiral type ground heat exchanger for enhancing heat transfer performance of geothermal heat pump. Energy Convers. Manag. 168, 296–307. https://doi.org/10.1016/J.ENCONMAN.2018.05.015

Saner, D., Juraske, R., Kübert, M., Blum, P., Hellweg, S., Bayer, P., 2010. Is it only CO2 that matters? A life cycle perspective on shallow geothermal systems. Renew. Sustain. Energy Rev. 14, 1798–1813. https://doi.org/10.1016/j.rser.2010.04.002

Sani, A.K., Singh, R.M., Amis, T., Cavarretta, I., 2019. A review on the performance of geothermal energy pile foundation, its design process and applications. Renew. Sustain. Energy Rev. 106, 54–78. https://doi.org/10.1016/J.RSER.2019.02.008

Sanner, B., Mands, E., Sauer, M., Grundmann, E., 2008. Thermal Response Test: a routine method to determine thermal ground properties for GSHP design. Proc. IEA HPC 20–22.

Sass, J.H.H., Lachenbruch, A.H., Munroe, R.J., Lachenbruch, H., Munro, R.J., 1971. Thermal conductivity of rocks from measurements on fragments and its application to heat-flow determinations. J. Geophys. Res. 76, 3391–3401. https://doi.org/10.1029/jb076i014p03391

Seddiki, M., Bennadji, A., 2019. Multi-criteria evaluation of renewable energy alternatives for electricity generation in a residential building. Renew. Sustain. Energy Rev. 110, 101–117. https://doi.org/10.1016/j.rser.2019.04.046

Sekine, K., Ooka, R., Yokoi, M., Shiba, Y., Hwang, S., 2007. Development of a ground-source heat pump system with ground heat exchanger utilizing the cast-in-place concrete pile foundations of buildings. ASHRAE Trans. 113, 558–566.

Selamat, S., Miyara, A., Kariya, K., 2016. Numerical study of horizontal ground heat exchangers for design optimization. Renew. Energy 95, 561–573. https://doi.org/10.1016/j.renene.2016.04.042

Serghides, D.K., Dimitriou, S., Katafygiotou, M.C., Michaelidou, M., 2015. Energy Efficient Refurbishment towards Nearly Zero Energy Houses, for the Mediterranean Region. Energy Procedia 83, 533–543. https://doi.org/10.1016/J.EGYPRO.2015.12.173

Shonder, J., Beck, J., 1999. Determining effective soil temperature thermal properites from field data using parameter estimation technique. ASHRAE Trans. 105, 458–466.

Signorelli, S., Bassetti, S., Pahud, D., Kohl, T., 2007. Numerical evaluation of thermal response tests. Geothermics 36, 141–166. https://doi.org/10.1016/j.geothermics.2006.10.006

Sivasakthivel, T., Philippe, M., Murugesan, K., Verma, V., Hu, P., 2017. Experimental thermal performance analysis of ground heat exchangers for space heating and cooling applications. Renew. Energy 113, 1168–1181. https://doi.org/10.1016/j.renene.2017.06.098

Smith, M.D., Perry, R.L., 1999. Borehole grouting: Field studies and thermal performance testing. ASHRAE Trans. 105, 451.

Spilker, E., 1998. Ground-coupled heat pump loop design using thermal conductivity testing and the effect of different backfill materials on vertical bore length. ASHRAE Trans. 33, 775–779.

Spitler, J.D., Cullin, J.R., Lee, E., Fisher, D.D.E., Bernier, M., Kummert, M., Cui, P., Liu, X., 2009. Preliminary Intermodel Comparison of Ground Heat Exchanger Simulation Models. Proc. Effstock 2009 11th Int. Conf. Therm. energy storages 14–17.

Sterpi, D., Tomaselli, G., Angelotti, A., 2020. Energy performance of ground heat exchangers embedded in diaphragm walls: Field observations and optimization by numerical modelling. Renew. Energy 147, 2748–2760. https://doi.org/10.1016/J.RENENE.2018.11.102

Steubing, B., Wernet, G., Reinhard, J., Bauer, C., Moreno-Ruiz, E., 2016. The ecoinvent database version 3 (part II): analyzing LCA results and comparison to version 2. Int. J. Life Cycle Assess. 21, 1269–1281. https://doi.org/10.1007/s11367-016-1109-6

Stylianou, I.I., Christodoulides, P., Aresti, L., Tassou, S., Florides, G., 2018. Borehole Ground Heat Exchangers and the flow of underground water. Int. J. Ind. Electron. Electr. Eng. 67–72.

Stylianou, I.I., Tassou, S., Christodoulides, P., Aresti, L., Florides, G., 2019. Modeling of Vertical Ground Heat Exchangers in the Presence of Groundwater Flow and Underground Temperature Gradient. Energy Build. https://doi.org/10.1016/j.enbuild.2019.03.020

Stylianou, I.I., Tassou, S., Christodoulides, P., Panayides, I., Florides, G., 2016. Measurement and analysis of thermal properties of rocks for the compilation of geothermal maps of Cyprus. Renew. Energy 88, 418–429. https://doi.org/10.1016/J.RENENE.2015.10.058

Sullivan, W.G.., Wicks, E.M., Koelling, P.C.., 2014. Engineering economy, Sixteenth. ed. Pearson Education Limited, London.

Suryatriyastuti, M.E., Mroueh, H., Burlon, S., 2012. Understanding the temperature-induced mechanical behaviour of energy pile foundations. Renew.

Sustain. Energy Rev. 16, 3344–3354. https://doi.org/10.1016/J.RSER.2012.02.062

Suzuki, M., Yoneyama, K., Amemiya, S., Oe, M., 2016. Development of a Spiral Type Heat Exchanger for Ground Source Heat Pump System. Energy Procedia 96, 503–510. https://doi.org/10.1016/J.EGYPRO.2016.09.091

Tassou, S.A., Marquand, C.J., Wilson, D.R., 1986. Energy and economic comparisons of domestic heat pumps and conventional heating systems in the British climate. Appl. Energy 24, 127–138. https://doi.org/10.1016/0306-2619(86)90065-6

Thornton, J., McDowell, T., Shonder, J., Hughes, P., Pahud, D., Hellstrom, G., 1997. Residential Vertical Geothermal Heat Pump System Models: Calibration to Data. ASHRAE Trans. 103, 660–674.

Tsagarakis, K.P., 2019. Shallow geothermal energy under the microscope: Social, economic, and institutional aspects. Renew. Energy. https://doi.org/10.1016/J.RENENE.2019.01.004

Tsagarakis, K.P., 2007. Optimal number of energy generators for biogas utilization in wastewater treatment facility. Energy Convers. Manag. 48, 2694–2698. https://doi.org/10.1016/J.ENCONMAN.2007.04.025

Tsagarakis, K.P., Efthymiou, L., Michopoulos, A., Mavragani, A., Anđelković, A.S., Antolini, F., Bacic, M., Bajare, D., Baralis, M., Bogusz, W., Burlon, S., Figueira, J., Genç, M.S., Javed, S., Jurelionis, A., Koca, K., Ryżyński, G., Urchueguia, J.F., Žlender, B., 2018. A review of the legal framework in shallow geothermal energy in selected European countries: Need for guidelines. Renew. Energy. https://doi.org/10.1016/J.RENENE.2018.10.007

Weidema, B.P., 2015. Comparing Three Life Cycle Impact Assessment Methods from an Endpoint Perspective. J. Ind. Ecol. 19, 20–26. https://doi.org/10.1111/jiec.12162

Wernet, G., Bauer, C., Steubing, B., Reinhard, J., Moreno-Ruiz, E., Weidema, B., 2016. The ecoinvent database version 3 (part I): overview and methodology. Int. J. Life Cycle Assess. 21, 1218–1230. https://doi.org/10.1007/s11367-016-

1087-8

Wood, C.J., Liu, H., Riffat, S.B., 2012. Comparative performance of ‘U-tube’ and ‘coaxial’ loop designs for use with a ground source heat pump. Appl. Therm. Eng. 37, 190–195. https://doi.org/10.1016/j.applthermaleng.2011.11.015

Xu, X., 2007. Simulation and optimal control of hybrid ground source heat pump systems. Oklahoma State University, Oklahoma State, USA.

Yang, H., Cui, P., Fang, Z., 2010. Vertical-borehole ground-coupled heat pumps: A review of models and systems. Appl. Energy 87, 16–27. https://doi.org/10.1016/j.apenergy.2009.04.038

Yang, Y., Li, M., 2014. Short-time performance of composite-medium line-source model for predicting responses of ground heat exchangers with single U-shaped tube. Int. J. Therm. Sci. 82, 130–137. https://doi.org/10.1016/j.ijthermalsci.2014.04.002

Yavuzturk, C., 1988. Modeling of vertical ground loop heat exchangers for ground source heat pump systems. Stillwater, Oklahoma.

Yavuzturk, C., Spitler, J., 2000. Comparative study of operating and control strategies for hybrid ground-source heat pump systems using a short time step simulation model. ASHRAE Transctions 106, 192–209.

Yavuzturk, C., Spitler, J., 1999. A short time step response factor model for vertical ground loop heat exchangers. ASHRAE Trans. 105, 475–485.

Yoon, S., Lee, S.-R., Go, G.-H., Park, S., 2015a. An experimental and numerical approach to derive ground thermal conductivity in spiral coil type ground heat exchanger. J. Energy Inst. 88, 229–240. https://doi.org/10.1016/J.JOEI.2014.10.002

Yoon, S., Lee, S.-R., Xue, J., Zosseder, K., Go, G.-H., Park, H., 2015b. Evaluation of the thermal efficiency and a cost analysis of different types of ground heat exchangers in energy piles. Energy Convers. Manag. 105, 393–402. https://doi.org/10.1016/J.ENCONMAN.2015.08.002

Young, T., 2004. Development, verification, and design analysis of the borehole fluid thermal mass model for approximating short term borehole thermal

response. Oklahoma, USA.

Yu, M.Z., Peng, X.F., Li, X.D., Fang, Z.H., 2004. A simplified model for measuring thermal properties of deep ground soil. Exp. Heat Transf. 17, 119–130. https://doi.org/10.1080/08916150490271845

Yu, X., Zhang, Y., Deng, N., Wang, J.J., Zhang, D., Wang, J.J., 2013. Thermal response test and numerical analysis based on two models for ground-source heat pump system. Energy Build. 66, 657–666. https://doi.org/10.1016/j.enbuild.2013.07.074

Zanchini, E., Lazzari, S., Priarone, A., 2010a. Effects of flow direction and thermal short-circuiting on the performance of small coaxial ground heat exchangers. Renew. Energy 35, 1255–1265. https://doi.org/10.1016/j.renene.2009.11.043

Zanchini, E., Lazzari, S., Priarone, A., 2010b. Improving the thermal performance of coaxial borehole heat exchangers. Energy 35, 657–666. https://doi.org/10.1016/j.energy.2009.10.038

Zarrella, A., De Carli, M., Galgaro, A., 2013. Thermal performance of two types of energy foundation pile: Helical pipe and triple U-tube. Appl. Therm. Eng. 61, 301–310. https://doi.org/10.1016/j.applthermaleng.2013.08.011

Zeng, H., Diao, N., Fang, Z., 2003. Heat transfer analysis of boreholes in vertical ground heat exchangers. Int. J. Heat Mass Transf. 46, 4467–4481. https://doi.org/10.1016/S0017-9310(03)00270-9

Zeng, H.Y., Diao, N.R., Fang, Z.H., 2002. A finite line-source model for boreholes in geothermal heat exchangers. Heat Transf. Res. 31, 558–567. https://doi.org/10.1002/htj.10057

Zhang, C., Guo, Z., Liu, Y., Cong, X., Peng, D., 2014. A review on thermal response test of ground-coupled heat pump systems. Renew. Sustain. Energy Rev. 40, 851–867. https://doi.org/10.1016/j.rser.2014.08.018

Zhang, L., Zhang, Q., Huang, G., Du, Y., 2014. A p(t)-linear average method to estimate the thermal parameters of the borehole heat exchangers for in situ thermal response test. Appl. Energy 131, 211–221. https://doi.org/10.1016/j.apenergy.2014.06.031

Zhang, W., Cui, P., Liu, J., Liu, X., 2017. Study on heat transfer experiments and mathematical models of the energy pile of building. Energy Build. 152, 643–652. https://doi.org/10.1016/J.ENBUILD.2017.07.041

Zhao, Q., Chen, B., Liu, F., 2016. Study on the thermal performance of several types of energy pile ground heat exchangers: U-shaped, W-shaped and spiral-shaped. Energy Build. 133, 335–344. https://doi.org/10.1016/j.enbuild.2016.09.055

Zhao, Q., Liu, F., Liu, C., Tian, M., Chen, B., 2017. Influence of spiral pitch on the thermal behaviors of energy piles with spiral-tube heat exchanger. Appl. Therm. Eng. 125, 1280–1290. https://doi.org/10.1016/J.APPLTHERMALENG.2017.07.099

Zhou, S., Cui, W., Tao, J., Peng, Q., 2016. Study on ground temperature response of multilayer stratums under operation of ground-source heat pump. Appl. Therm. Eng. 101, 173–182. https://doi.org/10.1016/j.applthermaleng.2016.02.130

Zhu, Y., Tao, Y., Rayegan, R., 2012. A comparison of deterministic and probabilistic life cycle cost analyses of ground source heat pump (GSHP) applications in hot and humid climate. Energy Build. 55, 312–321. https://doi.org/10.1016/j.enbuild.2012.08.039